Institut für Molekulare und Klinische Immmunologie

der Medizinischen Fakultät

der Otto-von-Guericke-Universität Magdeburg

Beeinflussung primärer und leukämischer T-Lymphozyten über $K_v1.3$-Kanäle mittels Memantin

D i s s e r t a t i o n

zur Erlangung des Doktorgrades

Dr. med.

(doctor medicinae)

an der Medizinischen Fakultät

der Otto-von-Guericke-Universität Magdeburg

vorgelegt von Theresa Lowinus

aus Berlin-Pankow

Magdeburg, 2019

Bibliographische Beschreibung

Bei der vorliegenden Arbeit handelt es sich um eine kumulative Promotionsschrift, in der die Ergebnisse von drei Publikationen zusammenhängender Thematik präsentiert werden. Im Text wird durch **Px.Abb.y** auf die zugehörigen Daten und Abbildungen aus den folgenden drei Publikationen (siehe Anhang) verwiesen:

P1: Kahlfuß S, Simma N, Mankiewicz J, Bose T, **Lowinus T**, Klein-Hessling S, Sprengel R, Schraven B, Heine M, Bommhardt U: Immunosuppression by N-methyl-D-aspartate receptor antagonists is mediated through inhibition of $K_v1.3$ and $K_{Ca}3.1$ channels in T cells. **Mol Cell Biol. 2014,** Mar;34(5):820-31.

P2: Lowinus T, Bose T, Busse S, Busse M, Reinhold D, Schraven B, Bommhardt UH: Immunomodulation by memantine in therapy of Alzheimer's disease is mediated through inhibition of $K_v1.3$ channels and T cell responsiveness. **Oncotarget. 2016,** Aug 16;7(33):53797-53807.

P3: Lowinus T, Heidel FH, Bose T, Nimmagadda SC, Schnöder T, Cammann C, Schmitz I, Seifert U, Fischer T, Schraven B, Bommhardt U: Memantine potentiates cytarabine-induced cell death of acute leukemia correlating with inhibition of Kv1.3 potassium channels, AKT and ERK1/2 signaling. **Cell Commun Signal. 2019** Jan 16;17(1):5.

Eigene, während der Promotionszeit erhobene Daten sind in zwei weitere Publikationen eingeflossen; die Daten sind jedoch nicht zentraler Bestandteil der vorliegenden kumulativen Dissertationsschrift:

- Simma N, Bose T, Kahlfuss S, Mankiewicz J, **Lowinus T**, Lühder F, Schüler T, Schraven B, Heine M, Bommhardt U: NMDA-receptor antagonists block B-cell function but foster IL-10 production in BCR/CD40-activated B cells. **Cell Commun Signal. 2014,** Dec 5;12:75.

- Pierau M, Na SY, Simma N, **Lowinus T**, Marx A, Schraven B, Bommhardt UH: Constitutive Akt1 signals attenuate B-cell receptor signaling and proliferation, but enhance B-cell migration and effector function. **Eur J Immunol. 2012** Dec;42(12):3381-93.

Kurzreferat

K_v1.3-Kaliumkanäle spielen eine zentrale Rolle bei der Aktivierung, Proliferation und Apoptose von T-Lymphozyten und sind vielversprechende therapeutische Zielstrukturen. Bisher sind jedoch keine Pharmaka zur K_v1.3-Kanal-Blockade klinisch lizensiert. Memantin, ein gut verträglicher, bei der Behandlung der Alzheimer Demenz eingesetzter NMDA-Rezeptor (NMDAR)-Antagonist, hemmt in Lymphozyten K_v1.3-Kanäle. In dieser Arbeit wird aufgezeigt, dass die NMDAR-Antagonisten Memantin, Ifenprodil und MK-801 die Proliferation und Migration muriner und humaner T-Lymphozyten *in vitro* reduzieren. In Memantin-behandelten Alzheimer-Patienten wurde eine veränderte Zusammensetzung der T-Zellpopulationen im peripheren Blut sowie eine reduzierte T-Zellreaktivität *ex vivo* nachgewiesen. Memantin-induzierte inhibitorische Effekte auf T-Zellfunktionen, und somit auf die adaptive Immunantwort, könnten einerseits vorteilhaft die Neuroinflammation der Alzheimer Demenz beeinflussen, andererseits die unter Memantin-Behandlung auftretende erhöhte Infektionsrate mitbedingen. Im zweiten Schwerpunkt der Dissertation wird dargestellt, dass Memantin die Cytarabin-induzierte Proliferationshemmung und den Zelltod von ALL- und AML-Zelllinien sowie primären leukämischen Blasten von Patienten mit akuter Leukämie potenziert. Dabei wurden eine verstärkte Hemmung der ERK1/2- und AKT-Signalwege und eine Steigerung der mitochondrialen Apoptose nachgewiesen. Memantin könnte daher als K_v1.3-Kanal-Inhibitor bei der Cytarabin-basierten Chemotherapie akuter Leukämien von klinischem Interesse sein. Kombinationsstrategien mit Memantin und Cytarabin wären fortführend in geeigneten Leukämiemodellen zu überprüfen.

Schlüsselwörter

T-Lymphozyt, K_v1.3-Kanal, Memantin, NMDA-Rezeptor-Antagonist, Alzheimer Demenz, Migration, Proliferation, Immunmodulation, akute lymphatische und myeloische Leukämie, Cytarabin, Zelltod, AKT, ERK1/2, c-MYC, Zytochrom C

Inhaltsverzeichnis

Abkürzungsverzeichnis

Aß	Amyloid beta
Abb.	Abbildung
AKT	AKT/Proteinkinase B
ALL	akute lymphatische Leukämie
AMPAR	α-Amino-3-hydroxy-5-methyl-4-isoxazolpropionat-Rezeptor
AML	akute myeloische Leukämie
Apaf-1	*apoptotic protease activating factor*
AraC	Cytarabin
ATP	Adenosintriphosphat
Bax	Bcl-2-associated X protein
CCL21	*CC motif chemokine ligand 21*
CD	*cluster of differentiation*
CI	*combination index* (Kombinationsindex)
CRAC	c*alcium release-activated calcium channel*
CTL	zytotoxischer T-Lymphozyt
CytC	Zytochrom C
DC	dendritische Zelle
DNA	Desoxyribonukleinsäure
DRI	*dose reduction index* (Dosisreduktionsindex)
ERK1/2	*extracellular-signal regulated kinase 1/2*
F_a	affektierte Fraktion
GvHD	*graft-versus-host disease*
HEV	hochendotheliale Venolen
HIV	humanes Immundefizienz-Virus
HLA	humanes Leukozytenantigen
IFN-γ	Interferon-gamma
iGluR	ionotroper Glutamatrezeptor
IL-2	Interleukin-2
IS	immunologische Synapse

ITAM	*immunoreceptor tyrosine-based activation motif*
JNK	c-Jun-N-terminale Kinase
$K_{Ca}3.1$	calciumgesteuerter Kaliumkanal Typ 3.1
kDa	Kilodalton
$K_v1.3$	spannungsgesteuerter Kaliumkanal Typ 1.3
LAT	Linker für aktivierte T-Zellen
^{p56}Lck	*lymphocyte specific protein tyrosin kinase of 56 kDa*
LDAC	*low dose* AraC
LFA-1	*lymphocyte function-associated antigen 1*
mGluR	metabotroper Glutamatrezeptor
MHC	*major histocompatibility complex*
mito$K_v1.3$	mitochondrialer $K_v1.3$-Kanal
MLR	*mixed lymphocyte reaction*
mTOR	*mammalian target of rapamycin*
NF-AT	*nuclear factor of activated T cells*
NF-κB	*nuclear factor ´kappa-light-chain-enhancer` of activated B cells*
NMDAR	N-Methyl-D-Aspartat-Rezeptor
PBMC	mononukleäre Zellen des peripheren Blutes
PI	Propidiumjodid
PI-3K	Phosphoinositid-3-Kinase
ROS	reaktive Sauerstoffspezies
SDF-1α	*stromal cell-derived factor-1*α
shRNA	*small hairpin* Ribonukleinsäure
SMAC	supramolekularer Aktivierungskomplex
TCR	T-Zellrezeptor
T_H-Zelle	T-Helfer-Zelle
ZNS	zentrales Nervensystem

1 EINFÜHRUNG

1.1 T-Lymphozyten: Funktion und Signalgebung

1.1.1 Funktion von T-Lymphozyten

T-Lymphozyten bilden zusammen mit B-Zellen den zellulären Teil der adaptiven Immunantwort. T-Zellen reifen im Thymus und wandern von dort entlang Chemokingradienten über das periphere Blut und durch hochendotheliale Venolen (HEV) in die Milz und Lymphknoten [1, 2]. Treffen naive T-Zellen in der T-Zellzone von Milz oder Lymphknoten auf dendritische Zellen (DCs), die das kognate Antigen auf Molekülen des Haupthistokompatibilitätskomplexes (MHC) präsentieren, werden sie über T-Zellrezeptor (TCR)-Ligation aktiviert und bei gleichzeitiger Kostimulation über CD28-Signale zur Proliferation (klonale Expansion) angeregt [3]. Aktivierte T-Zellen differenzieren sodann zu Effektorzellen, die über efferente Lymphbahnen in die Blutzirkulation eintreten und dort durch Chemokine, wie SDF-1α (*stromal cell-derived factor 1α*, CXCL12), in die verschiedenen Gewebe zur Immunüberwachung dirigiert werden [4, 5]. Naive $CD4^+$T-Helfer-Zellen (T_H) differenzieren in verschiedene T_H-Effektorpopulationen, deren Spezialisierung wesentlich durch das Zytokinmilieu determiniert wird und die durch spezifische Zytokinprofile ausgewiesen sind [6, 7]. Aktivierte $CD8^+$ T-Zellen differenzieren zu zytotoxischen T-Lymphozyten (CTLs). Ihre Aufgabe ist die Induktion von Apoptose in infizierten und pathologischen Zielzellen sowie in Effektorzellen, um die Immunreaktion abzuschalten (aktivierungsinduzierter Zelltod, AICD) [8, 9]. Nach Beseitigung des Krankheitserregers sterben die meisten Effektor-T-Zellen durch Apoptose, während einige zu Gedächtnis-T-Zellen differenzieren und längerfristig überleben.

1.1.2 Aktivierung, Proliferation und Zelltod von T-Lymphozyten

Um die Funktion von T-Lymphozyten gezielt beeinflussen zu können, ist es notwendig, die molekularen Mechanismen der T-Zell-Aktivierung genau zu verstehen. Im Folgenden sind wichtige Signalwege, die in der Arbeit untersucht wurden, kurz dargestellt. Jede T-Zelle exprimiert ca. 30000 TCRs einheitlicher Antigenspezifität auf ihrer Oberfläche. α/ß-T-Zellen tragen einen TCR bestehend aus einem α-ß-Heterodimer, der durch die ζ-Ketten und γ-, δ-, ε-Ketten des CD3-Komplexes stabilisiert wird [10]. Jeder TCR/CD3-Komplex enthält 10 ITAMs (*immunoreceptor tyrosine-based activation motifs*) zur initialen Signalübertragung [11, 12]. Wird der $CD4^+$ bzw. $CD8^+$ T-Zelle kognates Antigen als Peptid:MHCII- bzw. Peptid:MHCI-Komplex auf antigenpräsentierenden Zellen (APCs) präsentiert, kommt es bei Interaktion zur TCR-Ligation [10, 13], und in der Kontaktzone zwischen T-Zelle und APC verdichten sich wichtige an der Signaltransduktion beteiligte Proteine zu einem

supramolekularen Aktivierungskomplex (SMAC). Diese Zone wird auch als immunologische Synapse (IS) bezeichnet. Der zentrale SMAC (c-SMAC) integriert neben dem TCR die Korezeptoren CD4/CD8, den Kostimulator CD28 sowie das Adhäsionsmolekül CD2 und die Proteinkinase PKC-θ. Im peripheren SMAC (p-SMAC) finden sich wichtige Adhäsions- und Zytoskelettproteine, wie LFA-1 (*lymphocyte function-associated antigen-1*), ICAM-1 (*intercellular adhesion molecule-1*) und Talin [14, 15]. Zentral für die Aktivierung von T-Lymphozyten nach TCR-Ligation ist ein anhaltender Calciuminflux über CRAC (*calcium release-activated calcium*)-Kanäle [16, 17]. Um deren frühzeitige Inaktivierung aufgrund der Depolarisation der T-Zelle zu verhindern, werden Mitochondrien zur reversiblen Calciumaufnahme zur IS rekrutiert [18, 19]. Weiterhin lokalisieren spannungsabhängige Kaliumkanäle vom Typ $K_v1.3$ in der IS und ermöglichen durch kompensatorischen Kaliumefflux einen anhaltenden Calciuminflux über CRAC-Kanäle [20-22]. $K_v1.3$-Kanäle sind somit für die T-Zellaktivierung von großer Bedeutung [23, 24]. Nach TCR-Ligation wird initial die Tyrosin-Proteinkinase ^{p56}Lck (*lymphocyte-specific protein tyrosine kinase*) aktiviert, die teils mit den intrazellulären Domänen der Korezeptoren CD4/CD8 assoziiert ist. Nach Aktivierung durch die Tyrosin-Phosphatase CD45 und Autophosphorylierung phosphoyliert ^{p56}Lck die ITAM-Sequenzen der ζ-Ketten, was zur Rekrutierung von Zap70 (*zeta-chain-associated protein kinase 70*) und dessen Phosphorylierung und Aktivierung durch ^{p56}Lck führt. Zap70 wiederum phosphoryliert LAT (Linker für aktivierte T-Zellen) und nach Rekrutierung und Aktivierung weiterer Signalproteine kommt es zur Aktivierung der Phospholipase C-γ1 (PLCγ1) [12, 25, 26]. PLCγ1 generiert aus Phosphatidylinositol 4,5-bisphosphat (PIP_2) Diacylglycerol (DAG) und Inositol-1,4,5-triphosphat (IP_3). DAG aktiviert Proteinkinase C (PKC) und initiiert damit die NF-κB (*nuclear factor 'kappa-light-chain-enhancer' of activated B cells)*-Signalgebung. IP_3-Bindung an IP_3-Rezeptoren des endoplasmatischen Retikulums (ER) induziert die Calciumfreisetzung aus dem ER, was zur Translokation von STIM1(stromal interaction molecule 1)-Molekülen im ER und Aktivierung von Orai-Proteinen und der Öffnung der CRAC-Kanäle in der Plasmamembran führt [27]. Anstieg der intrazellulären Calciumkonzentration bewirkt u.a. die Aktivierung der NF-AT (*nuclear factor of activated T cells*)-Transkriptionsfaktoren. Über DAG und die Kinasen Raf (*rapidly accelerated fibrosarcoma*) und MEK (*mitogen-activated protein kinase/ERK kinase*) erfolgt die Aktivierung der MAPKinasen Erk1/2 (*extracellular signal-regulated kinase 1/2*) (**Abb.1a**). Die Transkription des IL-2-Gens erfordert die konzertierte Aktivität der Transkriptionsfaktoren NF-AT, NF-κB und AP-1 [28-31]. Sezerniertes IL-2 fördert sodann die Proliferation und Differenzierung naiver T-Zellen zu Effektorzellen [32]. TCR-Ligation führt zudem zur Aktivierung der Lipidkinase PI3-K (Phosphoinositid-3-Kinase) und zur Bildung von PIP3 (Phosphatidylinositol-(3,4,5)-Triphosphat). An PIP3 binden über ihre PH (*pleckstrin homology*)-Domänen die zytosolischen Serin/Threonin-Proteinkinasen Akt (auch als

Proteinkinase B/PKB bekannt) sowie PDK1 (*Phosphoinositide-dependent kinase-1*). Aktive PDK1 und mTORC2 (*mammalian target of rapamycin complex 2*) phosphorylieren und aktivieren Akt, was zur Aktivierung der Kinase mTOR (*mammalian target of rapamycin*) und nachfolgend zur Phosphorylierung des ribosomalen Proteins S6 und zur Steigerung der Proteinsynthese führt. Der PI3K-Akt-mTOR-Signalweg ist ein zentraler Regulator des Zellwachstums und Überlebens und in vielen Tumoren hyperaktiv [33-35]. Eine wichtige gemeinsame Zielstruktur der bei Tumoren häufig überaktivierten Kinasen Akt und Erk1/2 ist der Transkriptionsfaktor c-Myc, ein zentraler Regulator von Zellwachstum, Proliferation und Apoptose [36, 37].

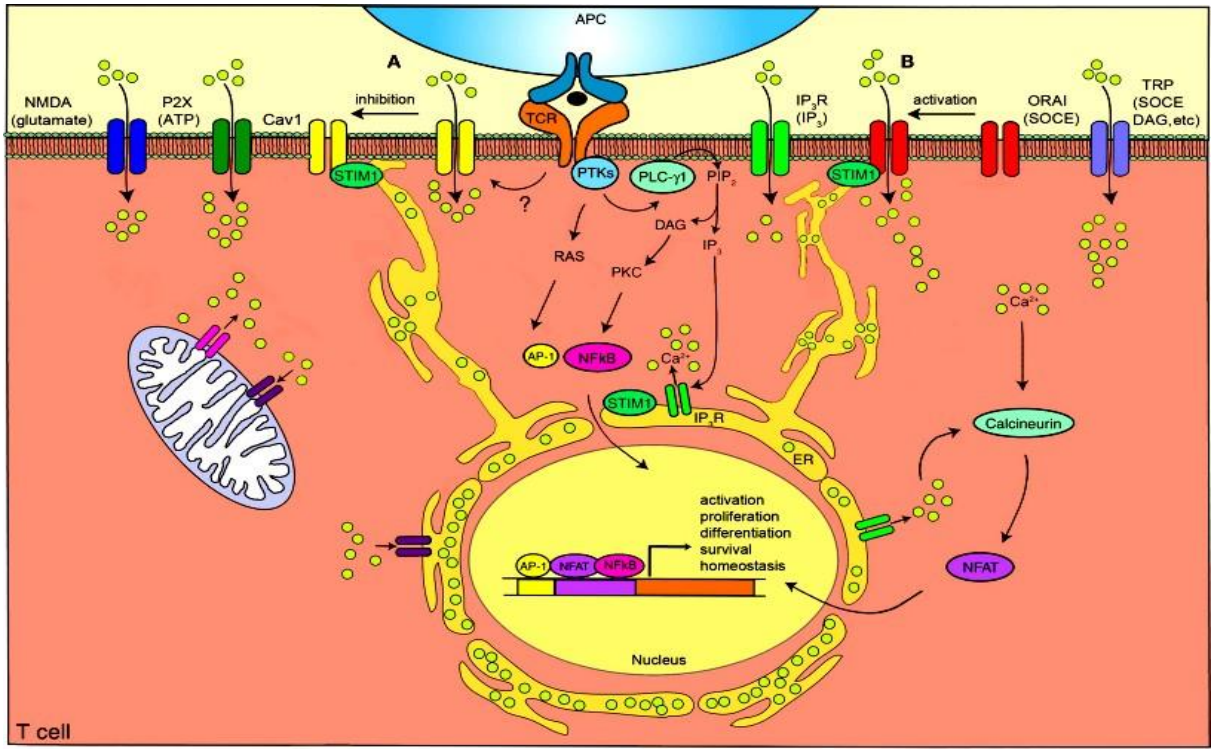

Abb.1a: TCR-Signalgebung. Die Interaktion des TCRs mit antigenspezifischen Peptid-MHC-Komplexen auf APCs führt über Aktivierung von Proteintyrosinkinasen, wie ^{p56}Lck, der Aktivierung von PLC-γ1 (Phospholipase C-γ1) und MAPKinasen (mitogenaktivierte Poteinkinase) zur Aktivierung der Transkriptionsfaktoren NF-AT (*nuclear factor of activated T cells*), NFκB *(nuclear factor kappa B*) und AP-1. Calciumkanäle, wie CRAC (*calcium-release activated channel*) und Ca_V1-Kanäle, sowie NMDA-, P2X- und TRP-Rezeptoren, sollen an der Calciumsignalgebung beteiligt sein. Ihre Existenz in T-Zellen ist teils unzureichend geklärt. *Abb. modifiziert aus: Kyla et al. 2013.*

Für die Aktivierung, Proliferation und Differenzierung naiver T-Zellen zu Effektorzellen sind drei Signale notwendig. Signal 1, Bindung des TCR an spezifische Antigen:MHC-Komplexe, führt zur T-Zellaktivierung. Signal 2, Bindung des kostimulatorischen Moleküls CD28 an die Liganden CD80/CD86 auf APCs, steigert die Proliferation und das Überleben der T-Zelle [38, 39]. Signal 3 über Zytokinrezeptoren dirigiert die T-Zelldifferenzierung über ein spezifisches

Zytokinmilieu [6, 7]. T-Effektorzellen können ohne CD28-Kostimulation aktiviert werden. Sie wandern aufgrund der hohen Expression von CD44 ($CD44^{high}$), der fehlenden Expression von CD62L ($CD62L^{low}$) und des Sphingosin-1-Phosphat-Rezeptors präferentiell in entzündetes Gewebe und nicht in die Lymphknoten [40]. Während naive humane T-Zellen die CD45RA-Isoform der CD45-Tyrosinphosphatase exprimieren [41-43], weisen T-Gedächtniszellen die CD45RO-Isoform auf, wodurch ihre Aktivierung über den TCR erleichtert wird, so dass eine Infektion mit einem bekannten Antigen schneller und effektiver abgewehrt werden kann [44]. Gedächtniszellen exprimieren zudem vermehrt anti-apoptotische Proteine, wie Bcl-2 (*B-cell lymphoma 2*), und können über Jahrzehnte in einem „Ruhestadium“ verharren, wobei ihre antigenspezifische Anzahl durch seltene Teilungsvorgänge und Apoptose konstant gehalten wird [44, 45].

Nur ein kleiner Anteil der T-Effektorzellen bleibt nach Beenden der Immunantwort als Gedächtniszellen erhalten, der Großteil stirbt durch Apoptose [46]. Im Gegensatz zur Nekrose verbraucht Apoptose Energie und führt zum Abschnüren von kleinen Zellteilen (*apoptotic bodies*), die ohne Entzündungsreaktionen von Makrophagen entfernt werden. Der extrinsische Apoptoseweg wird über Todesrezeptoren der TNF (Tumornekrosefaktor)-Familie initiiert [47, 48]. Der intrinsische Apoptoseweg wird über Mitochondrien bei Einwirken schädlicher Reize, wie Zytostatika, zellulärem Stress oder Entzug von Wachstumsfaktoren, eingeleitet [49, 50] (**Abb.1b**).

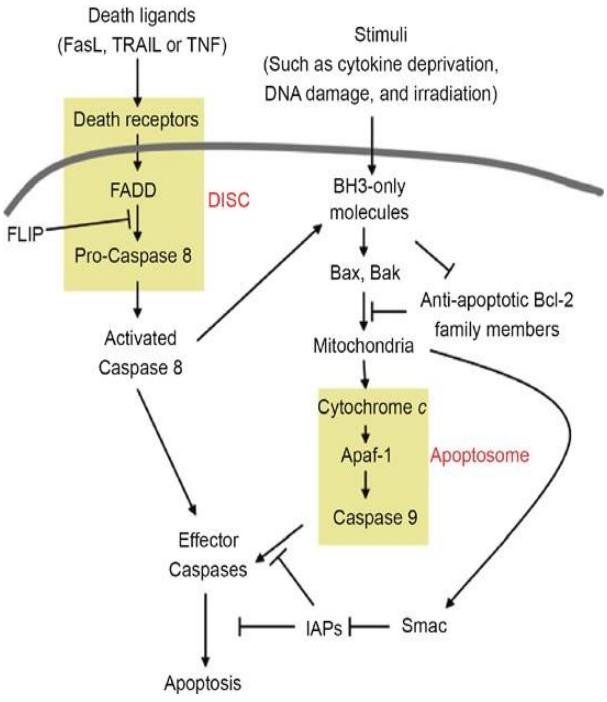

Abb.1b: Extrinsischer und intrinsischer Apoptoseweg in Lymphozyten. Der extrinsische Apoptoseweg (links) wird durch Ligation von Todesrezeptoren der Tumornekrosefaktor-Rezeptor-Superfamilie mit ihren Liganden initiiert und führt zur Aktivierung der Caspase-8. Der intrinsische Apoptoseweg wird durch Zytokinentzug, toxische Einwirkungen oder Zellschäden ausgelöst (rechts). Zentrale Ereignisse sind die Formation einer mitochondrialen Permeabilisationspore, Austritt von Zytochrom C in das Zytoplasma und Aktivierung der Caspase-9. Extrinsischer und intrinsischer Apoptoseweg konvergieren in der Aktivierung der Effektor-Caspase-3, und Endonukleasen fragmentieren die DNA. *Abb. aus: Leanza et al. 2007.*

Zytochrom C (CytC) dringt durch den Apoptose-induzierten Kanal der äußeren mitochondrialen Membran, der aus oligomerisertem Bax (*Bcl-2-associated X protein*) und anderen bisher nicht-identifizierten Proteinen besteht, in das Zytoplasma [51-53]. Dort bindet CytC an Apaf-1 (*apoptotic protease activating factor*-1) und nach dessen Oligomerisierung wird die Caspase-9 aktiviert [54, 55]. Caspasen (Aspartat-spezifische Proteasen) liegen initial als inaktive Pro-Caspasen vor und agieren in einer Kaskade, wobei die Initiator-Caspasen nachgeschaltete Effektor-Caspasen, insbesondere Caspase-3, aktivieren [56]. Initiator-Caspase des intrinsischen Apoptosewegs ist Caspase-9, für den extrinsischen Apoptoseweg agiert Caspase-8 [54, 57, 58]. Die Effektor-Caspasen spalten wichtige zelluläre Proteine und aktivieren Enzyme, wie Endonukleasen, die die DNA fragmentieren, wodurch der Zelltod eingeleitet wird [59] (**Abb.1b**). Die Dysregulation von Zelltodmechanismen kann zu Autoimmunerkrankungen, neurodegenerativen Erkrankungen und Neoplasien führen [60-62].

1.1.3 T-Zell-assoziierte Erkrankungen

T-Lymphozyten tragen wesentlich zu den protektiven Funktionen der adaptiven Immunantwort bei. Eine pathologisch verminderte Immunantwort liegt bei angeborenen Immundefekten [63, 64] oder erworbenen Störungen der T-Lymphozyten vor, etwa durch das humane Immundefizienz-Virus (HIV), was häufig tödlich verlaufende Infektionen zur Folge hat [65]. Andererseits führt eine übermäßige, unkontrollierte T-Zellaktivierung zu schwerwiegenden Erkrankungen, die jedes Organ betreffen können und teilweise lebensbedrohliche Auswirkungen haben, etwa bei Allergien und Autoimmunerkrankungen, wie multipler Sklerose. Die Immunantwort auf Alloantigene ist prinzipiell eine physiologische Reaktion, die bei der Transplantation von Organen jedoch unerwünscht ist. Grundlage für die Abstoßung transplantierter Organe sind die von T_{H1}-Effektorzellen und CTLs vermittelten Alloantigenreaktionen, bei denen Spender-MHC/Peptid-Moleküle als "fremd" erkannt werden (MHC-Restriktion) [66-68]. *In vitro* kann eine Alloantigenreaktion in *mixed lymphocyte reaction*s (MLRs) durch Stimulation von T-Zellen mit HLA-inkompatiblen Donor-Zellen induziert und zur antigenspezifischen Aktivierung von T-Zellen eingesetzt werden [69]. Eine auf dem gleichen Prinzip basierende Abstoßungsreaktion der Spender-T-Zellen gegen als "fremd" erkannte Empfänger-Körperzellen ist die *graft-versus-host* Reaktion (GvHD), die bei der Transplantation hämatopoetischer Stammzellen auftreten kann. Kommt es zur malignen Transformation von Lymphozyten, resultieren lebensbedrohliche Leukämien/Lymphome, z.B. die akute T-Zell-Leukämie. Angesichts der Schwere T-Zell-asssoziierter Erkrankungen besteht weiterhin ein dringlicher Bedarf an neuen, effektiven und dabei gut verträglichen Pharmaka zur Modulation der T-Zellfunktion.

1.2 NMDA-Rezeptoren: Einfluss von Antagonisten auf die T-Zell-Funktion

1.2.1 N-Methyl-D-Aspartat-Rezeptoren (NMDARen) und NMDAR-Antagonisten

Neuronale NMDARen sind liganden-gesteuerte Kationenkanäle mit hoher Calcium-permeabilität. Sie sind für die synaptische Plastizität und Langzeitpotenzierung verantwortlich und bilden somit die molekulare Basis für Lernen und Gedächtnis [70, 71]. Allerdings kann eine pathologisch erhöhte Aktivierung von NMDARen mit massivem Calciumeinstrom zu Exzitotoxizität und Neurodegeneration führen [72, 73]. Hinsichtlich des klinischen Einsatzes von NMDAR-Antagonisten ist aufgrund zu starker neuronaler Toxizität nur der *open channel* Blocker Memantin für die Behandlung der fortgeschrittenen Alzheimer Demenz lizensiert [74]. Weitere NMDAR-Antagonisten sind das selten als Narkotikum applizierte Ketamin [75] sowie die ausschließlich experimentell verwendeten Inhibitoren MK-801, ein *open channel* Blocker, D-AP-V, ein kompetitiver Antagonist der Glutamat-Bindungsstelle, und Ifenprodil, ein unkompetitiver Antagonist der Polyaminbindungsstelle der GluN2B-Untereinheit [76-78] (**Abb.2a**).

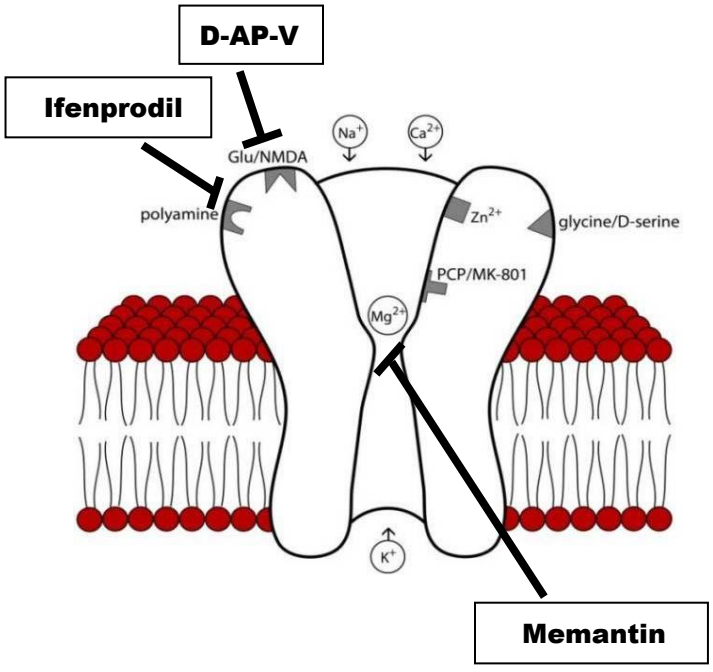

Abb.2a: Aufbau des NMDARs und Bindungsstellen der Antagonisten. Der NMDAR bildet ein Heterotetramer aus 2 GluN1- und 2 GluN2-Untereinheiten. Der Ionenkanal wird durch Bindung von Glutamat/Aspartat sowie Glycin/D-Serin bei vordepolarisierter Zellmembran aktiviert. Im inaktiven Zustand ist der Ionenkanal durch ein zentrales Magnesiumion blockiert. Memantin und MK-801 wirken als *open channel* Blocker direkt im Ionenkanal, D-AP-V ist ein kompetitiver Antagonist und blockiert die Glutamat-Bindungsstelle. Ifenprodil inhibiert den Rezeptor un-kompetitiv an der Polyaminbindungsstelle. *Abb. modifiziert aus: Tomek et al. 2013.*

T-Zellen exprimieren mehrere Typen von Ionenkanälen, die das Membranpotential und den Calciumeinstrom regulieren [24, 79, 80]. 1997 postulierten Kostanyan *et al.* anhand der Bindung von radioaktiv-markiertem Glutamat erstmals die Expression von Glutamatrezeptoren (GluRen) auf peripheren Blut-Lymphozyten [81]. Wenige Jahre später wurde die Existenz von metabotropen GluRen (mGluRen) [82-86] sowie von ionotropen GluRen (iGluRen) vom α-Amino-3-hydroxy-5-methyl-4-isoxazolpropionat (AMPAR)- und NMDAR-Typ in humanen T-Lymphozyten beschrieben [87-91]. GluRen in T-Zellen könnten

insbesondere nach Eindringen der T-Zelle ins ZNS aktiviert werden. Glutamat liegt zudem mit einer Konzentration von ~100 µM (dem Hundertfachen der Konzentrationen im *Liquor cerebrospinalis*) im peripheren Blut, in peripheren lymphatischen Geweben und innervierten Organen vor [92, 93]. Pathologisch erhöhte Glutamat-Plasmaspiegel wurden bei HIV-Immundefizienz und Neoplasien beobachtet [94-97]. Über sezerniertes Glutamat könnten T-Lymphozyten bei Kontakt mit DCs koaktiviert werden [98], aber auch Makrophagen und Neutrophile wurden neben DCs als Quelle für Glutamat identifiziert [99, 100]. Affaticati *et al.* publizierten 2011, dass DCs in Kontakt mit Thymozyten aus Vesikeln Glutamat in die Kontaktzone sezernieren. Glutamat würde sodann an die NMDARen auf Thymozyten binden, da NMDAR-Antagonisten den Calciuminflux in $CD4^+CD8^+$ Thymozyten und deren Apoptose minderten [101].

Der Nachweis von NMDARen in T-Zellen erfolgte hauptsächlich anhand der mRNA-Expression von NMDAR-Untereinheiten und indirekt durch die Wirkung von Glutamat und NMDAR-Antagonisten auf verschiedene T-Zellfunktionen [89, 102-106]. Dabei ist zu beachten, dass Glutamat auch an $K_v1.3$-Kanäle bindet [107]. Funktionale NMDARen auf Thymozyten oder peripheren T-Zellen konnten mittels Patch-Clamp-Technik, wie für Neurone umfangreich vorgefunden, weder durch Affaticati *et al*. noch durch meine Kollegin Dr. T. Bose im SFB854-Twin-Forschungsprojekt nachgewiesen werden. Ihre Patch-Clamp-Untersuchungen zeigten vielmehr, dass die NMDAR-Antagonisten Memantin, Ifenprodil und MK-801 $K_v1.3$- und $K_{Ca}3.1$-Kaliumkanäle auf humanen und murinen T-Lymphozyten hemmen [108, 109]. Die Auswirkungen der $K_v1.3$-Kanal-Blockade durch NMDAR-Antagonisten, insbesondere von Memantin, auf verschiedene Effektorfunktionen von T-Lymphozyten waren zu Projektbeginn weitgehend unbekannt.

1.2.2 Wirkmechanismus und unerwünschte Wirkungen von Memantin

Memantin ist strukturell von Amantadin abgeleitet und wird chemisch als Dimethyladamantan oder nach IUPAC (*International Union of Pure and Applied Chemistry*) als Dimethyl-trizyklo-decanamin beschrieben [74] (**Abb.2b,** oben). Memantin wurde erstmals in den 1960er Jahren synthetisiert [110] und 1975 von Merz & Co. für seine Wirkung auf das ZNS patentiert [74, 111]. Erst 1989 wurde der Wirkmechanismus von Memantin auf Neurone als NMDAR-Antagonist aufgeklärt [112, 113]. Memantin ist ein *open channel* Blocker, d.h. es kann nur im aktivierten offenen Zustand des NMDARs in den Ionenkanal eintreten und ihn im Bereich der Mg^{2+}-Bindungsstelle blockieren („besseres Mg^{2+}“) (**Abb.2b,** unten) [114]. Memantin ist daher bei pathologisch erhöhter NMDAR-Aktivität am wirksamsten, wobei physiologische NMDAR-Funktionen weiterhin möglich sind [115-117]. Memantin ist zur Behandlung der moderaten bis fortgeschrittenen Alzheimer Demenz zugelassen und soll die neuronale Exzitotoxizität

verringern und die Neurodegeneration verlangsamen [118]. Aufgrund der *open channel* Blockade, seiner niedrigen Affinität und schnellen *off-rate* am NMDAR ist Memantin im Vergleich zu anderen NMDAR-Antagonisten auch bei Dauergabe gut verträglich und seit fast vier Jahrzehnten im klinischen Einsatz [115, 117, 119]. Häufigste unerwünschte Wirkungen von Memantin auf das ZNS sind Schläfrigkeit und Kopfschmerzen. Zudem wurde von gehäuft auftretenden Infektionen der Atemwege und des Urogenitaltraktes berichtet [120]. Im Rahmen der Überwachung von Nebenwirkungen nach der Zulassung durch die EMA (*European Medicines Agency*) treten Pilzinfektionen bei 1-10 von 1000 Patienten auf. Im schwersten Fall wurden Panzytopenien beobachtet [121]. Memantin-Behandlung könnte daher das Immunsystemn beeinflussen.

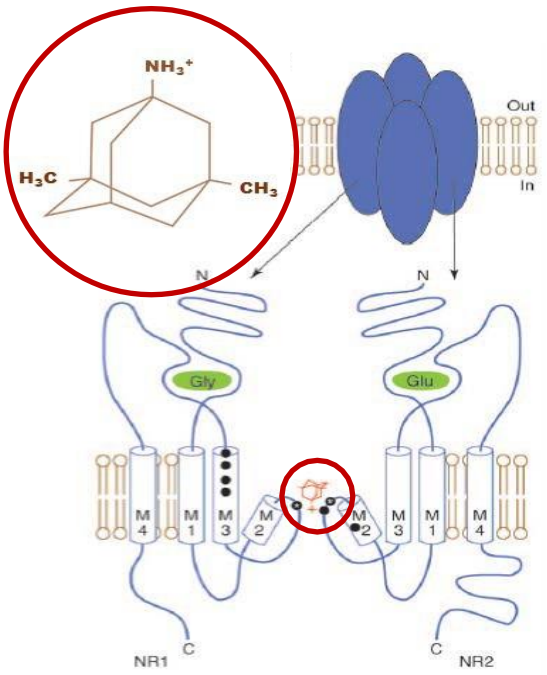

Abb.2b: Struktur von Memantin und Bindung im NMDAR-Ionenkanal. Memantin (3,5-Dimethyl-1-aminoadamantan) besteht aus einer Dreiring-struktur mit einer Amino- und zwei Methylgruppen (links oben, rot umrandet). Memantin blockiert den Ionenkanal des NMDARs an der Magnesium-bindungsstelle. Die Aminogruppe von Memantin kontaktiert kritische Aspartatreste der M2-Domänen, die Methylgruppen stabilisieren das Pharmakon innerhalb des NMDARs (unten). *Abb. modifiziert aus: Johnson et al. 2006.*

1.2.3 Immunpathogenese der Alzheimer Demenz

Die Alzheimer Demenz ist eine Hauptform der Demenz und zunehmendes Alter ein wesentlicher Risikofaktor [122]. Trotz intensiver Forschungstätigkeit fehlen effektive Therapiestrategien [123, 124]. Aktuelle Hypothesen zur Pathophysiologie gehen von einem ursächlichen Zusammenhang mit Proteinablagerungen von Amyloid-ß (Aß) und Tau im Gehirn der Patienten aus [125]. Auch Neuroinflammation spielt eine wichtige, aber noch unzureichend charakterisierte pathogenetische Rolle bei der Alzheimer Demenz [126-129]. Das Binden von Aß an Mikroglia soll die Sekretion pro-inflammatorischer Zytokine anregen und damit die Aggregation von Aß weiter begünstigen [128, 130]. Zudem wird eine reduzierte *Aß-clearance* durch gestörte Phagozytosefunktion der Mikroglia sowie die pathogenetische Beteiligung von Makrophagen, Astrozyten und Endothelzellen vermutet [126, 131-133]. T-

Lymphozyten könnten bei der Pathogenese der Alzheimer Demenz von diagnostischem (Biomarker) sowie therapeutischem Interesse (Immuntherapie) sein [134-136]. Es wurde berichtet, dass in Alzheimer-Patienten T-Zellen das Hirnparenchym nahe der Aß-Plaques aufgrund pathologisch gesteigerter Migration über die Blut-Hirn-Schranke infiltrieren [137, 138]. Aß-reaktive T_H1- sowie T_H17-T-Zellen fördern neuroinflammatorische Prozesse, während eine stark immunsupprimierende Funktion regulatorischer T-Zellen (Treg) mit einer niedrigeren kognitiven Einschränkung der Patienten einherzugehen scheint [139-142]. Im peripheren Blut zeigen Alzheimer-Patienten eine übermäßige Anzahl Aß-reaktiver T-Zellen [143], aktivierter $CD4^+$ und $CD8^+$ T-Zellen [144], IFN-γ-sezernierender T_H1-Zellen [145] und von Gedächtnis-T-Zellen [146-150]. Zudem ist die Proliferation von T-Zellen von Alzheimer-Patienten auf allogene Stimuli in MLRs und gegenüber Aß gesteigert [143]. Insgesamt ist die Bedeutung von T-Zellen für die Immunpathogenese der Alzheimer Demenz jedoch wenig verstanden.

1.3 $K_v1.3$-Ionenkanäle: „Spannende“ Zielstrukturen für T-Zellpathologien?

1.3.1 Aufbau und Expression von $K_v1.3$-Kanälen

Während Calciumkanäle eine entscheidende Rolle bei der Erregungsbildung von Neuronen spielen, sind Kaliumkanäle für die Repolarisation der Zelle essentiell. 1984 wurde erstmals die Existenz von spannungsgesteuerten Kaliumkanälen in T-Lymphozyten beschrieben [151-155] und anschließend u.a. der Subtyp $K_v1.3$ charakterisiert [156]. Kaliumkanäle werden anhand ihrer Struktur und Aktivierbarkeit in mehrere Gruppen eingeteilt.

Spannungsgesteuerte Kaliumkanäle gehören zur Kanal-Gruppe mit sechs Transmembrandomänen und werden durch Depolarisation der Zellmembran aktiviert. Sie umfassen 12 Unterfamilien (K_v1-K_v12), wobei die K_v1-Unterfamilie als *Shaker* Typ bezeichnet wird [157]. Spannungsgesteuerte Kaliumkanäle in Lymphozyten zeigen eine Homotetramerstruktur aus vier α-Untereinheiten mit einem zentralen Ionenkanal [158-160]. Jede α-Untereinheit besteht aus sechs Transmembrandomänen (S1-S6). S4 stellt aufgrund der vielen positiv-geladenen Aminosäurenreste den Spannungssensor dar. Zwischen S5 und S6 befindet sich die P-Schleife, die als Selektivitätsfilter für Kaliumionen agiert (**Abb.3a**) [161-163]. Am intrazellulär gelegenen N- und C-Terminus liegen Phosphorylierungsstellen und Interaktionsstellen für andere Proteine, etwa ^{p56}Lck, ß1-Integrine und Adapterproteine, zur weiteren Signaltransduktion [164-168]. Regulatorische Untereinheiten, wie K_vß, beeinflussen das *gating*, die Amplitude des Kaliumstroms und die Oberflächenexpression des Kanals [169, 170].

Das für den $K_v1.3$-Kanal kodierende Gen *KCNA3* ist für humane, murine und Ratten-T-Zellen gut charakterisiert [171]. Ruhende humane T-Zellen exprimieren ~200-400 $K_v1.3$-Kanäle/Zelle, aber nur 8-10 $K_{Ca}3.1$-Kanäle/Zelle. Bei Letzteren handelt es sich um Calcium-

aktivierte K^+-Kanäle, die durch ansteigende intrazelluläre Calciumkonzentrationen aktiviert werden. Nach T-Zellaktivierung werden ~500 $K_{Ca}3.1$-Kanäle/Zelle exprimiert und die relative Bedeutung von $K_v1.3$-Kanälen am Kaliumefflux sinkt. Ruhende T_{CM} (zentrale T-Gedächtniszellen, $CCR7^+$ $CD45RA^-$) erhöhen bei Aktivierung zu Effektorzellen ihre Expression von $K_{Ca}3.1$-Kanälen vergleichbar zu naiven T-Zellen. Bei T_{EM} (Effektor-T-Gedächtniszellen, $CCR7^-$ $CD45RA^-$) hingegen kommt es zur prädominanten Expression von $K_v1.3$-Kanälen mit ~1500 Kanälen/Zelle. Ruhende Maus- und Ratten-T-Zellen weisen im Vergleich zu ruhenden humanen T-Zellen eine deutlich geringere Anzahl an $K_v1.3$-Kanälen (<10/Zelle) auf und erst nach Aktivierung erhöht sich die Anzahl an $K_v1.3$-Kanälen auf vergleichbares Niveau [24]. Neben neuronalen Zellen und Lymphozyten exprimieren auch andere hämatopoetische Zellen, Muskelzellen, Drüsenzellen und weitere Zelltypen funktionell bedeutsame Kaliumkanäle [157].

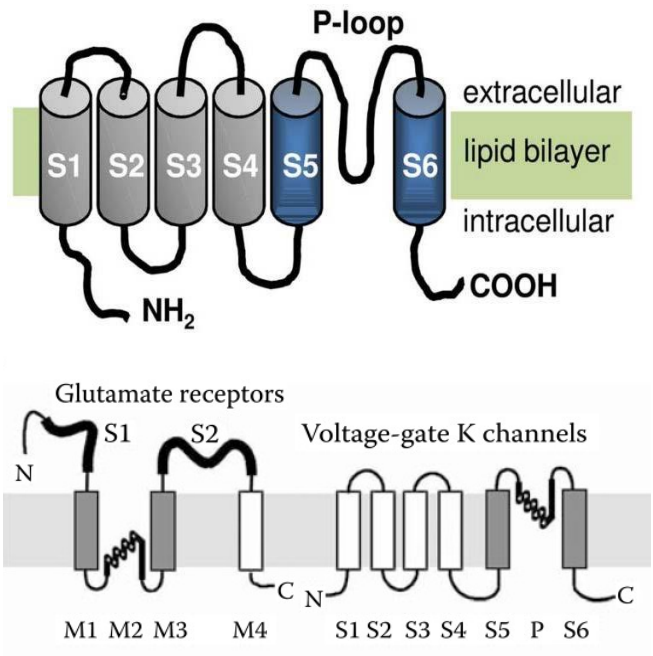

Abb.3a: Struktur spannungsgesteuerter Kaliumkanäle. Jede der vier α-Untereinheiten besteht aus sechs Transmembrandomänen S1-S6, einer P-Schleife und den intrazellulär gelegenen Amino (NH_2)- und Carboxyl (COOH)-Enden. S4 repräsentiert den Spannungssensor und S5-P-S6 bilden im Tetramer die Kalium-Permeationspore (oben). Spannungsgesteuerte Kaliumkanäle zeigen strukturelle Ähnlichkeiten mit GluRen und könnten daher aus einer gemeinsamen Ionenkanal-Familie hervorgegangen sein: die Sequenz der P-Schleife von Kaliumkanälen ähnelt der M2-Domäne von iGluRen, die Transmembrandomänen S5 und S6 entsprechen den M1- und M3-Domänen (unten). *Abb. aus: Alain et al. 2009.*

1.3.2 Funktion von $K_v1.3$-Kanälen in T-Lymphozyten

$K_v1.3$-Kanäle regulieren das Ruhemembranpotential von T-Zellen auf -50 bis -60 mV. Bei ansteigendem Membranpotential werden sie zunehmend aktiviert und verhindern durch Kaliumefflux die akzidentielle Depolarisation der T-Zelle [20, 21]. Nach Aktivierung des TCR werden $K_v1.3$-Kanäle in die IS rekrutiert und verhindern durch Kaliumefflux eine vorzeitige Inaktivierung der CRAC-Kanäle (permissive Hyperpolarisation) [23, 172]. $K_v1.3$-Kanäle ermöglichen somit einen starken und anhaltenden Anstieg der intrazellulären Calciumkonzentration, der für die Aktivierung zahlreicher Ca^{2+}-abhängiger Proteine, etwa von NF-AT, essentiell ist [22, 173]. Daher sind $K_v1.3$-Kanäle kritisch an der Aktivierung von

T-Lymphozyten beteiligt. Ihre Hemmung blockiert den Zellzyklus in der G_1-Phase und somit die Proliferation der T-Zelle [23, 24, 174]. K_v1.3 *knock-out* Ratten bzw. Mäuse zeigen allerdings keine Immundefekte, was auf die kompensatorisch verstärkte Expression von K_{Ca}3.1- bzw. Chloridkanälen zurückgeführt wurde [175, 176].

K_v1.3-Kanäle sind nicht nur in der Plasmamembran und der nukleären Membran lokalisiert, sondern wurden auch in der inneren mitochondrialen Membran nachgewiesen [177, 178]. Da kein struktureller Unterschied zwischen K_v1.3-Kanälen der Plasmamembran und des Mitochondriums vorliegt und keine spezifische Translokationssequenz detektiert wurde, bleibt unklar, welcher Mechanismus die Verteilung der Kanäle steuert [177, 179]. K_v1.3-Kanäle des Mitochondriums (mitoK_v1.3) sind zentrale Mediatoren der intrinsischen Apoptose und interagieren mit dem pro-apoptotischen Bcl-2-Familienprotein Bax der äußeren mitochondrialen Membran [180-182]. Bei apoptotischem Stimulus transloziert Bax zum mitoK_v1.3-Kanal und inhibiert diesen in der Kanalpore über Lysin 128, analog zu einem für K_v1.3-Kanal-Toxine beschriebenen Mechanismus [183, 184] (**Abb.3b**).

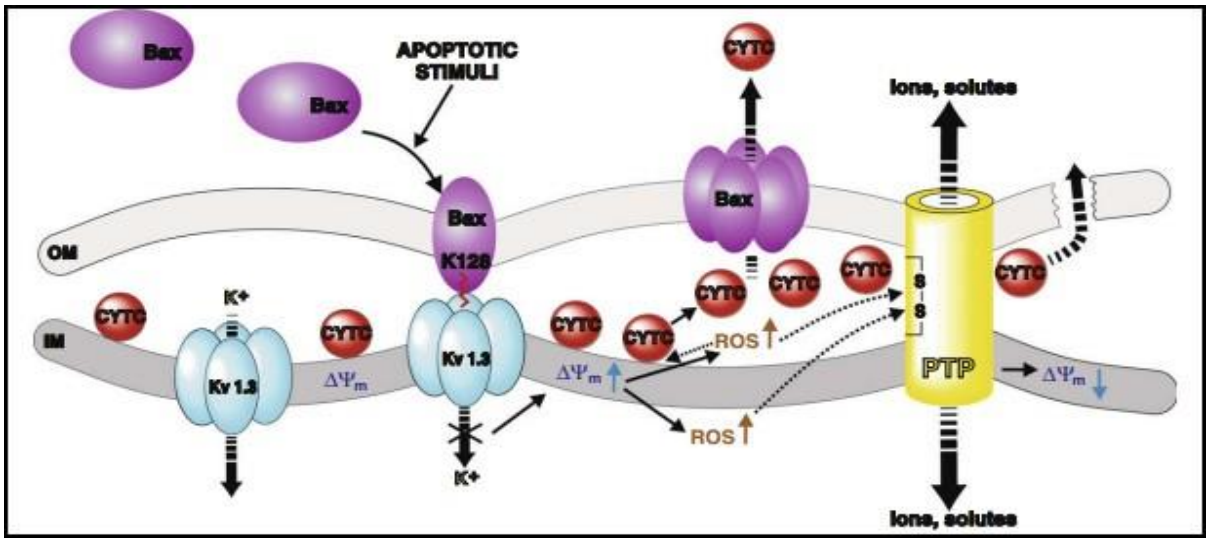

Abb.3b: Rolle von mitoK_v1.3-Kanälen bei der Apoptose. Ausgelöst durch einen apoptotischen Stimulus transloziert Bax zur OMM (äußere mitochondriale Membran) und inhibiert K_v1.3-Kanäle der IMM (innere mitochondriale Membran) durch Interaktion von Lysin 128 mit der Kanalpore. Die konsekutive Hyperpolarisation der IMM stört die Funktion der Atmungskette, wodurch sich die Produktion von ROS (reaktive Sauerstoffspezies) erhöht. Diese lösen CytC (Zytochrom C) aus der Cardiolipin-Bindung und aktivieren die PTP (Permeabilitätstransistionspore). CytC gelangt über den MAC (mitochondrialer Apoptose-induzierter Kanal), u.a. bestehend aus oligomerisiertem Bax, ins Zytoplasma. Öffnung der PTP resultiert in Depolarisation der IMM sowie Schwellung und ggf. Ruptur der mitochondrialen Membranen und führt damit ebenfalls zur Freisetzung von CytC ins Zytoplasma. *Abb. aus: Szabò et al. 2010.*

Hemmung der mitoK_v1.3-Kanäle ändert das Membranpotential der inneren mitochondrialen Membran, was zur Störung der Atmungskettenkomplexe und verstärkter Produktion reaktiver

Sauerstoffspezies (ROS) führt. Letztere setzen an Cardiolipin gebundenes Zytochrom C (CytC) an der inneren mitochondrialen Membran frei [185, 186], wodurch der intrinsische Apoptoseweg initiiert wird (**Abb.3b**).

1.3.3 K_v1.3-Kanal-Inhibitoren

Aufgrund ihrer zentralen Funktion bei der Aktivierung, Proliferation und dem Zelltod von Lymphozyten sind K_v1.3-Kanäle eine vielversprechende Zielstruktur für die therapeutische Beeinflussung der adaptiven Immunabwehr, etwa bei der Behandlung von Autoimmun-erkrankungen [187-189]. Jedoch sind Pharmaka zur spezifischen K_v1.3-Kanal-Inhibition *in vivo* derzeit nicht zugelassen. Die bislang identifizierten spezifischen K_v1.3-Kanal-Blocker lassen sich in Peptidtoxine und niedermolekulare Blocker einteilen [190, 191].

Peptidtoxine umfassen Skorpion- und Seeanemone-Toxine bzw. deren Derivate mit einer Größe von ~4 kDa. Sie blockieren von extern die Kanalpore mit hoher Affinität und Selektivität und unabhängig vom Öffnungszustand des Kanals. Allerdings sind sie aufgrund ihrer positiven Ladung membran-impermeabel und können nur K_v1.3-Kanäle der Plasmamembran, aber nicht Apoptose-vermittelnde mitoK_v1.3-Kanäle hemmen. Weiterhin tragen sie das Risiko, allergische Reaktionen hervorzurufen und müssten für eine klinische Anwendung parenteral verabreicht werden. Bisher werden Peptidtoxine nur experimentell verwendet. Lediglich zum Pharmakon Dalazatid liegen neuerdings erste Ergebnisse der Phase I/Ib Studien von gesunden Probanden und Psoriasis-Patienten vor [192].

Zu den niedermolekularen K_v1.3-Kanal-Inhibitoren mit einer Größe <0.8 kDa gehören PAP-1, Psora-4 und Clofazimin. Aufgrund ihrer Hydrophobizität sind sie membranpermeabel, binden intrazellulär an den Kanal und können über die Blockade von mitoK_v1.3-Kanälen Apoptose induzieren. Pharmakologisch vorteilhaft ist ihre bessere Bioverfügbarkeit und einfachere Produktion im Vergleich zu Peptidtoxinen. Hingegen ist ihre Affinität und Selektivität nicht optimal, so dass verstärkt Nebenwirkungen auftreten können, berücksichtigt man die weitverbreitete Expression von Kaliumkanälen [157, 191].

Neue K_v1.3-Kanal-Hemmstoffe werden mittels Punktmutationen von Toxinen oder in Hochdurchsatztechnologien gesucht [193-195]. Komplizierend ist, dass bisher kein gemeinsames Strukturmerkmal von K_v1.3-Kanal-Hemmstoffen gefunden wurde [196], während detaillierte Analysen zur Struktur des K_v1.3-Kanals vorliegen [158, 159, 161, 197, 198]. Die Struktur von Kaliumkanälen ähnelt dem Aufbau von GluRen, so dass sie aus einer gemeinsamen Ionenkanalfamilie hervorgegangen sein könnten. Eine signifikante Aminosäure-Homologie wurde in den Kanalpore-bildenden Domänen gefunden. Die

Sequenz der P-Schleife von Kaliumkanälen ähnelt der M2-Domäne und die flankierenden Transmembrandomänen S5 und S6 entsprechen den M1- und M3-Domänen von iGluRen [199-201] (**Abb.3a**). Diese Strukturähnlichkeit könnte erklären, dass Memantin K_v1.3-Kanäle humaner und muriner T-Lymphozyten blockiert [108, 109, 202]. Auch für Makrophagen und Neurone wurde gezeigt, dass Memantin Kaliumkanäle hemmt [203, 204]. Memantin könnte daher als K_v1.3-Kanal-Antagonist für klinische Therapieansätze von Interesse sein.

1.3.4 Potential der K_v1.3-Kanal-Inhibition für die Therapie akuter Leukämien

Die akute lymphatische (ALL) und akute myeloische Leukämie (AML) erfordern intensive Therapieregime, die für ältere Patienten häufig zu große toxische Nebenwirkungen aufweisen. Daher erhalten nur 30% der älteren AML-Patienten eine intensive Chemotherapie [205, 206]. Auch nimmt die Mutationslast, genetische Heterogenität und pathologische Aktivierung onkogener Signalkaskaden in AML-Blasten älterer Patienten zu [207-209]. Palliative Therapien mit demethylierenden Zytostatika (Azazytidin/Decitabin), DNA-interkalierenden Chemotherapeutika, etwa *low-dose* AraC (LDAC), und experimentellen Therapieansätzen sind begrenzt [210, 211] und bei älteren Patienten mit einer hohen Komplikationsrate und Frühmortalität verbunden [212]. Neue Therapiestrategien werden daher dringend benötigt und gesucht.

Akute Leukämien sind meist durch eine gesteigerte Aktivität der PI-3K-AKT-mTOR- und ERK1/2-Signalwege gekennzeichnet, die einen aggressiven Phänotyp und Therapieresistenz bedingen [213-217]. ERK1/2- und AKT-Signale fördern die Aktivierung des Transkriptions-faktors c-MYC [218], ein an der leukämischen Transformation beteiligtes Protoonkogen [219-221]. Da der PI-3K-AKT-mTOR- und ERK1/2-Signalweg sowie c-MYC die Zellproliferation und den Zelltod von ALL- und AML-Zellen regulieren [222-225], ist deren Inhibition ein vielversprechender Therapieansatz [226-230]. Bei rezidivierten/refraktären AML-Patienten wurde allerdings keine Synergie zwischen klassischer Chemotherapie und mTOR-Inhibition [231] und keine Korrelation zwischen mTOR-Inhibition und Gesamtüberleben [232] vorgefunden. Mechanistisch könnte dies durch eine kompensatorische Hochregulation anderer Signalwege bedingt sein, etwa verstärkter ERK1/2- und c-MYC-Aktivität [233]. Eine aberrante Expression von K_v1.3-Kanälen wurde bei Leukämien und malignen soliden Tumoren nachgewiesen und die Inhibition von K_v1.3-Kanälen wird derzeit als neue potente Therapiestrategie angesehen [234-239]. Die Bedeutung von K_v1.3-Kanälen als Zielstruktur für die Therapie akuter Leukämien wurde bisher nicht untersucht.

2 ZIELE, MATERIAL UND METHODEN

2.1 Ziele

Zu den weltweit führenden Ursachen für Morbidität gehören Demenzerkrankungen. Trotz intensiver Forschungstätigkeit besteht für die Therapie der Alzheimer Demenz weiterhin ein dringlicher Bedarf an effektiven Therapiestrategien. Die Mortalität in „entwickelten" Ländern wird neben kardiovaskulären Erkrankungen wesentlich durch Neoplasien bestimmt. Insbesondere für den wachsenden Anteil älterer Patienten sind hoch-intensive Chemotherapien jedoch oft intolerabel toxisch und neue, verträglichere und wirksamere Therapiestrategien sind erforderlich.

Die Beeinflussung des Immunsystems hat in den letzten Jahren herausragende Erfolge in der Therapie von Neoplasien erzielt. Immuntherapien befinden sich in einer hochaktiven Entwicklungsphase mit vielversprechendem Potential und könnten auch für die Therapie der Alzheimer Demenz interessant sein. Beispielsweise ist die Rolle von Lymphozyten und anderen Immunzellen bei der Pathogenese der Alzheimer Demenz unzureichend untersucht. Ionenkanäle sind für die Aktivierung und Funktion von T-Zellen von großer Bedeutung und damit potente therapeutische Zielstrukturen. Die Expression funktionaler NMDARen in Immunzellen wurde zwar mehrfach postuliert, ihre potentielle Funktion in Lymphozyten ist jedoch unzureichend geklärt. Unsere Patch-Clamp-Untersuchungen zeigten vielmehr, dass NMDAR-Antagonisten, inklusive Memantin, $K_v1.3$- und $K_{Ca}3.1$-Kaliumkanäle auf T-Zellen hemmen [108, 109]. $K_v1.3$-Kanäle sind zentrale Regulatoren des Membranpotentials, der Proliferation und des Zelltodes von T-Zellen und verschiedenen Tumorentitäten und daher hochinteressante pharmakologische Zielstrukturen. Obwohl Memantin als zugelassenes Medikament in der Therapie der Alzheimer Demenz seit Jahren eingesetzt wird, lagen zu den direkten Auswirkungen von Memantin auf humane T-Zellen *in vitro* und *in vivo* keine Untersuchungen vor. Im Rahmen der Dissertation sollten folgende Fragestellungen bearbeitet werden:

- **Welche Auswirkungen haben NMDAR-Antagonisten (Memantin, MK-801 und Ifenprodil) auf die Proliferation und Migration muriner und humaner T-Lymphozyten?**
- **Wirkt Memantin bei der Therapie von Alzheimer-Patienten auf periphere Blut-T-Lymphozyten?**
- **Beeinflusst die Inhibition von $K_v1.3$-Kanälen durch Memantin den Zelltod akuter Leukämiezellen?**

2.2 Material und Methoden

2.2.1 Verwendete Zellen

Die zellulären und molekularen Analysen zur Signalgebung, Proliferation, Migration und dem Zelltod erfolgten an:

(1) $CD3^+$ und $CD4^+$ T-Zellen aus der Milz oder den Lymphknoten von C57BL/6 Mäusen
(2) humanen $CD3^+$ bzw. $CD4^+$ T-Lymphozyten aus dem peripheren Blut gesunder Probanden und Patienten mit Alzheimer Demenz
(3) humanen lymphatischen und myeloischen akuten Leukämie-Zelllinien
(4) peripheren mononukleären Blutzellen und Knochenmarkzellen von Patienten mit akuter Leukämie (ALL, AML).

Für die Versuche mit murinen Lymphozyten wurden keine Tierversuchsgenehmigungen benötigt. Peripheres Blut von gesunden Spendern und Alzheimer-Patienten (Ethiknummer: MD133/13) sowie peripheres Blut und Knochenmarkzellen von Patienten mit akuter Leukämie (Ethiknumer: MD 115/08, MD 40/13) wurden nach schriftlichem Konsent der Patienten und in Übereinstimmung mit der "Deklaration von Helsinki" gewonnen und eingesetzt.

2.2.2 Methoden

Methodisch eingesetzt wurden: Zellisolation mittels MACS, *Multi-colour* Durchfluss-zytometrie, Western-Blot, quantitative PCR (qPCR), Migration im Transwell-System, Lumineszenzmessung mittels Photometer, [^{3}H]-Thymidin-Einbau und lentivirale Transduktion (**Abb.4a-c**). Einige methodische Besonderheiten werden zum besseren Verständnis der Versuche in den entsprechenden Ergebniskapiteln aufgeführt. Detaillierte Kultur- und Stimulationsbedingungen, Methoden und Materialien sind in den Abschnitten *Material and Methods* der jeweiligen Veröffentlichung angegeben.

3 ERGEBNISSE

3.1 Auswirkungen von NMDAR-Antagonisten auf die Funktion muriner T-Zellen

3.1.1 Proliferation muriner T-Zellen unter Einfluss von NMDAR-Antagonisten

Die Existenz funktionaler NMDARen in T-Lymphozyten wurde aufgrund des Nachweises von NMDAR-Untereinheiten auf mRNA-Ebene und der Wirkung von Glutamat und NMDAR-Antagonisten auf humane Lymphozyten-Effektorfunktionen postuliert. In unserem SFB854-Twin-Forschungsprojekt wurde mittels Patch-Clamp-Analysen und GluN1 (NMDAR) *knock-*

out Mäusen jedoch aufgedeckt, dass die Existenz funktionaler NMDARen in T-Zellen zumindest fragwürdig ist, und die NMDAR-Antagonisten Memantin, Ifenprodil und MK-801 in humanen und murinen T-Lymphozyten $K_v1.3$- und $K_{Ca}3.1$-Kaliumkanäle hemmen [108, 109]. Im Rahmen der Dissertation habe ich die Auswirkungen der NMDAR-Antagonisten auf die Alloantigen-induzierte Proliferation und Chemokin-induzierte Migration von Lymphozyten untersucht. Die dazu gewonnenen Daten sind in die Publikation P1 eingeflossen.

Zur Analyse der Proliferation muriner T-Lymphozyten unter Einwirkung von NMDAR-Antagonisten wurden $CD4^+$ T-Lymphozyten aus den Lymphknoten von C57/BL6 Mäusen isoliert, diese in MLRs durch bestrahlte (30 Gy) Splenozyten aus Balb/C Mäusen aktiviert und für 5 Tage in Anwesenheit der NMDAR-Antagonisten kultiviert. Die allogene T-Zellstimulation stellt im Vergleich zur CD3-Antikörper-basierten Stimulation einen physiologischeren Ansatz der T-Zellaktivierung dar. Die Proliferation wurde mittels [^{3}H]-Thymidineinbau bestimmt (**Abb.4a**). Zugabe von Memantin, MK-801 oder Ifenprodil führte zu einer dosisabhängigen Reduktion der allogenen Aktivierung und Proliferation muriner $CD4^+$ T-Zellen. Die IC_{50} für Memantin lag bei 5-10 µM und eine Proliferationsinhibition war ab 1 µM Memantin nachweisbar. Ifenprodil hemmte die Proliferation am effektivsten, mit einer IC_{50} von 1 µM (**P1, Abb.1D**).

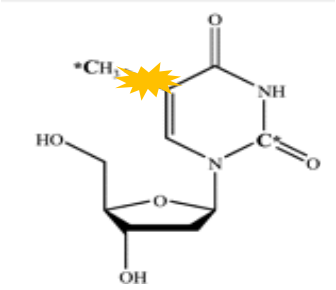

[^{3}H-Methyl]-Thymidin

Abb.4a: Messung der Proliferation von Lymphozyten *in vitro* mittels [^{3}H-Methyl]-Thymidin. Bei der [^{3}H]-Thymidin-Inkorporation wird der Zellkultur radioaktiv-markiertes [^{3}H-Methyl]-Thymidin) zugesetzt. Dieses wird nach Aufnahme von den Zellen durch die Thymidinkinase zu Thymidintriphosphat (TTP) phosphoryliert und während der S-Phase des Zellzyklus in die DNA eingebaut. Die eingebaute Radioaktivität kann mittels Szintillationszähler (Betastrahler) gemessen werden und ist proportional zur Zellteilung. *Abb. modifiziert nach: Bading et al. 1994.*

3.1.2 Migration muriner T-Zellen unter Einfluss von NMDAR-Antagonisten

Aktivierte Lymphozyten migrieren entlang Chemokingradienten, z.B. von SDF-1α und CCL21, vom peripheren Blut in die verschiedenen Gewebe, um dort ihre spezifische Funktion auszuüben. SDF-1α bindet an CXCR4-Rezeptoren und CCL21 an CCR7-Rezeptoren auf Lymphozyten. Die Chemokin-induzierte Migration muriner T-Zellen der Milz in An- und Abwesenheit des NMDAR-Antagonisten Ifenprodil wurde *in vitro* im Transwell-Migrationssystem bestimmt (**Abb.4b**). Ifenprodil (10 µM und 50 µM) hemmte die SDF-1α-induzierte Migration von $CD4^+$ und $CD8^+$ T-Lymphozyten dosisabhängig um 60-90%. Die CCL21-induzierte Migration der T-Zellen wurde durch Ifenprodil ebenfalls um 50-70% reduziert (**P1, Abb.4E**).

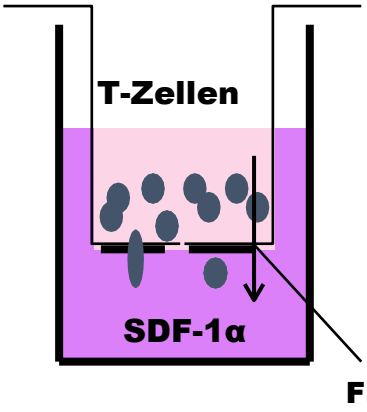

Abb.4b: Migration von T-Lymphozyten im Transwell-System. Nach Vorbehandlung mit Memantin oder Ifenprodil werden die T-Zellen im zuvor mit Fibronektin beschichteten Insert platziert. Durch dessen Poren (Durchmesser 3.0 µm) migrieren die Zellen bei 37°C in Richtung des Chemokins SDF-1α oder CCL21. Nach 150 min wird die Migration durch Zugabe von EDTA beendet. Die Zellzahl der migrierten Zellen im Medium wird mittels Durchflusszytometrie bestimmt. *Abb.: eigene Darstellung.*

Erwähnt sei in diesem Zusammenhang, dass auch die SDF-1α- und CCL21-induzierte Migration muriner B-Zellen im Transwell-Migrationssystem durch Ifenprodil (30 µM) um ~70% im Vergleich zu unbehandelten B-Zellen vermindert wurde ([240], Simma *et al*., 2014: Figure 4A).

- **NMDAR-Antagonisten inhibieren die Alloantigen-induzierte Proliferation muriner T-Lymphozyten sowie die SDF-1α- und CCL21-induzierte Migration muriner T- und B-Lymphozyten.**
- **Über die Hemmung der Proliferation und Migration könnten NMDAR-Antagonisten die adaptive Immunantwort wesentlich beeinflussen.**

3.2 Auswirkungen von Memantin auf humane T-Zellen

3.2.1 Wirkung von Memantin auf T-Zellen gesunder Spender

Zur Wirkung des NMDAR-Antagonisten Memantin auf humane T-Zellen *in vitro* oder *in vivo* lagen keine Veröffentlichungen vor. In Hinblick auf die berichteten infektiösen Komplikationen bei Memantin-behandelten Patienten und der möglichen Beteiligung von T-Zellen an der Immunpathogenese der Alzheimer Demenz war ein Schwerpunkt meiner Arbeit zu klären, inwieweit Memantin humane T-Lymphozyten beeinflusst. Die dazu gewonnenen Daten wurden in der Publikation P2 veröffentlicht.

Zunächst habe ich die Auswirkungen von Memantin auf die Proliferation $CD3^+$ T-Zellen aus dem peripheren Blut gesunder Probanden in MLRs mittels [^{3}H]-Thymidineinbau bestimmt. Memantin hemmte die Proliferation humaner T-Zellen auf allogene Stimuli von bestrahlten HLA-inkompatiblen Spenderzellen dosisabhängig und mit einer IC_{50} von ~20 µM (**P2, Abb.1A**, rechts). Auf Alloantigene reagieren in MLRs vorwiegend T_H1-Zellen, für deren Differenzierung der Transkriptionsfaktor T-bet maßgeblich ist [241, 242]. Intrazelluläre Färbungen für T-bet mittels Durchflusszytometrie zeigten, dass Memantin (20 µM und 50 µM) die Anzahl T-bet-positiver T-Zellen in den MLRs konzentrationsabhängig um 50-65%

reduziert. Dies weist auf eine supprimierte T-Zellaktivierung und T_H1-Bildung unter Memantingabe hin (**P2, Abb.1B**). Die Proliferation humaner T-Zellen nach Stimulation mit einem "starken" TCR-Stimulus durch CD3-Antikörper wurde durch Memantin ebenfalls gehemmt (IC_{50} ~40 µM) (**P2, Abb.1A**, links). Dagegen wurde die durch die Mitogene PMA/Ionomycin induzierte Proliferation humaner T-Zellen durch Memantin nur marginal reduziert (**P2, Abb.1A**, mittig). Somit scheint die inhibitorische Wirkung von Memantin auf die Proliferation mit der Dosis des Pharmakons und invers mit der „Stärke“ der T-Zellstimulation zu korrelieren. Gedächtnis-T-Zellen weisen eine niedrigere Aktivierungsschwelle auf als naive T-Zellen [43]. Es war daher interessant zu klären, ob Memantin die Proliferation spezifischer T-Zellsubpopulationen aus dem peripheren Blut gesunder Spender unterschiedlich beeinflusst. Memantin hemmte die Proliferation naiver $CD45RO^-$ $CD4^+$ T-Zellen sowie von $CD45RO^+$ $CD4^+$ Gedächtnis-T-Zellen. Letztere waren allerdings weniger sensitiv für Memantin, da sie erst bei einer Konzentration von 30-50 µM Memantin, naive $CD45RO^-$ $CD4^+$ T-Zellen dagegen bereits durch 1-10 µM Memantin signifikant gehemmt wurden (**P2, Abb.1C**). In Übereinstimmung mit den Ergebnissen zur Proliferation zeigte meine Kollegin Dr. T. Bose in Patch-Clamp-Analysen, dass zur Blockade von $K_v1.3$-Kanälen auf aktivierten $CD3^+$ T-Zellen und $CD45RO^+$ $CD4^+$ Gedächtnis-T-Zellen höhere Memantin-konzentrationen notwendig sind als zur Blockade von $K_v1.3$-Kanälen auf ruhenden $CD3^+$ T-Zellen und naiven $CD45RO^-$ $CD4^+$ T-Zellen [109, 202].

Analog zu murinen T-Zellen wurde die Migration humaner T-Zellen in Anwesenheit von SDF-1α und Memantin im Transwell-System untersucht. Bei Zugabe von 20 µM Memantin migrierten ca. 50% weniger $CD4^+$ und $CD8^+$ T-Zellen durch die Transwell-Membran in das SDF-1α-haltige Kulturmedium (**P2, Abb.3A**). Um auszuschließen, dass die verminderte Migration auf eine verringerte Adhäsion zurückzuführen ist, wurde der Migrationstest auch ohne Beschichtung der Transwell-Membran mit Fibronektin durchgeführt. Da vergleichbare Ergebnisse vorgefunden wurden, ist davon auszugehen, dass Memantin die Chemokin-induzierte Motilität humaner T-Zellen mindert (**P2, Abb.3B**).

- **Memantin reduziert die TCR-induzierte Proliferation naiver sowie aktivierter humaner $CD4^+$ T-Zellen und vermindert die SDF1α-induzierte Migration humaner T-Zellen *in vitro*.**

3.2.2 Reaktivität von T-Zellen Memantin-behandelter Alzheimer-Patienten

In den *in vitro* Analysen waren relativ hohe Memantin-Konzentrationen erforderlich, um die T-Zellaktivität zu blockieren. Die bei der Therapie der Alzheimer Demenz eingesetzte Standarddosierung von Memantin (10-20 mg/Tag) führt im *steady state* zu einer

Serumkonzentration von Memantin <1 µM [121]. Es stellte sich daher die Frage, ob die *in vitro* vorgefundenen inhibitorischen Effekte von Memantin auf humane T-Lymphozyten von klinischer Relevanz sind. Um diesen zentralen Punkt zu klären, habe ich die *ex vivo* T-Zellreaktivität von Alzheimer-Patienten analysiert, die mit Memantin in therapeutischer Standarddosierung behandelt wurden. Diese Versuche wurden in Kooperation mit PD Dr. S. Busse aus der Klinik für Psychiatrie und Psychotherapie der Medizinischen Fakultät Magdeburg durchgeführt. Schriftliches Einverständnis der Alzheimer-Patienten über Blutentnahmen zu Forschungszwecken und die Genehmigung durch die Ethikkommission lagen vor. Peripheres Blut der Alzheimer-Patienten wurde zu drei Zeitpunkten entnommen: zu Z1, nach Diagnosestellung und vor Memantin-Therapie; zu Z2, nach einer Woche Therapie mit 10 mg/Tag Memantin und zu Z3, nach weiteren 11 Wochen Therapie mit 20 mg/Tag Memantin, d.h. einer Gesamtbehandlungszeit von 12 Wochen (**P2, Abb.4A**).

Zu den Zeitpunkten Z1-Z3 wurden $CD4^+$ T-Zellen aus dem peripheren Blut der jeweils selben Alzheimer-Patienten isoliert und die T-Zell-Alloreaktivität auf PBMCs (periphere mononukleäre Blutzellen) eines jeweils gleichen gesunden Spenders in MLRs mittels [^{3}H]-Thymidineinbau bestimmt. Dadurch sollten mögliche individuelle Veränderungen in der Proliferationsfähigkeit der $CD4^+$ T-Zellen auf Alloantigene während der Memantin-Therapie aufgedeckt werden. Nach einer Woche Memantin-Behandlung proliferierten bei der Mehrzahl der untersuchten Patienten (10 von 13) die $CD4^+$ T-Zellen bereits signifikant schlechter im Vergleich zur Proliferationsaktivität vor Memantin-Gabe. Nach 12 Wochen Memantin-Therapie wurde nur noch ein Fünftel der initialen Proliferationswerte erreicht. Die $CD4^+$ T-Zellen von 3 Patienten zeigten ein anderes Verhalten, mit initial (nach 1 Woche) leicht gesteigerter und nach 12 Wochen wiederum reduzierter T-Zellproliferation. Die T-Zellproliferation aller getesteten Patienten zeigte nach 12 Wochen (Z3) eine Reduktion auf durchschnittlich 32% der Proliferationswerte vor Memantin-Behandlung (Z1) (**P2, Abb.4B**). Memantin-Behandlung der Alzheimer-Patienten induzierte somit eine ausgeprägte und über mehrere Wochen andauernde Proliferationshemmung der $CD4^+$ T-Zellen, die fortbestand, obwohl die $CD4^+$ T-Zellen *ex vivo* in Memantin-freiem Medium kultiviert wurden.

Weiterhin zeigte sich unter Therapie mit Memantin eine markante Veränderung in der Zusammensetzung der T-Zellpopulationen im Blut der Alzheimer-Patienten. Mittels Oberflächenfärbung und Durchflusszytometrie wurde eine Abnahme von $CD45RO^+$ $CD4^+$ Gedächtnis-T-Zellen im Blut nachgewiesen. Verglichen mit dem Zeitpunkt Z1 vor Memantin-Behandlung war der prozentuale Anteil $CD45RO^+$ $CD4^+$ Zellen zu Z2 um 22% und zu Z3 um 56% dezimiert, wobei der prozentuale Gesamtanteil von $CD4^+$ Zellen im Blut konstant blieb (**P2, Abb.4C**). Memantin scheint somit insbesondere auf Gedächtnis-T-Zellen zu wirken.

Wie durch meine Kollegin Dr. T. Bose gezeigt und zuvor erläutert, wird die Wirkung von Memantin auf humane T-Zellen höchstwahrscheinlich über die Hemmung von K_v1.3-Kanälen vermittelt. Daher wurde die Expression der K_v1.3-Kanäle unter Memantin-Behandlung mittels FACS-Färbung und Durchflusszytometrie bestimmt. Sowohl naive CD45RO$^-$ CD4$^+$ als auch CD45RO$^+$ CD4$^+$ Gedächtnis-T-Zellen der Alzheimer-Patienten wiesen bei Memantingabe eine gesteigerte Expression von K_v1.3-Kanälen auf. Die relative K_v1.3-Oberflächenexpression auf CD45RO$^-$ und CD45RO$^+$ CD4$^+$ T-Zellen war zu Z2 um 60% bzw. 55% und zu Z3 um 29% und 18% erhöht (**P2, Abb.5B**). Dies könnte eine kompensatorische Hochregulation der K_v1.3-Kanäle als Toleranzmechanismus bei pharmakologischer Hemmung darstellen. Die erhöhte Expression von K_v1.3-Kanälen korrelierte mit verminderten K_v1.3-Kanalströmen zum Zeitpunkt Z2 nach 1 Woche Memantin-Behandlung, während die K_v1.3-Ströme zum Zeitpunkt Z3 nach 12 Wochen vergleichbar mit denen zu Z1 vor Memantin-Behandlung waren (Patch-Clamp-Daten meiner Kollegin Dr. T. Bose) [109, 202]. Es ist zu betonen, dass trotz einer „Normalisierung" der K_v1.3-Kanalexpression und des K_v1.3-Stromes zum Zeitpunkt Z3 auf Werte vor Memantin-Behandlung (Z1), die T-Zellreaktiviät auf allogene Stimulation zu Z3 dennoch gestört war. Somit scheint eine „transiente" Hemmung von K_v1.3-Kanälen durch Memantin eine länger andauernde Verminderung der T-Zell-Reaktivität hervorrufen zu können.

- **Therapeutische Memantingabe bei Alzheimer-Patienten führt zu einer Hemmung von K_v1.3-Kanälen auf CD4$^+$ T-Lymphozyten, vermindert deren *ex vivo* Reaktivität auf allogene Stimuli und führt zu einer Abnahme CD45RO$^+$ CD4$^+$ Gedächtnis-T-Zellen im peripheren Blut.**

3.3 K_v1.3-Kanal-Inaktivierung als neue Therapieoption für akute Leukämien

3.3.1 Genetische und pharmakologische K_v1.3-Kanal-Inaktivierung in T-ALL-Zellen

Abnorm gesteigerte Proliferation und aberrante Migration sind Merkmale neoplastischer Zellen. In Hinblick auf die suppressive Wirkung von Memantin auf die Proliferation und Migration humaner T-Zellen und der signifikanten Reaktivitätshemmung von CD4$^+$ T-Zellen Memantin-behandelter Patienten, habe ich im zweiten Schwerpunkt meiner Dissertationsarbeit untersucht, inwiefern eine Hemmung von K_v1.3-Kanälen durch Memantin für die Behandlung akuter Leukämien von Bedeutung sein könnte (Publikation P3).

Die im Folgenden dargestellten Untersuchungen wurden mit der akuten T-Zell-Leukämie-Zelllinie Jurkat (JE6-1) durchgeführt. Die Expression von K_v1.3-Kanälen auf Jurkat-Zellen wurde mehrfach beschrieben [156, 243] und mit K_v1.3-Antikörperfärbung und

Durchflusszytometrie von mir bestätigt (**P3, Abb.S1a**). In Zusammenarbeit mit Prof. T. Fischer und Prof. F. Heidel (Klinik für Hämatologie und Onkologie der Medizinischen Fakultät Magdeburg) wurde K_v1.3 mRNA in Jurkat-Zellen mittels RNA-Interferenz durch lentivirale Transduktion herunterreguliert, um die Bedeutung von K_v1.3-Kanälen für Jurkat-Zellen zu untersuchen. Die Selektion virus-infizierter Jurkat-Zellen erfolgte über Puromycin-Resistenz. Von fünf getesteten K_v1.3 shRNAs (*small hairpin* Ribonukleinsäure) wurden zwei shRNAs mit der höchsten Effizienz des K_v1.3 *knock-down* für die weiteren Versuche eingesetzt. Die Effizienz der lentiviralen Transduktion betrug ca. 85% und resultierte in einer 40-50%igen Reduktion der K_v1.3 mRNA im Vergleich zu Kontrollinfektionen mit *scrambled* shRNA (scr-shRNA) (**P3, Abb.S1b**). Der Zelltod der Jurkat-Zellen wurde mit Propidiumjodid (PI)- oder SYTOX-Färbung bestimmt (**Abb.4c**). An Tag 7 nach Infektion betrug der Anteil SYTOX-positiver toter Zellen 90%, während die scr-shRNA Kontrollzellen zu mehr als 90% vital blieben (**P3, Abb.1d**).

Methode	Messinstrument	Prinzip	Darstellung avitaler Zellen
FSC/SSC	Durchflusszytometrie	Größe und Granularität	klein, z.T. erhöhte Granularität
SYTOX ® Blue	Durchflusszytometrie	Aufnahme durch Zellen mit defekter Zellmembran und Bindung an Nukleinsäuren	avitale Zellen SYTOX®-positiv
Propidium-jodid (PI)	Durchflusszytometrie	Aufnahme durch Zellen mit defekter Zellmembran und Bindung an Nukleinsäuren	avitale Zellen PI-positiv
Annexin V-FITC	Durchflusszytometrie	Bindung an externalisiertes Phosphatidylserin	früh-apoptotische Zellen positiv für Annexin V-Fluoreszenz
Zytochrom C (CytC)	Durchflusszytometrie	Bindung eines fluoreszenz-markierten monoklonalen CytC-Antikörpers an mitochondriales CytC	apoptotische Zellen mit intrinsischem Apoptoseweg zeigen niedrige CytC-Fluoreszenz
Caspasen	Western-Blot	Nachweis fragmentierter aktivierter Caspasen	apoptotische Zelle über intrinsischen/extrinsischen/terminalen Weg: Fragmentierung von Caspase-9/ Caspase-8/Caspase-3

Abb.4c: Verwendete Methoden zur Bestimmung des Zelltodes von T-Lymphozyten. Die Tabelle gibt einen Überblick über die in der Arbeit verwendeten *in vitro* Methoden zur Bestimmung des Zelltodes.

Cytarabin (AraC) ist ein sehr wirksames und häufig eingesetztes Zytostatikum bei der Behandlung akuter Leukämien. Es wurde daher getestet, welchen Einfluss eine zusätzliche AraC-Exposition auf die K_v1.3-shRNA-infizierten Jurkat-Zellen hat. Die Gabe von 20 nM AraC 48 Stunden nach lentiviraler shRNA-Infektion steigerte den Zelltod der Jurkat-Zellen an Tag 5 von 70-80% auf über 95% (**P3, Abb.2c**). Diese Daten unterstreichen die Bedeutsamkeit von K_v1.3-Kanälen für das Überleben neoplastischer T-Lymphozyten und weisen darauf hin, dass K_v1.3-Kanal-Inaktivierung in Kombination mit Chemotherapie die Todesrate akut leukämischer Zellen steigern könnte.

Für die klinische Anwendung ist nur eine pharmakologische K_v1.3-Kanal-Inaktivierung zweckmäßig. Zur spezifischen Hemmung von K_v1.3-Kanälen wurden zahlreiche Pharmaka entwickelt und getestet [193, 194, 244]. Jedoch sind bisher keine spezifischen K_v1.3-Inhibitoren klinisch zugelassen. Wie in Patch-Clamp-Analysen von Dr. Bose gezeigt, blockiert Memantin K_v1.3-Kanäle auf Jurkat-Zellen [109, 202]. Da Memantin auch von älteren Patienten gut vertragen wird [74] und wie von uns gezeigt in der Standarddosierung eine T-Zell-Hemmung *in vivo* hervorruft [202], wurde die Wirkung von Memantin auf Jurkat-Zellen detaillierter untersucht. FSC/SSC (*forward scatter/side scatter*)-Profile und PI-Färbungen in der Durchflusszytometrie zeigten, dass Memantin allein in Konzentrationen >200 µM in Jurkat-Zellen Zelltod induziert (**P3, Abb.1c**). Somit könnte Memantin zur pharmakologischen Blockade von K_v1.3-Kanälen auf neoplastischen T-Lymphozyten geeignet sein.

- **Partieller *knock-down* von K_v1.3 mRNA führt zum Zelltod von Jurkat-Zellen.**
- **Memantin in hohen Konzentrationen (> 200 µM) induziert Zelltod in Jurkat-Zellen.**

3.3.2 Kombinationsbehandlung von Jurkat-Zellen mit Memantin und AraC

Für die weiteren Analysen wurde Memantin zur pharmakologischen Blockade von K_v1.3-Kanälen eingesetzt und mit AraC kombiniert. Diese Versuche sollten klären, ob und wie Memantin den zytotoxischen Effekt von AraC verstärkt. Dabei wurde Memantin meistens in einer Konzentration von 100 µM eingesetzt, da diese Konzentration allein keinen relevanten Effekt auf den Zelltod von Jurkat-Zellen hatte und inhibitorische Wirkungen von Memantin in dieser Konzentration voll abgedeckt sein sollten. Jurkat-Zellen blieben jeweils unbehandelt, wurden mit AraC allein, mit Memantin allein oder mit AraC plus Memantin kultiviert.

Als Maß für die Vitalität der Jurkat-Zellen nach Behandlung mit Memantin und AraC für 72 h wurde der zelluläre ATP-Gehalt mittels Cell Titer Glo Assay® bestimmt. AraC (30 nM) allein reduzierte den ATP-Gehalt in Jurkat-Zellen um ~50%, während Memantin allein den ATP-Gehalt erst bei einer Konzentration von 200 µM verringerte. Kombination von AraC mit Memantin (50/100/200 µM) führte dosisabhängig zu einer weiteren Reduktion des ATP-Gehalts um 13-67% im Vergleich zu alleiniger AraC-Behandlung (**P3, Abb.2d**), so dass eine Kobehandlung mit Memantin die Vitalität der Jurkat-Zellen deutlich reduziert. Memantin allein zeigte keinen Einfluss auf die Proliferation der Jurkat-Zellen. In Kombination verstärkte Memantin jedoch die AraC-induzierte proliferative Inhibition um das 3-fache (**P3, Abb.2e**) und arretierte den Zellzyklus in der S-Phase im Vergleich zu alleiniger AraC-Behandlung (**Abb.5a**).

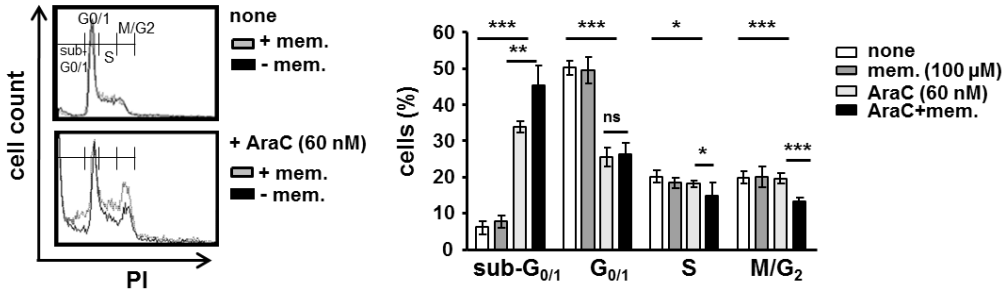

Abb.5a: Memantin/AraC-Behandlung von Jurkat-Zellen führt zu Zellzyklusarrest. Jurkat-Zellen wurden mit den angegebenen Konzentrationen von Memantin und AraC behandelt und der Zellzyklus nach 72 h mittels PI-Färbung und Durchflusszytometrie analysiert (links ist ein repräsentatives Histogramm gezeigt). Der Graph zeigt den Prozentsatz von Zellen in den Zellzyklusphasen sub-$G_{o/1}$, $G_{o/1}$, S und M/G_2 von n=5 Experimenten mit Mittelwert +/- SD. Signifikanzen wurden mittels Student's *t*-Test bestimmt; p*<0.05, p**< 0.01, p***<0.001.

Hinsichtlich der Induktion von Zelltod in Jurkat-Zellen bei Memantin/AraC-Behandlung wurde AraC (20-100 nM) und Memantin (25, 50, 100 µM) titriert. Bei AraC-Konzentrationen von 40-60 nM war die Zunahme des Zelltodes durch Memantin am größten (**P3, Abb.2a**). Versuche zum Zelltod mit konstanten Pharmaka-Verhältnissen (*constant drug ratio*) und Bestimmung des *combination index* (CI) und *dose reduction index* (DRI) mit der Chou-Talalay-Methode [245] zeigten bei Memantin/AraC-Kombination additive (CI=1) bis synergistische (CI<1) Effekte auf den Zelltod von Jurkat-Zellen. Der DRI von AraC bei Zugabe von Memantin für Jurkat-Zellen war >1 ab einer affektierten Fraktion (F_a) von 0.1. Bei der für die Therapie von Neoplasien relevant erachteten F_a von 0.97 betrug der DRI von AraC 2.4, d.h. dass bei 97% abgetöteter Zellen die Dosis von AraC um das 2,4-fache gegenüber alleiniger AraC-Behandlung reduziert werden kann (**P3, Abb.2b**).

- **Memantin verstärkt die AraC-induzierte Proliferationshemmung und steigert synergistisch den AraC-induzierten Zelltod in Jurkat-Zellen.**

3.3.3 Signalgebung in Memantin/AraC-behandelten Jurkat-Zellen

Die PI-3K-AKT-mTOR- und ERK1/2-Signalwege sind in akuten Leukämien oftmals überaktiviert und vermitteln einen aggressiven Phänotyp und Therapieresistenz [213-217]. Beide Signalwege sind daher wichtige therapeutische Zielstrukturen [219-221]. Allerdings wird zunehmend ersichtlich, dass aufgrund kompensatorischer Verstärkung anderer Signalwege bei Hemmung einzelner Signalproteine oder Signalkaskaden mehrere Signalwege gleichzeitig gehemmt werden müssen, um eine effektive Proliferationshemmung oder klinisch relevanten Zelltod zu erreichen.

Mittels Western-Blot wurde die Wirkung der Memantin/AraC-Koapplikation auf die Signalgebung in Jurkat-Zellen bestimmt. Im Vergleich zu alleiniger AraC-Gabe führte Memantin/AraC-Kombinationsbehandlung zu einer verstärkten Reduktion von pAKT, pS6 sowie von pERK1/2 und c-MYC, einem gemeinsamen Zielprotein von AKT und ERK1/2 (**P3, Abb.3**). Die Expression von pJNK (c-Jun-N-terminale Kinase) und dem Transkriptionsfaktor c-Jun wurde durch Memantin dagegen nicht beeinflusst.

- **Memantin-Koapplikation verstärkt die Inhibition der AKT-mTOR-S6 und ERK1/2-c-MYC-Signalgebung in AraC-behandelten Jurkat-Zellen.**

3.3.4 Zelltodmechanismen in Memantin/AraC-behandelten Jurkat-Zellen

Weiterführend wurde untersucht, ob die Förderung des Zelltodes in Jurkat-Zellen durch Memantin über den extrinsischen (Caspase-8-abhängigen) oder intrinsischen mitochondrialen (CytC- und Caspase-9-vermittelten) Apoptoseweg verläuft. In Western Blot-Analysen zeigten weder AraC noch Memantin oder die Kombination beider Pharmaka einen Einfluss auf die Aktivierung der Caspase-8 (**P3, Abb.S2a**), in Einklang mit der Literatur über den AraC-vermittelten Zelltod [246]. Caspase-8-defiziente Jurkat-Zellen wiesen zudem eine vergleichbare Steigerung des AraC-induzierten Zelltods durch Memantin auf wie rekonstitutierte Caspase-8-haltige Kontrollzellen (**P3, Abb.S2b**).

Beim intrinsischen Apoptoseweg transloziert das pro-apoptotische Protein Bax zur äußeren mitochondrialen Membran (OMM), hemmt die mitoK_v1.3-Kanäle und bewirkt die Freisetzung von CytC ins Zytoplasma. Der CytC-Gehalt in T-Zellen kann mittels fluorochrommarkierten CytC-spezifischen Antikörpern und Durchflusszytometrie quantitativ bestimmt werden [247]. Zellen, die dem intrinsischen Zelltod unterliegen, weisen eine geringere CytC-spezifische Fluoreszenz ($CytC^{low}$) auf. Memantin erhöhte den prozentualen Anteil an $CytC^{low}$ Jurkat-Zellen um das 1,9-fache im Vergleich zur alleinigen AraC-Behandlung (**P3, Abb.4a**). Die Expression aktiver Caspase-9, die durch mitochondriale CytC-Freisetzung aktiviert wird, war bei Memantin/AraC-Kobehandlung um das 1,6-fache gesteigert (**P3, Abb.4b links**) und die Expression aktiver Effektor-Caspase-3 um das 4-fache (**P3, Abb.4b rechts**). Konsistent mit diesen Ergebnissen war in Caspase-9-defizienten Jurkat-Zellen, im Gegensatz zu Caspase-9-rekonstituierten Kontrollzellen, keine Steigerung des AraC-induzierten Zelltods durch Memantin nachweisbar (**P3, Abb.4c**).

- **Memantin fördert die CytC-Freisetzung und Aktivierung von Caspase-9 und Caspase-3 in AraC-behandelten Jurkat-Zellen, d.h. steigert die intrinsische Apoptose.**

Eine zusammenfasende schematische Darstellung der durch Memantin/AraC-Behandlung beeinflussten Signalproteine in Jurkat-Zellen ist in **Abb.6** im Diskussionsteil gezeigt.

3.3.5 Kombinationsbehandlung von AML-Zelllinien mit Memantin und AraC

Etwa 80% der akuten Leukämien im Erwachsenenalter sind myeloischen Ursprungs. Es sollte daher geklärt werden, ob eine Memantin/AraC-Kombinationsbehandlung auch bei AML-Zelllinien zu verstärktem Zelltod führt. Dahingehend wurden die AML-Zelllinien OCI-AML-3 (NPM-1 (Nukleophosmin-1)-mutiert), Molm-13 (FLT-3-ITD-positiv (*fms like tyrosine kinase 3 internal tandem duplication*)) und HL-60 untersucht. In den AML-Zelllinien induzierte Memantin erst in hohen Dosen Zelltod (**Abb.5b**), steigerte jedoch dosisabhängig bei Konzentrationen von 25-100 µM den AraC-induzierten Zelltod (**P3, Abb.5b**).

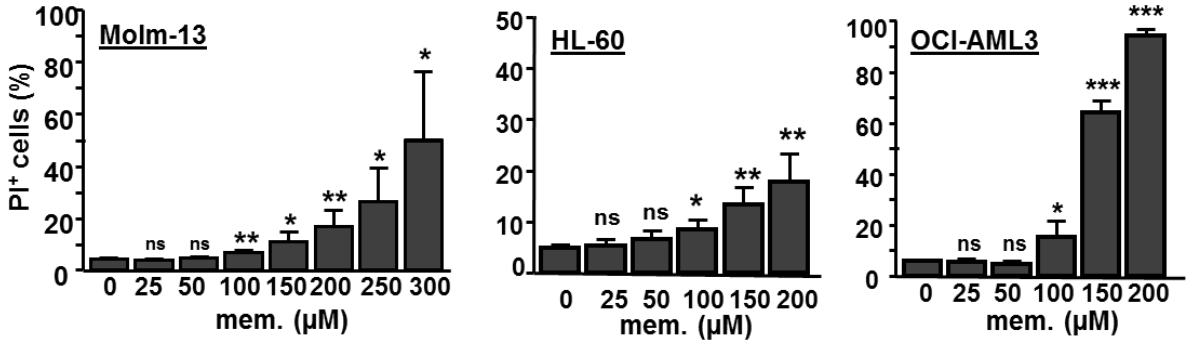

Abb.5b: Memantin in hohen Konzentrationen induziert Zelltod in AML-Zelllinien. Molm-13-, HL-60- und OCI-AML3-Zellen wurden 72 h mit Memantin kultiviert und der Zelltod mittels PI-Färbung bestimmt. Die Graphen zeigen den Prozentsatz PI^+ toter Zellen von n=5 Experimenten mit Mittelwert + SD. Signifikanzen wurden mittels Student´s *t*-Test bestimmt; p*<0.05, p**< 0.01, p***<0.001.

Chou-Talalay-Analysen von Experimenten mit konstanten Pharmaka-Verhältnissen zeigten synergistische Effekte der Memantin/AraC-Behandlung (CI-Werte von 0.46-0.97) für die drei AML-Zelllinien. DRI-Werte für AraC bei Memantin-Zugabe lagen bei 5.4 für OCI-AML3, 1.8 für Molm-13 und 7.7 für HL-60. Dies zeigt, dass durch Zugabe von Memantin die Dosis von AraC deutlich reduziert werden kann, um vergleichbar hohen Zelltod wie bei alleiniger AraC-Behandlung zu erreichen (**P3, Abb.S3c**). In den Zelllinien erhöhte Memantin auch den Anteil von $CytC^{low}$ Zellen um das 2-2.5-fache im Vergleich zur alleinigen AraC-Behandlung (**P3, Abb.5c**).

- **Memantin verstärkt die AraC-induzierte CytC-Freisetzung und damit den intrinsischen Apoptoseweg in Molm-13-, OCI-AML-3- und HL-60-Zellen.**
- **Memantin+AraC wirken synergistisch bei der Induktion des Zelltodes in den drei AML-Zelllinen.**

3.3.6 Wirkung von Memantin/AraC auf den Zelltod primärer Blasten von ALL- und AML-Patienten

Die Ergebnisse von den Analysen der akut leukämischen Zelllinien ließen vermuten, dass eine Memantin/AraC-Kombinationstherapie für Patienten mit akuter lymphatischer oder akuter myeloischer Leukämie unterschiedlichen genetischen Risikoprofils geeignet sein könnte. Um eine potentielle klinische Bedeutung einer Memantin/AraC-Kombinationstherapie zu bekräftigen, wurden primäre leukämische Blasten von Patienten mit ALL und AML hinsichtlich eines gesteigerten Zelltodes bei Memantin/AraC-Behandlung untersucht. Primäre ALL-Blasten (1 Patient) und AML-Blasten (6 Patienten) aus dem peripheren Blut oder Knochenmark waren im Gegensatz zu den ALL- und AML-Zelllinien sensitiver für Memantin, da alleinige Memantin-Behandlung bereits Zelltod induzierte (**Abb.5c**).

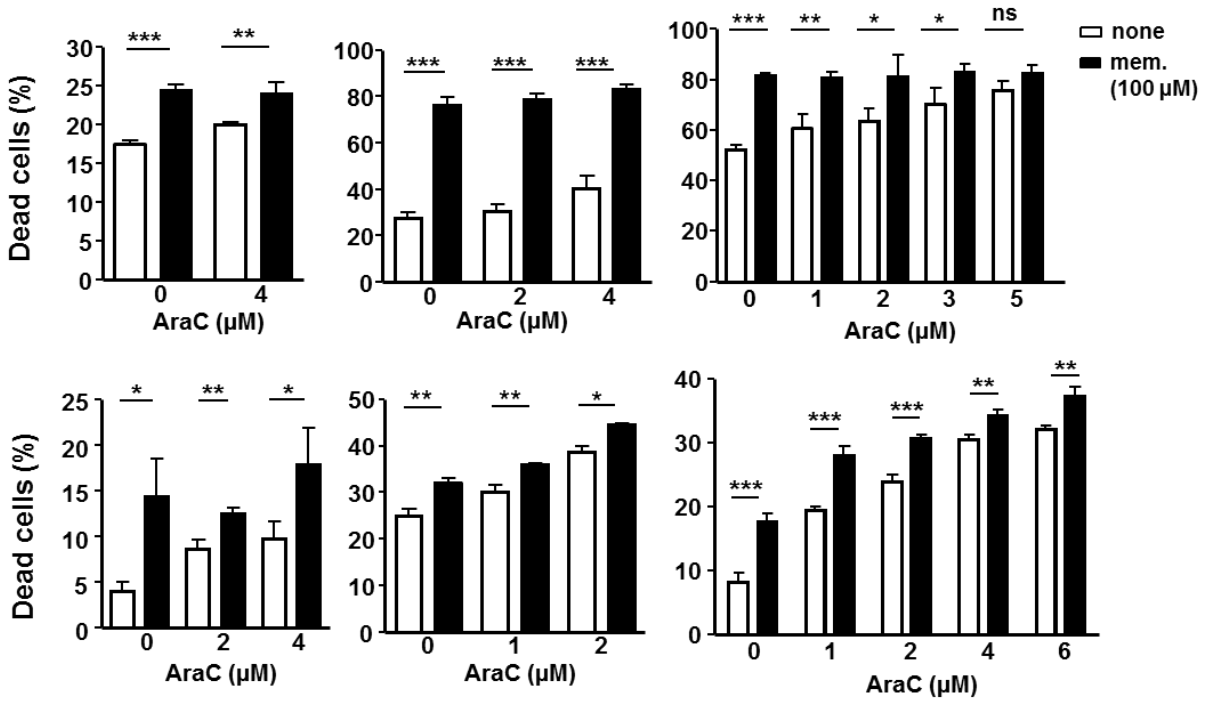

Abb.5c: Memantin steigert den AraC-induzierten Zelltod primärer AML-Blasten. PBMCs bzw. Knochenmarkzellen von 6 AML-Patienten wurden mit Memantin und AraC behandelt und der Zelltod nach 72 h mittels PI-Färbung bestimmt. Die Graphen zeigen den Prozentsatz PI^+ toter Zellen aus Triplett-Ansätzen mit Mittelwert + SD. Signifikanzen wurden mittels Student´s *t*-Test bestimmt; p*<0.05, p**< 0.01, p***<0.001.

Da primäre Blasten *ex vivo*, ungleich der Zelllinien, bereits nach kurzer Kulturzeit auch ohne AraC sterben, ist zu vermuten, dass Wachstumsfaktorentzug und Mangel anderer überlebensfördernder Signale einen initialen Apoptose-auslösenden Faktor darstellen, der durch Memantin sodann verstärkt wird. In allen untersuchten Patienten-Proben steigerte Memantin zudem den AraC-induzierten Zelltod (**P3,** T-ALL: **Abb.2g**; AML: **Abb.5c**). Analysen von Knochenmark-Blasten von 10 weiteren AML-Patienten durch Dr. S.C.

Nimmagadda und Prof. U. Bommhardt bestätigten, dass Memantin den AraC-induzierten Zelltod in primären AML-Blasten signifikant erhöht ([248], Figure 6b/c). In primären (nicht-neoplastischen) humanen T-Zellen führte Memantin (100 µM) sowohl bei alleiniger Exposition als auch in Kombination mit AraC zu keiner Steigerung des Zelltodes (**P3, Abb.2h**). Memantin/AraC-Kombinationsbehandlung scheint daher präferentiell auf neoplastische Zellen zu wirken und geringe Toxizität auf "normale" T-Zellen zu haben.

- **Memantin fördert synergistisch mit AraC den Zelltod primärer akut leukämischer Blasten.**
- **Kombination des klassischen Zytostatikum AraC mit dem K_v1.3-Kanal-Blocker Memantin könnte eine neue Therapieoption für ALL- und AML-Patienten darstellen.**

4 DISKUSSION UND AUSBLICK

Memantin wird als neuronaler NMDAR-Antagonist in der Therapie der Alzheimer Demenz langjährig klinisch eingesetzt und ist auch für ältere Patienten und in höheren Dosen gut verträglich. In der Arbeitsgruppe wurde zuvor nachgewiesen, dass Memantin in Lymphozyten K_v1.3-Kalium-Kanäle hemmt. In dieser Arbeit wurden fortführend die Auswirkungen von Memantin auf Lymphozytenfunktionen *in vitro* und *in vivo* untersucht. Memantin supprimierte die Alloantigen-induzierte Proliferation und Chemokin-induzierte Migration humaner und muriner T-Lymphozyten *in vitro*. Die Proliferationsinhibition durch Memantin war dabei invers mit der „Stärke“ der T-Zellstimulation korreliert (**P2, Abb.1A**), in Übereinstimmung mit K_v1.3-Kanal-Blockade durch spezifische K_v1.3-Blocker [249]. Im Vergleich zu murinen T-Lymphozyten (IC_{50}: 5-10 µM) waren zur Proliferationshemmung humaner T-Zellen (IC_{50}: ~20 µM) etwa doppelt so hohe Memantinkonzentrationen erforderlich (**P1, Abb.1D** und **P2, Abb.1A,** rechts). Dies könnte durch die höhere Expression von K_v1.3-Kanälen auf ruhenden humanen T-Zellen im Vergleich zu murinen T-Zellen [24] bedingt sein. Da Memantin auch die Proliferation von B-Lymphozyten inhibierte ([240], Daten hier nicht gezeigt) könnte Memantin die adaptive Immunanwort grundlegend beeinflussen.

Ausgehend von den *in vitro* erhobenen Daten mit relativ hohen Memantin-Konzentrationen stellte sich die Frage, ob Memantin Lymphozyten *in vivo* beeinflusst und somit für immunologische Prozesse von klinischer Bedeutung ist. Die Untersuchungen an Alzheimer-Patienten deckten auf, dass T-Zellen von Alzheimer-Patienten bei Memantin-Behandlung *ex vivo* eine reduzierte Proliferation gegenüber Alloantigenen aufweisen (**P2, Abb.4B**) und

bestätigen somit die klinische Relevanz einer T-Zell-Funktionshemmung durch Memantin. T-Zellen einzelner Alzheimer-Patienten (3 von 13) zeigten eine initial (Z2, nach 1 Woche Memantin-Behandlung) gesteigerte und erst nach längerer Behandlung (Z3, 12 Wochen) eine reduzierte Proliferationsrate (**P2, Abb.4B**, rechts). Dafür können Patienten-individuelle Faktoren, wie Komedikation und pharmakokinetische Faktoren sowie ggf. unregelmäßige Medikamenteneinnahme, ursächlich sein. Auffällig war weiterhin, dass die Alzheimer-Patienten nach Memantin-Behandlung eine Reduktion von $CD45RO^+$ $CD4^+$ Gedächtnis-T-Zellen im peripheren Blut aufwiesen (**P2, Abb.4C**). Die *in vitro* Proliferation $CD4^+$ Gedächtnis-T-Zellen gesunder Spender war im Vergleich zu naiven T-Zellen durch Memantin allerdings weniger supprimiert (**P2, Abb.1C**). Daher ist zu vermuten, dass die Abnahme $CD45RO^+$ $CD4^+$ Gedächtnis-T-Zellen im peripheren Blut der Alzheimer-Patienten unter Memantin-Behandlung auf eine verminderte Migration ins Blut bzw. Zirkulation im Blut zurückzuführen ist. Dies wäre in Einklang mit der nachgewiesen reduzierten *in vitro* Migration humaner T-Zellen gesunder Spender bei Memantin-Exposition (**P2, Abb.3A/B**) und ist möglicherweise durch die Assoziation von $K_v1.3$-Kanälen mit ß1-Integrinen bedingt [250]. Da in der Immunpathogenese der Alzheimer Demenz ein pathologisch erhöhter Anteil von Gedächtnis-T-Zellen im Blut beschrieben wurde [148, 251], könnte Memantin insbesondere $CD45RO^+$ $CD4^+$ Gedächtnis-T-Zellen modulieren und diese „Abweichung" korrigieren. Die vorliegenden *in vitro* und *ex vivo* Daten zur Inhibition der T- und B-Zellfunktion durch Memantin könnten auch zu den beobachteten infektiösen Komplikationen unter Memantin-Behandlung beitragen und weisen auf einen möglichen therapeutischen Benefit von Memantin im Rahmen der Immunpathogenese der Alzheimer Demenz hin. Daher sollte die Rolle von T-Zellen und B-Zellen bei der Neuroinflammation der Alzheimer Demenz zukünftig intensiver untersucht werden, etwa hinsichtlich der Aß-spezifischen T-Zellantwort und Zytokinexpressionsmustern. In Mausmodellen der Alzheimer Demenz wäre interessant zu klären, ob Memantin die beschriebenen abnormen T_H1- und Gedächtnis-T-Zellfunktionen sowie die Migration der Lymphozyten verändert. Zudem sollten die Auswirkungen von Memantin auf die Mikroglia, Endothelzellen und andere an der Neuroinflammation der Alzheimer Demenz beteiligten Zellen in Betracht gezogen werden.

Memantin in Standarddosierung (20 mg/Tag) zur Behandlung der Alzheimer Demenz liegt im *steady state in vivo* in Konzentrationen von <1 µM vor. Effektive Memantin-Konzentrationen *in vitro* liegen mit 10-50 µM wesentlich höher. Dies lässt vermuten, dass bei Memantin-Applikation *in vivo* weitere Aspekte relevant werden. Zu diesen gehören die Interaktion von T-Lymphozyten mit anderen Immunzellen, eine höhere Zelldichte, pharmakokinetische Parameter, wie transient hohe Spitzenkonzentrationen und Halbwertszeit, sowie die tägliche repetitive Gabe von Memantin, zumal *in vitro* Memantin nur einmal zu Beginn der

Zellkulturen zugesetzt wurde. In diesem Zusammenhang wäre auch die Bestimmung der K_v1.3-Expression und K_v1.3-Kanalströme zu weiteren Zeitpunkten der Memantin-Behandlung interessant, um zu klären, wie schnell und wie lange eine K_v1.3-Kanal-Inhibition vorliegt. Es müsste auch geklärt werden, wie lange die beoabachte reduzierte T-Zellreaktivität nach Absetzen von Memantin vorliegt.

Die vorliegenden Resultate sprechen dafür, dass Memantin als K_v1.3-Kanal-Blocker für neue therapeutische Ansätze zur Beeinflussung der Immunantwort von Interesse ist. Da Memantin die Alloreaktivität von T-Lymphoyzten supprimiert, könnte es ein vielversprechendes Therapeutikum bei der Therapie von Autoimmunerkrankungen, Transplantatabstoßungs-reaktionen oder der GvHD sein. K_v1.3-Kanäle regulieren die Proliferation und den Zelltod von Lymphozyten [23, 24, 180] und eine aberrante Expression von K_v1.3-Kanälen wurde in Leukämien und malignen soliden Tumoren nachgewiesen [179, 234, 236-239]. Es wurde daher fortführend untersucht, ob K_v1.3-Blockade mittels Memantin für Leukämietherapien von Interesse sein könnte, zumal kein Pharmakon zur spezifischen K_v1.3-Kanal-Blockade klinisch zugelassen ist. Meine Analysen bestätigen, dass das Überleben neoplastischer T-Zellen stark von K_v1.3-Kanälen abhängt und zeigen erstmals, dass pharmakologische K_v1.3-Kanal-Blockade mit Memantin den AraC-induzierten Zelltod von ALL- sowie AML-Zellen verstärkt. Insbesondere für betagte oder multimorbide Patienten mit akuter Leukämie werden dringlich adäquate Therapien benötigt. Die effektivere Zelltodinduktion durch die Kombination von AraC mit Memantin eröffnet daher eine interessante alternative Option zur palliativen Therapie akuter Leukämien.

Obgleich Memantin (100 µM) allein den Zelltod von Jurkat-Zellen kaum beeinflusste, steigerte es synergistisch den AraC-induzierten Zelltod und verstärkte signifikant die AraC-induzierte Proliferationshemmung. Dies deutet daraufhin, dass AraC als initialer apoptotischer Stimulus wirkt und die Translokation von Bax zum mitoK_v1.3-Kanal auslöst [180, 182]. Memantin verstärkt sodann durch Inhibition der mitoK_v1.3-Kanäle die mitochondriale CytC-Freisetzung und konsekutive Aktivierung von Caspase-9 und Caspase-3, was durch die vorliegenden Daten unterstützt wird (**P3, Abb.4k**). Diese Hypothese setzt voraus, dass Memantin in die Zelle eindringen kann, wozu bisher jedoch keine Publikationen vorliegen. Molekulare Untersuchungen zum synergistischen Effekt von Memantin und AraC zeigten eine verstärkte Blockade der AKT/mTOR/S6- sowie ERK1/2/c-MYC-Signalwege in Jurkat-Zellen. Die gleichzeitige Hemmung zweier zentraler Signalwege für Wachstum und Proliferation bei Memantin-Koappliaktion ist bedeutsam, weil die beschriebene kompensatorische Hochregulation von ERK1/2 bei alleiniger Hemmung des AKT-Signalwegs und eine dadurch hervorgerufene Resistenzentwicklung unterbunden werden könnte [229,

252, 253]. In **Abb.6** sind die untersuchten und durch Memantin beeinflussten Signalmoleküle/wege schematisch zusammengefasst.

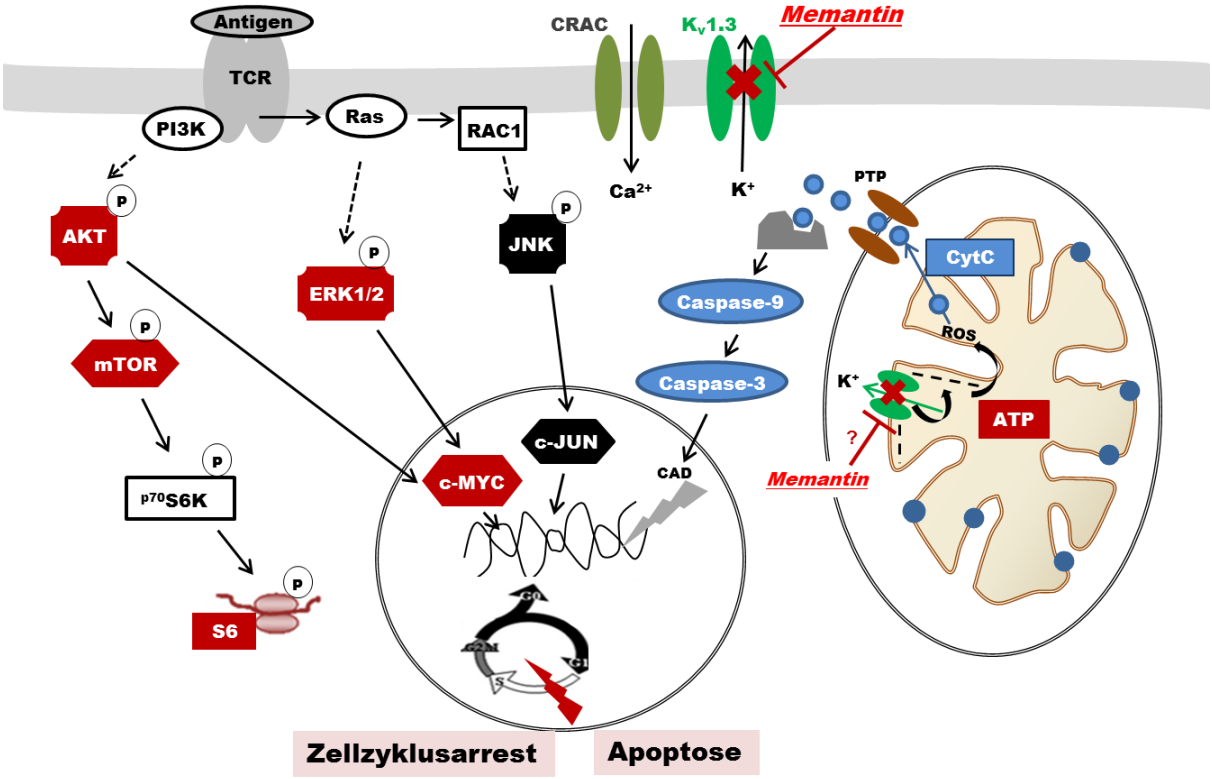

Abb.6: Memantin steigert den AraC-induzierten Zellzyklusarrest und Zelltod in Jurkat T-Zell-Leukämiezellen. Schematische Darstellung der untersuchten durch Memantin gehemmten (rot), aktivierten (blau) und unbeeinflussten (schwarz) Signalmoleküle. K_v1.3-Blockade durch Memantin verstärkt die AraC-induzierte Hemmung der Signalproteine AKT-mTOR-S6, ERK1/2 und c-MYC. Der Zellzyklus wird am Übergang der G_1-S-Phase arretiert. Weiterhin steigert Memantin den durch AraC induzierten Zelltod über den mitochondrialen Apoptoseweg mit Zytochrom C (CytC)-Freisetzung und Aktivierung der Caspase-9 und Caspase-3. PTP: Permeabilisationstransitionspore, ROS: reaktive Sauerstoffspezies, CAD: Caspasen-aktivierte DNAse. *Abb.: eigene Darstellung.*

Eine vergleichbare gesteigerte Hemmung von AKT und ERK1/2 wurde auch in der AML-Zelllinie Molm-13 vorgefunden (Daten von Dr. C. Cammann erhoben, [248]), ebenso wie eine gesteigerte CytC-Freisetzung. Es ist daher naheliegend, dass Memantin/AraC-Kobehandlung bei beiden Zelltypen - und wahrscheinlich einer Vielzahl unterschiedlicher akuter Leukämiezellen - den Zelltod über vergleichbare Mechanismen verstärkt. Dies ist in Hinblick auf die biologische Heterogenität akuter Leukämien, besonders bei älteren Patienten [207], von Interesse, da Memantin-Kobehandlung bei einer Vielzahl leukämischer Patientenblasten lymphatischen und myeloischen Ursprungs effektiv sein könnte, was durch die vorliegenden Patienten-Daten untermauert wird. Für Memantin als Adjuvanz im Rahmen eines palliativen Therapieschemas mit LDAC (*low dose AraC*) spricht weiterhin, dass die

synergistische Wirkung von Memantin auf den Zelltod bei niedrigen AraC-Konzentrationen, wie sie bei LDAC-Behandlung erreicht werden, auftritt. Da Memantin die Blut-Hirn-Schranke überwindet, ist es zudem im Rahmen der Prophylaxe bzw. Therapie einer *Meningeosis leukemica* mit AraC einsetzbar.

Da Memantin in Standarddosierung *in vivo* die Funktion nicht-neoplastischer T-Zellen beeinflusst, ist dies bei einer Memantin/AraC-Kombination zur ALL/AML-Therapie zu berücksichtigen. Das Ausmaß der T-Zellsuppression in der Leukämie-Therapie ist relevant hinsichtlich der verbundenen Infektanfälligkeit der Patienten, insbesondere auf Virusinfektionen. Zudem leisten T-Zellen einen kritischen Beitrag zur Antitumor-Immunität und die negative Beeinflussung von T-Zellen in der Umgebung solider Tumore über K_v1.3-Kanäle wurde bereits als interessante Immunevasion herausgestellt [254]. Im Weiteren wären *in vivo* Untersuchungen zur optimalen Dosierung von Memantin in Hinblick auf die T-Zell- und allgemeine hämatologische Inhibition notwendig. Aufgrund der stärkeren Vergleichbarkeit humaner T-Zellen mit Ratten-T-Zellen als mit murinen T-Zellen hinsichtlich des Expressions- und Regulationsmusters von K_v1.3-Kanälen, wären für *in vivo* Versuche Rattenmodelle in Betacht zu ziehen [188]. Fortführende *in vivo* Versuche waren im Rahmen der Dissertation leider nicht möglich. Memantin besitzt eine große therapeutische Breite, wobei akzidentielle Dosierungen bis zum 10-fachen der Standarddosis, d.h. 200 mg/Tag, ohne bedeutsame Toxizität beobachtet wurden [121]. Somit könnten für die Therapie akuter Leukämien auch punktuelle höhere Memantindosen eingesetzt werden. Dies eröffnet einen vielversprechenden Dosierungsspielraum für eine effektive und verträgliche Memantin/AraC-Kombinationsbehandlung bei akuten Leukämien.

Fortgeschrittenes Alter ist ein wesentlicher Risikofaktor für Neoplasien sowie Alzheimer Demenz. Der Alterungsprozess geht mit gehäuftem Auftreten chronischer Inflammation, mitochondrialer Dysfunktion und oxidativem Stress einher. In Folge kommt es verstärkt zu DNA-Schäden, zur Störung der oxidativen Energiegewinnung im Mitochondrium sowie zu abnormen Mitosen und aberrantem Zellzyklus [53, 255-257]. Weiterhin werden in betroffenen Zellen zentrale Signalwege für Proliferation und Überleben übermäßig aktiviert, wie der ERK1/2- und der PI3-K-AKT-mTOR Signalweg [258, 259]. Im Rahmen der Kanzerogenese wird damit die ungehemmte Proliferation und Migration, d.h. Metastasierung, begünstigt, während bei neurodegenerativen Erkrankungen, wie der Alzheimer Demenz, der amyloidogene Signalweg und die Tau-Hyperphosphorylierung gefördert werden [256]. Dennoch wird eine inverse Assoziation zwischen Neoplasien und neurodegenerativen Erkrankungen beobachtet: Patienten mit Neoplasien haben ein geringeres Risiko für Alzheimer Demenz und umgekehrt [260, 261]. Vermutet wird, dass die gleichen zellulären Alterungsprozesse bei teilungsfähigen Zellen Proliferation, bei Neuronen aber Apoptose

auslösen [256, 257]. Aufgrund gemeinsamer pathophysiologischer Mechanismen zwischen Neoplasien und neurodegenerativen Erkrankungen könnten übertragbare Therapiestrategien gefunden werden [257]. Beispielweise sind mTOR-Inhibitoren vielversprechende Pharmaka für Neoplasien sowie für die Alzheimer-Behandlung [223, 228, 262, 263]. Der Einsatz verschiedener monoklonaler Antikörper gegen Oberflächenmarker der Zielzelle haben die Prognose vieler Neoplasien stark verbessert [264, 265] und diese Antikörper werden auch für die Therapie der Alzheimer Demenz getestet [124]. Zytostatika haben im Alzheimer-Mausmodell die Bildung von Aß reduziert und die kognitive Funktion verbessert [266-268]. Meine Untersuchungen zur Wirkung von Memantin auf Lymphozyten und akute Leukämiezellen liefern erste Ansatzpunkte, dass Memantin, bisher für die Therapie der Alzheimer Demenz zugelassen, für Neoplasien ein vielversprechendes Ko-Therapeutikum sein könnte.

Zusammenfassung

Das Pharmakon Memantin ist ein NMDA-Rezeptor-Antagonist und wird zur Behandlung der fortgeschrittenen Alzheimer Demenz klinisch eingesetzt. In Lymphozyten hemmt Memantin jedoch Kalium-Kanäle vom K_v1.3-Typ. Diese sind zentrale Regulatoren des Membranpotentials, der Proliferation und Apoptose von Lymphozyten und vielversprechende therapeutische Zielstrukturen. In der vorliegenden Promotionsschrift wurden die funktionellen Auswirkungen einer K_v1.3-Kanal-Hemmung mittels Memantin auf die Proliferation, Migration und den Zelltod von T-Lymphozyten und akuten Leukämiezellen untersucht. Memantin und die NMDA-Rezeptor-Antagonisten Ifenprodil und MK801 hemmten die Alloantigen-induzierte Proliferation sowie die Chemokin-induzierte Migration humaner und muriner T-Lymphozyten *in vitro*. In mit Memantin in Standarddosierung behandelten Alzheimer-Patienten wurde eine Abnahme $CD45RO^+$ $CD4^+$ Gedächtnis-T-Zellen im peripheren Blut festgestellt, eine vermutlich kompensatorische Hochregulation von K_v1.3-Kanälen auf den T_H-Zellen sowie eine verminderte *ex vivo* T_H-Zell-Proliferation und T_H1-Induktion auf Alloantigene. Klinisch eingesetzte Konzentrationen von Memantin bewirken demnach eine T-Zellfunktions-hemmung *in vivo.* Die inhibitorische Wirkung von Memantin auf T_H-Zellen könnte einerseits die Immunpathogenese der Alzheimer Demenz mildern, aber auch die unter Memantin-Behandlung auftretende erhöhte Infektionsrate mitbedingen. Aufgrund der reduzierten T_H1-Bildung und supprimierten Alloreaktivität könnte Memantin als Immunsuppressivum bei der Behandlung von Autoimmunerkrankungen oder der Transplantatabstoßung von Interesse sein. Weitere Untersuchungen zeigten, dass die Inaktivierung von K_v1.3-Kanälen mittels Memantin für die Therapie akuter lymphatischer (ALL) und akuter myeloischer Leukämien (AML) von Bedeutung sein könnte. In Kombination mit dem weitläufig eingesetzten Chemotherapeutikum Cytarabin (AraC) förderte Memantin die Proliferationshemmung und steigerte synergistisch mit AraC den Zelltod von ALL- und AML-Zelllinien sowie von primären Blasten von Patienten mit akuter Leukämie. Dabei wurde eine verstärkte Inhibition der AKT-mTOR-S6-, ERK1/2- und c-MYC-Signalgebung sowie eine Verstärkung des intrinsischen Apoptosewegs durch erhöhte Freisetzung von mitochondrialem Zytochrom C und gesteigerter Aktivierung der Caspase-9 und Caspase-3 nachgewiesen. Da Memantin eine große therapeutische Breite besitzt und auch für ältere Patienten gut verträglich ist, könnte die Hemmung von K_v1.3-Kanälen mittels Memantin in Kombination mit dem klassischen Zytostatikum AraC eine vielversprechende neue Therapieoption, insbesondere für betagte oder multimorbide Patienten mit akuter Leukämie darstellen.

Literaturverzeichnis

1. Miller, J.F., THE THYMUS AND THE DEVELOPMENT OF IMMUNOLOGIC RESPONSIVENESS. Science, 1964. 144(3626): p. 1544-51.
2. von Andrian, U.H. and T.R. Mempel, Homing and cellular traffic in lymph nodes. Nat Rev Immunol, 2003. 3(11): p. 867-78.
3. Itano, A.A. and M.K. Jenkins, Antigen presentation to naive CD4 T cells in the lymph node. Nat Immunol, 2003. 4(8): p. 733-9.
4. Bleul, C.C., et al., A highly efficacious lymphocyte chemoattractant, stromal cell-derived factor 1 (SDF-1). J Exp Med, 1996. 184(3): p. 1101-9.
5. Luster, A.D., Chemokines--chemotactic cytokines that mediate inflammation. N Engl J Med, 1998. 338(7): p. 436-45.
6. Abbas, A.K., K.M. Murphy, and A. Sher, Functional diversity of helper T lymphocytes. Nature, 1996. 383(6603): p. 787-93.
7. Murphy, K.M. and S.L. Reiner, The lineage decisions of helper T cells. Nat Rev Immunol, 2002. 2(12): p. 933-44.
8. Barry, M. and R.C. Bleackley, Cytotoxic T lymphocytes: all roads lead to death. Nat Rev Immunol, 2002. 2(6): p. 401-9.
9. Green, D.R., N. Droin, and M. Pinkoski, Activation-induced cell death in T cells. Immunol Rev, 2003. 193: p. 70-81.
10. Murphy, K. and C. Weaver, Janeway's immunobiology. 2016: Garland Science.
11. Flaswinkel, H., M. Barner, and M. Reth, The tyrosine activation motif as a target of protein tyrosine kinases and SH2 domains. Semin Immunol, 1995. 7(1): p. 21-7.
12. Reth, M., Pillars article: antigen receptor tail clue. Nature. 1989. 338: 383-384. J Immunol, 2014. 192(9): p. 4015-6.
13. Smith-Garvin, J.E., G.A. Koretzky, and M.S. Jordan, T cell activation. Annu Rev Immunol, 2009. 27: p. 591-619.
14. Dustin, M.L. and A.S. Shaw, Costimulation: building an immunological synapse. Science, 1999. 283(5402): p. 649-50.
15. Dustin, M.L. and C.T. Baldari, The Immune Synapse: Past, Present, and Future. Methods Mol Biol, 2017. 1584: p. 1-5.
16. Zweifach, A. and R.S. Lewis, Mitogen-regulated Ca2+ current of T lymphocytes is activated by depletion of intracellular Ca2+ stores. Proc Natl Acad Sci U S A, 1993. 90(13): p. 6295-9.
17. Lewis, R.S., Calcium signaling mechanisms in T lymphocytes. Annu Rev Immunol, 2001. 19: p. 497-521.
18. Quintana, A., et al., T cell activation requires mitochondrial translocation to the immunological synapse. Proc Natl Acad Sci U S A, 2007. 104(36): p. 14418-23.
19. Martin-Cofreces, N.B., F. Baixauli, and F. Sanchez-Madrid, Immune synapse: conductor of orchestrated organelle movement. Trends Cell Biol, 2014. 24(1): p. 61-72.
20. Lin, C.S., et al., Voltage-gated potassium channels regulate calcium-dependent pathways involved in human T lymphocyte activation. J Exp Med, 1993. 177(3): p. 637-45.
21. Defarias, F.P., S.P. Stevens, and R.J. Leonard, Stable expression of human Kv1.3 potassium channels resets the resting membrane potential of cultured mammalian cells. Receptors Channels, 1995. 3(4): p. 273-81.
22. Nicolaou, S.A., et al., Localization of Kv1.3 channels in the immunological synapse modulates the calcium response to antigen stimulation in T lymphocytes. J Immunol, 2009. 183(10): p. 6296-302.
23. Panyi, G., et al., Kv1.3 potassium channels are localized in the immunological synapse formed between cytotoxic and target cells. Proc Natl Acad Sci U S A, 2004. 101(5): p. 1285-90.
24. Cahalan, M.D. and K.G. Chandy, The functional network of ion channels in T lymphocytes. Immunol Rev, 2009. 231(1): p. 59-87.
25. Thome, M., et al., Syk and ZAP-70 mediate recruitment of p56lck/CD4 to the activated T cell receptor/CD3/zeta complex. J Exp Med, 1995. 181(6): p. 1997-2006.
26. Philipsen, L., et al., De novo phosphorylation and conformational opening of the tyrosine kinase Lck act in concert to initiate T cell receptor signaling. Sci Signal, 2017. 10(462).
27. Feske, S., Calcium signalling in lymphocyte activation and disease. Nat Rev Immunol, 2007. 7(9): p. 690-702.
28. Jain, J., et al., The T-cell transcription factor NFATp is a substrate for calcineurin and interacts with Fos and Jun. Nature, 1993. 365(6444): p. 352-5.
29. Serfling, E., et al., NFATc1 autoregulation: a crucial step for cell-fate determination. Trends Immunol, 2006. 27(10): p. 461-9.
30. Rao, A., Signaling to gene expression: calcium, calcineurin and NFAT. Nat Immunol, 2009. 10(1): p. 3-5.
31. Hock, M., et al., NFATc1 induction in peripheral T and B lymphocytes. J Immunol, 2013. 190(5): p. 2345-53.
32. Serfling, E., A. Avots, and M. Neumann, The architecture of the interleukin-2 promoter: a reflection of T lymphocyte activation. Biochim Biophys Acta, 1995. 1263(3): p. 181-200.
33. Cantrell, D., Protein kinase B (Akt) regulation and function in T lymphocytes. Semin Immunol, 2002. 14(1): p. 19-26.

34. Patra, A.K., S.Y. Na, and U. Bommhardt, Active protein kinase B regulates TCR responsiveness by modulating cytoplasmic-nuclear localization of NFAT and NF-kappa B proteins. J Immunol, 2004. 172(8): p. 4812-20.
35. Manning, B.D. and A. Toker, AKT/PKB Signaling: Navigating the Network. Cell, 2017. 169(3): p. 381-405.
36. Dang, C.V., MYC on the path to cancer. Cell, 2012. 149(1): p. 22-35.
37. Gabay, M., Y. Li, and D.W. Felsher, MYC activation is a hallmark of cancer initiation and maintenance. Cold Spring Harb Perspect Med, 2014. 4(6).
38. Jenkins, M.K., et al., CD28 delivers a costimulatory signal involved in antigen-specific IL-2 production by human T cells. J Immunol, 1991. 147(8): p. 2461-6.
39. Esensten, J.H., et al., CD28 Costimulation: From Mechanism to Therapy. Immunity, 2016. 44(5): p. 973-88.
40. Masopust, D. and J.M. Schenkel, The integration of T cell migration, differentiation and function. Nat Rev Immunol, 2013. 13(5): p. 309-20.
41. Schraven, B., et al., Association of CD2 and CD45 on human T lymphocytes. Nature, 1990. 345(6270): p. 71-4.
42. Hermiston, M.L., Z. Xu, and A. Weiss, CD45: a critical regulator of signaling thresholds in immune cells. Annu Rev Immunol, 2003. 21: p. 107-37.
43. Zamoyska, R., Why is there so much CD45 on T cells? Immunity, 2007. 27(3): p. 421-3.
44. Farber, D.L., N.A. Yudanin, and N.P. Restifo, Human memory T cells: generation, compartmentalization and homeostasis. Nat Rev Immunol, 2014. 14(1): p. 24-35.
45. Sprent, J. and C.D. Surh, Normal T cell homeostasis: the conversion of naive cells into memory-phenotype cells. Nat Immunol, 2011. 12(6): p. 478-84.
46. Kaech, S.M., et al., Selective expression of the interleukin 7 receptor identifies effector CD8 T cells that give rise to long-lived memory cells. Nat Immunol, 2003. 4(12): p. 1191-8.
47. Krammer, P.H., CD95's deadly mission in the immune system. Nature, 2000. 407(6805): p. 789-95.
48. Schmitz, I., et al., Differences between CD95 type I and II cells detected with the CD95 ligand. Cell Death Differ, 1999. 6(9): p. 821-2.
49. Zhang, N., et al., The role of apoptosis in the development and function of T lymphocytes. Cell Res, 2005. 15(10): p. 749-69.
50. Xu, G. and Y. Shi, Apoptosis signaling pathways and lymphocyte homeostasis. Cell Res, 2007. 17(9): p. 759-71.
51. Skulachev, V.P., Cytochrome c in the apoptotic and antioxidant cascades. FEBS Lett, 1998. 423(3): p. 275-80.
52. Martinez-Caballero, S., et al., Assembly of the mitochondrial apoptosis-induced channel, MAC. J Biol Chem, 2009. 284(18): p. 12235-45.
53. Peixoto, P.M., L.M. Dejean, and K.W. Kinnally, The therapeutic potential of mitochondrial channels in cancer, ischemia-reperfusion injury, and neurodegeneration. Mitochondrion, 2012. 12(1): p. 14-23.
54. Kuida, K., Caspase-9. Int J Biochem Cell Biol, 2000. 32(2): p. 121-4.
55. Pinkoski, M.J., N.J. Waterhouse, and D.R. Green, Mitochondria, apoptosis and autoimmunity. Curr Dir Autoimmun, 2006. 9: p. 55-73.
56. Harvey, N.L. and S. Kumar, The role of caspases in apoptosis. Adv Biochem Eng Biotechnol, 1998. 62: p. 107-28.
57. Tang, J., H. Kawadler, and X. Yang, Lymphocyte life and death: the caspase-8 connection. Cancer Biol Ther, 2005. 4(7): p. 700-2.
58. Samraj, A.K., et al., Loss of caspase-9 provides genetic evidence for the type I/II concept of CD95-mediated apoptosis. J Biol Chem, 2006. 281(40): p. 29652-9.
59. Nagata, S., et al., Degradation of chromosomal DNA during apoptosis. Cell Death Differ, 2003. 10(1): p. 108-16.
60. Ekshyyan, O. and T.Y. Aw, Apoptosis: a key in neurodegenerative disorders. Curr Neurovasc Res, 2004. 1(4): p. 355-71.
61. Vermeulen, K., D.R. Van Bockstaele, and Z.N. Berneman, Apoptosis: mechanisms and relevance in cancer. Ann Hematol, 2005. 84(10): p. 627-39.
62. Plaza-Sirvent, C., et al., c-FLIP Expression in Foxp3-Expressing Cells Is Essential for Survival of Regulatory T Cells and Prevention of Autoimmunity. Cell Rep, 2017. 18(1): p. 12-22.
63. Bosma, G.C., R.P. Custer, and M.J. Bosma, A severe combined immunodeficiency mutation in the mouse. Nature, 1983. 301(5900): p. 527-30.
64. Cirillo, E., et al., Severe combined immunodeficiency--an update. Ann N Y Acad Sci, 2015. 1356: p. 90-106.
65. Barre-Sinoussi, F., HIV as the cause of AIDS. Lancet, 1996. 348(9019): p. 31-5.
66. Zinkernagel, R.M. and P.C. Doherty, Restriction of in vitro T cell-mediated cytotoxicity in lymphocytic choriomeningitis within a syngeneic or semiallogeneic system. Nature, 1974. 248(5450): p. 701-2.
67. Strom, T.B., et al., The Th1/Th2 paradigm and the allograft response. Curr Opin Immunol, 1996. 8(5): p. 688-93.
68. Carbone, F.R., et al., Cross-presentation: a general mechanism for CTL immunity and tolerance. Immunol Today, 1998. 19(8): p. 368-73.
69. Arakelov, A. and F.G. Lakkis, The alloimmune response and effector mechanisms of allograft rejection. Semin Nephrol, 2000. 20(2): p. 95-102.

70. Seeburg, P.H., et al., The NMDA receptor channel: molecular design of a coincidence detector. Recent Prog Horm Res, 1995. 50: p. 19-34.
71. Dingledine, R., et al., The glutamate receptor ion channels. Pharmacol Rev, 1999. 51(1): p. 7-61.
72. Boeckman, F.A. and E. Aizenman, Pharmacological properties of acquired excitotoxicity in Chinese hamster ovary cells transfected with N-methyl-D-aspartate receptor subunits. J Pharmacol Exp Ther, 1996. 279(2): p. 515-23.
73. Cull-Candy, S., S. Brickley, and M. Farrant, NMDA receptor subunits: diversity, development and disease. Curr Opin Neurobiol, 2001. 11(3): p. 327-35.
74. Parsons, C.G., W. Danysz, and G. Quack, Memantine is a clinically well tolerated N-methyl-D-aspartate (NMDA) receptor antagonist--a review of preclinical data. Neuropharmacology, 1999. 38(6): p. 735-67.
75. Peltoniemi, M.A., et al., Ketamine: A Review of Clinical Pharmacokinetics and Pharmacodynamics in Anesthesia and Pain Therapy. Clin Pharmacokinet, 2016. 55(9): p. 1059-77.
76. Davies, J., et al., 2-Amino-5-phosphonovalerate (2APV), a potent and selective antagonist of amino acid-induced and synaptic excitation. Neurosci Lett, 1981. 21(1): p. 77-81.
77. Wong, E.H., et al., The anticonvulsant MK-801 is a potent N-methyl-D-aspartate antagonist. Proc Natl Acad Sci U S A, 1986. 83(18): p. 7104-8.
78. Carter, C., J.P. Rivy, and B. Scatton, Ifenprodil and SL 82.0715 are antagonists at the polyamine site of the N-methyl-D-aspartate (NMDA) receptor. Eur J Pharmacol, 1989. 164(3): p. 611-2.
79. Lewis, R.S. and M.D. Cahalan, Potassium and calcium channels in lymphocytes. Annu Rev Immunol, 1995. 13: p. 623-53.
80. Cahalan, M.D., H. Wulff, and K.G. Chandy, Molecular properties and physiological roles of ion channels in the immune system. J Clin Immunol, 2001. 21(4): p. 235-52.
81. Kostanyan, I.A., E.V. Navolotskaya, and R.I. Nurieva, Identification of Binding Sites for L-Glutamate on T Lymphocytes. Russ J Immunol, 1997. 2(2): p. 135-137.
82. Storto, M., et al., Expression of metabotropic glutamate receptors in murine thymocytes and thymic stromal cells. J Neuroimmunol, 2000. 109(2): p. 112-20.
83. Rezzani, R., et al., Cyclosporine-A treatment inhibits the expression of metabotropic glutamate receptors in rat thymus. Acta Histochem, 2003. 105(1): p. 81-7.
84. Pacheco, R., et al., Group I metabotropic glutamate receptors mediate a dual role of glutamate in T cell activation. J Biol Chem, 2004. 279(32): p. 33352-8.
85. Miglio, G., et al., Stimulation of group I metabotropic glutamate receptors evokes calcium signals and c-jun and c-fos gene expression in human T cells. Biochem Pharmacol, 2005. 70(2): p. 189-99.
86. Chiocchetti, A., et al., Group I mGlu receptor stimulation inhibits activation-induced cell death of human T lymphocytes. Br J Pharmacol, 2006. 148(6): p. 760-8.
87. Lombardi, G., et al., Characterization of ionotropic glutamate receptors in human lymphocytes. Br J Pharmacol, 2001. 133(6): p. 936-44.
88. Ganor, Y., et al., Human T cells express a functional ionotropic glutamate receptor GluR3, and glutamate by itself triggers integrin-mediated adhesion to laminin and fibronectin and chemotactic migration. J Immunol, 2003. 170(8): p. 4362-72.
89. Boldyrev, A.A., et al., Rodent lymphocytes express functionally active glutamate receptors. Biochem Biophys Res Commun, 2004. 324(1): p. 133-9.
90. Boldyrev, A.A., D.O. Carpenter, and P. Johnson, Emerging evidence for a similar role of glutamate receptors in the nervous and immune systems. J Neurochem, 2005. 95(4): p. 913-8.
91. Mashkina, A.P., et al., NMDA receptors are expressed in lymphocytes activated both in vitro and in vivo. Cell Mol Neurobiol, 2010. 30(6): p. 901-7.
92. Divino Filho, J.C., et al., Glutamate concentration in plasma, erythrocyte and muscle in relation to plasma levels of insulin-like growth factor (IGF)-I, IGF binding protein-1 and insulin in patients on haemodialysis. J Endocrinol, 1998. 156(3): p. 519-27.
93. Levite, M., Neurotransmitters activate T-cells and elicit crucial functions via neurotransmitter receptors. Curr Opin Pharmacol, 2008. 8(4): p. 460-71.
94. Droge, W., et al., Elevated plasma glutamate levels in colorectal carcinoma patients and in patients with acquired immunodeficiency syndrome (AIDS). Immunobiology, 1987. 174(4-5): p. 473-9.
95. Eck, H.P., P. Drings, and W. Droge, Plasma glutamate levels, lymphocyte reactivity and death rate in patients with bronchial carcinoma. J Cancer Res Clin Oncol, 1989. 115(6): p. 571-4.
96. Eck, H.P., H. Frey, and W. Droge, Elevated plasma glutamate concentrations in HIV-1-infected patients may contribute to loss of macrophage and lymphocyte functions. Int Immunol, 1989. 1(4): p. 367-72.
97. Ollenschlager, G., et al., Plasma glutamate--a prognostic marker of cancer and of other immunodeficiency syndromes? Scand J Clin Lab Invest, 1989. 49(8): p. 773-7.
98. Pacheco, R., et al., Glutamate released by dendritic cells as a novel modulator of T cell activation. J Immunol, 2006. 177(10): p. 6695-704.
99. Rimaniol, A.C., et al., Role of glutamate transporters in the regulation of glutathione levels in human macrophages. Am J Physiol Cell Physiol, 2001. 281(6): p. C1964-70.
100. Collard, C.D., et al., Neutrophil-derived glutamate regulates vascular endothelial barrier function. J Biol Chem, 2002. 277(17): p. 14801-11.
101. Affaticati, P., et al., Sustained calcium signalling and caspase-3 activation involve NMDA receptors in thymocytes in contact with dendritic cells. Cell Death Differ, 2011. 18(1): p. 99-108.
102. Lombardi, G., et al., Glutamate modulation of human lymphocyte growth: in vitro studies. Biochem Biophys Res Commun, 2004. 318(2): p. 496-502.

103. Miglio, G., et al., Stimulation of N-methyl-D-aspartate receptors modulates Jurkat T cell growth and adhesion to fibronectin. Biochem Biophys Res Commun, 2007. 361(2): p. 404-9.
104. Kvaratskhelia, E., et al., N-methyl-D-aspartate and sigma-ligands change the production of interleukins 8 and 10 in lymphocytes through modulation of the NMDA glutamate receptor. Neuroimmunomodulation, 2009. 16(3): p. 201-7.
105. Gao, M., et al., Effect of N-methyl-D-aspartate receptor antagonist on T helper cell differentiation induced by phorbol-myristate-acetate and ionomycin. Cytokine, 2011. 56(2): p. 458-65.
106. Zainullina, L.F., et al., NMDA receptors as a possible component of store-operated Ca(2)(+) entry in human T-lymphocytes. Biochemistry (Mosc), 2011. 76(11): p. 1220-6.
107. Poulopoulou, C., et al., Modulation of voltage-gated potassium channels in human T lymphocytes by extracellular glutamate. Mol Pharmacol, 2005. 67(3): p. 856-67.
108. Kahlfuss, S., et al., Immunosuppression by N-methyl-D-aspartate receptor antagonists is mediated through inhibition of Kv1.3 and KCa3.1 channels in T cells. Mol Cell Biol, 2014. 34(5): p. 820-31.
109. Bose, T., Crosstalk between NMDAR antagonists and potassium channels in murine and human lymphocytes. Dissertation 2014.
110. Gerzon, K., et al., The Adamantyl Group in Medicinal Agents. I. Hypoglycemic N-Arylsulfonyl-N' -Adamantylureas. J Med Chem, 1963. 6: p. 760-3.
111. Grossmann, A., W. Grossmann, and I. Jurna, The effect of dimethylaminoadamantane on neuronal membranes. Eur J Pharmacol, 1976. 35(2): p. 379-88.
112. Bormann, J., Memantine is a potent blocker of N-methyl-D-aspartate (NMDA) receptor channels. Eur J Pharmacol, 1989. 166(3): p. 591-2.
113. Kornhuber, J., et al., Memantine displaces [3H]MK-801 at therapeutic concentrations in postmortem human frontal cortex. Eur J Pharmacol, 1989. 166(3): p. 589-90.
114. Mayer, M.L., G.L. Westbrook, and P.B. Guthrie, Voltage-dependent block by Mg2+ of NMDA responses in spinal cord neurones. Nature, 1984. 309(5965): p. 261-3.
115. Chen, H.S., et al., Open-channel block of N-methyl-D-aspartate (NMDA) responses by memantine: therapeutic advantage against NMDA receptor-mediated neurotoxicity. J Neurosci, 1992. 12(11): p. 4427-36.
116. Chen, H.S. and S.A. Lipton, Mechanism of memantine block of NMDA-activated channels in rat retinal ganglion cells: uncompetitive antagonism. J Physiol, 1997. 499 (Pt 1): p. 27-46.
117. Danysz, W. and C.G. Parsons, The NMDA receptor antagonist memantine as a symptomatological and neuroprotective treatment for Alzheimer's disease: preclinical evidence. Int J Geriatr Psychiatry, 2003. 18(Suppl 1): p. S23-32.
118. Kornhuber, J., et al., Amantadine and memantine are NMDA receptor antagonists with neuroprotective properties. J Neural Transm Suppl, 1994. 43: p. 91-104.
119. Rammes, G., W. Danysz, and C.G. Parsons, Pharmacodynamics of memantine: an update. Curr Neuropharmacol, 2008. 6(1): p. 55-78.
120. Thomas, S.J. and G.T. Grossberg, Memantine: a review of studies into its safety and efficacy in treating Alzheimer's disease and other dementias. Clin Interv Aging, 2009. 4: p. 367-77.
121. Agency, E.M. Memantine (Axura). Available from: https://www.ema.europa.eu/en/documents/product-information/axura-epar-product-information_en.pdf.
122. Querfurth, H.W. and F.M. LaFerla, Alzheimer's disease. N Engl J Med, 2010. 362(4): p. 329-44.
123. Smith, A.D., Why are drug trials in Alzheimer's disease failing? Lancet, 2010. 376(9751): p. 1466.
124. Sacks, C.A., J. Avorn, and A.S. Kesselheim, The Failure of Solanezumab - How the FDA Saved Taxpayers Billions. N Engl J Med, 2017. 376(18): p. 1706-1708.
125. Bloom, G.S., Amyloid-beta and tau: the trigger and bullet in Alzheimer disease pathogenesis. JAMA Neurol, 2014. 71(4): p. 505-8.
126. Pimplikar, S.W., Neuroinflammation in Alzheimer's disease: from pathogenesis to a therapeutic target. J Clin Immunol, 2014. 34 Suppl 1: p. S64-9.
127. Heneka, M.T., et al., Neuroinflammation in Alzheimer's disease. Lancet Neurol, 2015. 14(4): p. 388-405.
128. Heppner, F.L., R.M. Ransohoff, and B. Becher, Immune attack: the role of inflammation in Alzheimer disease. Nat Rev Neurosci, 2015. 16(6): p. 358-72.
129. Guerriero, F., et al., Neuroinflammation, immune system and Alzheimer disease: searching for the missing link. Aging Clin Exp Res, 2017. 29(5): p. 821-831.
130. Da Mesquita, S., et al., Insights on the pathophysiology of Alzheimer's disease: The crosstalk between amyloid pathology, neuroinflammation and the peripheral immune system. Neurosci Biobehav Rev, 2016. 68: p. 547-562.
131. Tahara, K., et al., Role of toll-like receptor signalling in Abeta uptake and clearance. Brain, 2006. 129(Pt 11): p. 3006-19.
132. Heneka, M.T., D.T. Golenbock, and E. Latz, Innate immunity in Alzheimer's disease. Nat Immunol, 2015. 16(3): p. 229-36.
133. Goldeck, D., et al., Peripheral Immune Signatures in Alzheimer Disease. Curr Alzheimer Res, 2016. 13(7): p. 739-49.
134. Monsonego, A., A. Nemirovsky, and I. Harpaz, CD4 T cells in immunity and immunotherapy of Alzheimer's disease. Immunology, 2013. 139(4): p. 438-46.
135. Gonzalez, H. and R. Pacheco, T-cell-mediated regulation of neuroinflammation involved in neurodegenerative diseases. J Neuroinflammation, 2014. 11: p. 201.
136. Jevtic, S., et al., The role of the immune system in Alzheimer disease: Etiology and treatment. Ageing Res Rev, 2017. 40: p. 84-94.

137. Man, S.M., et al., Peripheral T cells overexpress MIP-1alpha to enhance its transendothelial migration in Alzheimer's disease. Neurobiol Aging, 2007. 28(4): p. 485-96.
138. McManus, R.M., K.H. Mills, and M.A. Lynch, T Cells-Protective or Pathogenic in Alzheimer's Disease? J Neuroimmune Pharmacol, 2015. 10(4): p. 547-60.
139. Saresella, M., et al., PD1 negative and PD1 positive CD4+ T regulatory cells in mild cognitive impairment and Alzheimer's disease. J Alzheimers Dis, 2010. 21(3): p. 927-38.
140. Browne, T.C., et al., IFN-gamma Production by amyloid beta-specific Th1 cells promotes microglial activation and increases plaque burden in a mouse model of Alzheimer's disease. J Immunol, 2013. 190(5): p. 2241-51.
141. Zhang, J., et al., Th17 cell-mediated neuroinflammation is involved in neurodegeneration of abeta1-42-induced Alzheimer's disease model rats. PLoS One, 2013. 8(10): p. e75786.
142. Gonzalez, H., et al., Neuroimmune regulation of microglial activity involved in neuroinflammation and neurodegenerative diseases. J Neuroimmunol, 2014. 274(1-2): p. 1-13.
143. Monsonego, A., et al., Increased T cell reactivity to amyloid beta protein in older humans and patients with Alzheimer disease. J Clin Invest, 2003. 112(3): p. 415-22.
144. Lueg, G., et al., Clinical relevance of specific T-cell activation in the blood and cerebrospinal fluid of patients with mild Alzheimer's disease. Neurobiol Aging, 2015. 36(1): p. 81-9.
145. Fiala, M., et al., Amyloid-beta induces chemokine secretion and monocyte migration across a human blood--brain barrier model. Mol Med, 1998. 4(7): p. 480-9.
146. Speciale, L., et al., Lymphocyte subset patterns and cytokine production in Alzheimer's disease patients. Neurobiol Aging, 2007. 28(8): p. 1163-9.
147. Schindowski, K., et al., Increased T-cell reactivity and elevated levels of CD8+ memory T-cells in Alzheimer's disease-patients and T-cell hyporeactivity in an Alzheimer's disease-mouse model: implications for immunotherapy. Neuromolecular Med, 2007. 9(4): p. 340-54.
148. Larbi, A., et al., Dramatic shifts in circulating CD4 but not CD8 T cell subsets in mild Alzheimer's disease. J Alzheimers Dis, 2009. 17(1): p. 91-103.
149. Saresella, M., et al., Increased activity of Th-17 and Th-9 lymphocytes and a skewing of the post-thymic differentiation pathway are seen in Alzheimer's disease. Brain Behav Immun, 2011. 25(3): p. 539-47.
150. Pellicano, M., et al., Immune profiling of Alzheimer patients. J Neuroimmunol, 2012. 242(1-2): p. 52-9.
151. Matteson, D.R. and C. Deutsch, K channels in T lymphocytes: a patch clamp study using monoclonal antibody adhesion. Nature, 1984. 307(5950): p. 468-71.
152. Chandy, K.G., et al., Voltage-gated potassium channels are required for human T lymphocyte activation. J Exp Med, 1984. 160(2): p. 369-85.
153. Cahalan, M.D., et al., A voltage-gated potassium channel in human T lymphocytes. J Physiol, 1985. 358: p. 197-237.
154. Chandy, K.G., et al., Ion channels in lymphocytes. J Clin Immunol, 1985. 5(1): p. 1-6.
155. DeCoursey, T.E., et al., Voltage-dependent ion channels in T-lymphocytes. J Neuroimmunol, 1985. 10(1): p. 71-95.
156. Spencer, R.H., K.G. Chandy, and G.A. Gutman, Immunological identification of the Shaker-related Kv1.3 potassium channel protein in T and B lymphocytes, and detection of related proteins in files and yeast. Biochem Biophys Res Commun, 1993. 191(1): p. 201-6.
157. Wickenden, A., K(+) channels as therapeutic drug targets. Pharmacol Ther, 2002. 94(1-2): p. 157-82.
158. MacKinnon, R., Determination of the subunit stoichiometry of a voltage-activated potassium channel. Nature, 1991. 350(6315): p. 232-5.
159. Doyle, D.A., et al., The structure of the potassium channel: molecular basis of K+ conduction and selectivity. Science, 1998. 280(5360): p. 69-77.
160. Jiang, Y., et al., X-ray structure of a voltage-dependent K+ channel. Nature, 2003. 423(6935): p. 33-41.
161. Tytgat, J., Mutations in the P-region of a mammalian potassium channel (RCK1): a comparison with the Shaker potassium channel. Biochem Biophys Res Commun, 1994. 203(1): p. 513-8.
162. Bright, J.N., et al., Conformational dynamics of helix S6 from Shaker potassium channel: simulation studies. Biopolymers, 2002. 64(6): p. 303-13.
163. Treptow, W., et al., Coupled motions between pore and voltage-sensor domains: a model for Shaker B, a voltage-gated potassium channel. Biophys J, 2004. 87(4): p. 2365-79.
164. Bowlby, M.R., et al., Modulation of the Kv1.3 potassium channel by receptor tyrosine kinases. J Gen Physiol, 1997. 110(5): p. 601-10.
165. Chung, I. and L.C. Schlichter, Native Kv1.3 channels are upregulated by protein kinase C. J Membr Biol, 1997. 156(1): p. 73-85.
166. Hanada, T., et al., Human homologue of the Drosophila discs large tumor suppressor binds to p56lck tyrosine kinase and Shaker type Kv1.3 potassium channel in T lymphocytes. J Biol Chem, 1997. 272(43): p. 26899-904.
167. Gong, J., et al., Differential stimulation of PKC phosphorylation of potassium channels by ZIP1 and ZIP2. Science, 1999. 285(5433): p. 1565-9.
168. Cook, K.K. and D.A. Fadool, Two adaptor proteins differentially modulate the phosphorylation and biophysics of Kv1.3 ion channel by SRC kinase. J Biol Chem, 2002. 277(15): p. 13268-80.
169. Nakahira, K., et al., Selective interaction of voltage-gated K+ channel beta-subunits with alpha-subunits. J Biol Chem, 1996. 271(12): p. 7084-9.
170. McCormack, T., et al., The effects of Shaker beta-subunits on the human lymphocyte K+ channel Kv1.3. J Biol Chem, 1999. 274(29): p. 20123-6.

171. Grissmer, S., et al., Expression and chromosomal localization of a lymphocyte K+ channel gene. Proc Natl Acad Sci U S A, 1990. 87(23): p. 9411-5.
172. Panyi, G., et al., Colocalization and nonrandom distribution of Kv1.3 potassium channels and CD3 molecules in the plasma membrane of human T lymphocytes. Proc Natl Acad Sci U S A, 2003. 100(5): p. 2592-7.
173. Toth, A., et al., Functional consequences of Kv1.3 ion channel rearrangement into the immunological synapse. Immunol Lett, 2009. 125(1): p. 15-21.
174. Panyi, G., Biophysical and pharmacological aspects of K+ channels in T lymphocytes. Eur Biophys J, 2005. 34(6): p. 515-29.
175. Koni, P.A., et al., Compensatory anion currents in Kv1.3 channel-deficient thymocytes. J Biol Chem, 2003. 278(41): p. 39443-51.
176. Chiang, E.Y., et al., Potassium channels Kv1.3 and KCa3.1 cooperatively and compensatorily regulate antigen-specific memory T cell functions. Nat Commun, 2017. 8: p. 14644.
177. Szabo, I., et al., A novel potassium channel in lymphocyte mitochondria. J Biol Chem, 2005. 280(13): p. 12790-8.
178. Jang, S.H., et al., Nuclear localization and functional characteristics of voltage-gated potassium channel Kv1.3. J Biol Chem, 2015. 290(20): p. 12547-57.
179. Leanza, L., et al., Targeting a mitochondrial potassium channel to fight cancer. Cell Calcium, 2015. 58(1): p. 131-8.
180. Szabo, I., et al., Mitochondrial potassium channel Kv1.3 mediates Bax-induced apoptosis in lymphocytes. Proc Natl Acad Sci U S A, 2008. 105(39): p. 14861-6.
181. Gulbins, E., et al., Role of Kv1.3 mitochondrial potassium channel in apoptotic signalling in lymphocytes. Biochim Biophys Acta, 2010. 1797(6-7): p. 1251-9.
182. Szabo, I., M. Zoratti, and E. Gulbins, Contribution of voltage-gated potassium channels to the regulation of apoptosis. FEBS Lett, 2010. 584(10): p. 2049-56.
183. Antignani, A. and R.J. Youle, How do Bax and Bak lead to permeabilization of the outer mitochondrial membrane? Curr Opin Cell Biol, 2006. 18(6): p. 685-9.
184. Szabo, I., et al., Single-point mutations of a lysine residue change function of Bax and Bcl-xL expressed in Bax- and Bak-less mouse embryonic fibroblasts: novel insights into the molecular mechanisms of Bax-induced apoptosis. Cell Death Differ, 2011. 18(3): p. 427-38.
185. Narita, M., et al., Bax interacts with the permeability transition pore to induce permeability transition and cytochrome c release in isolated mitochondria. Proc Natl Acad Sci U S A, 1998. 95(25): p. 14681-6.
186. Ott, M., et al., Cytochrome c release from mitochondria proceeds by a two-step process. Proc Natl Acad Sci U S A, 2002. 99(3): p. 1259-63.
187. Wulff, H., C. Beeton, and K.G. Chandy, Potassium channels as therapeutic targets for autoimmune disorders. Curr Opin Drug Discov Devel, 2003. 6(5): p. 640-7.
188. Zhao, Y., et al., Toxins Targeting the Kv1.3 Channel: Potential Immunomodulators for Autoimmune Diseases. Toxins (Basel), 2015. 7(5): p. 1749-64.
189. Chandy, K.G. and R.S. Norton, Peptide blockers of Kv1.3 channels in T cells as therapeutics for autoimmune disease. Curr Opin Chem Biol, 2017. 38: p. 97-107.
190. Chandy, K.G., et al., K+ channels as targets for specific immunomodulation. Trends Pharmacol Sci, 2004. 25(5): p. 280-9.
191. Varga, Z., P. Hajdu, and G. Panyi, Ion channels in T lymphocytes: an update on facts, mechanisms and therapeutic targeting in autoimmune diseases. Immunol Lett, 2010. 130(1-2): p. 19-25.
192. Tarcha, E.J., et al., Safety and pharmacodynamics of dalazatide, a Kv1.3 channel inhibitor, in the treatment of plaque psoriasis: A randomized phase 1b trial. PLoS One, 2017. 12(7): p. e0180762.
193. Middleton, R.E., et al., Substitution of a single residue in Stichodactyla helianthus peptide, ShK-Dap22, reveals a novel pharmacological profile. Biochemistry, 2003. 42(46): p. 13698-707.
194. Vennekamp, J., et al., Kv1.3-blocking 5-phenylalkoxypsoralens: a new class of immunomodulators. Mol Pharmacol, 2004. 65(6): p. 1364-74.
195. Murray, J.K., et al., Pharmaceutical Optimization of Peptide Toxins for Ion Channel Targets: Potent, Selective, and Long-Lived Antagonists of Kv1.3. J Med Chem, 2015. 58(17): p. 6784-802.
196. Batista, C.V., et al., Two novel toxins from the Amazonian scorpion Tityus cambridgei that block Kv1.3 and Shaker B K(+)-channels with distinctly different affinities. Biochim Biophys Acta, 2002. 1601(2): p. 123-31.
197. Lange, A., et al., Toxin-induced conformational changes in a potassium channel revealed by solid-state NMR. Nature, 2006. 440(7086): p. 959-62.
198. Gill, S., et al., A cell-based Rb(+)-flux assay of the Kv1.3 potassium channel. Assay Drug Dev Technol, 2007. 5(3): p. 373-80.
199. Wood, M.W., H.M. VanDongen, and A.M. VanDongen, Structural conservation of ion conduction pathways in K channels and glutamate receptors. Proc Natl Acad Sci U S A, 1995. 92(11): p. 4882-6.
200. Kuner, T., P.H. Seeburg, and H.R. Guy, A common architecture for K+ channels and ionotropic glutamate receptors? Trends Neurosci, 2003. 26(1): p. 27-32.
201. Zhorov, B.S. and D.B. Tikhonov, Potassium, sodium, calcium and glutamate-gated channels: pore architecture and ligand action. J Neurochem, 2004. 88(4): p. 782-99.
202. Lowinus, T., et al., Immunomodulation by memantine in therapy of Alzheimer's disease is mediated through inhibition of Kv1.3 channels and T cell responsiveness. Oncotarget, 2016. 7(33): p. 53797-53807.

203. Giustizieri, M., et al., Memantine inhibits ATP-dependent K+ conductances in dopamine neurons of the rat substantia nigra pars compacta. J Pharmacol Exp Ther, 2007. 322(2): p. 721-9.
204. Tsai, K.L., H.F. Chang, and S.N. Wu, The inhibition of inwardly rectifying K+ channels by memantine in macrophages and microglial cells. Cell Physiol Biochem, 2013. 31(6): p. 938-51.
205. Menzin, J., et al., The outcomes and costs of acute myeloid leukemia among the elderly. Arch Intern Med, 2002. 162(14): p. 1597-603.
206. Gokbuget, N., How I treat older patients with ALL. Blood, 2013. 122(8): p. 1366-75.
207. Rao, A.V., et al., Age-specific differences in oncogenic pathway dysregulation and anthracycline sensitivity in patients with acute myeloid leukemia. J Clin Oncol, 2009. 27(33): p. 5580-6.
208. Patel, C., et al., Multidrug resistance in relapsed acute myeloid leukemia: evidence of biological heterogeneity. Cancer, 2013. 119(16): p. 3076-83.
209. Heidel, F.H., et al., Evolutionarily conserved signaling pathways: acting in the shadows of acute myelogenous leukemia's genetic diversity. Clin Cancer Res, 2015. 21(2): p. 240-8.
210. Ossenkoppele, G. and B. Lowenberg, How I treat the older patient with acute myeloid leukemia. Blood, 2015. 125(5): p. 767-74.
211. Gokbuget, N., Treatment of Older Patients with Acute Lymphoblastic Leukaemia. Drugs Aging, 2018. 35(1): p. 11-26.
212. Pagano, L., et al., Acute lymphoblastic leukemia in the elderly. A twelve-year retrospective, single center study. Haematologica, 2000. 85(12): p. 1327-9.
213. McCubrey, J.A., et al., Roles of the Raf/MEK/ERK pathway in cell growth, malignant transformation and drug resistance. Biochim Biophys Acta, 2007. 1773(8): p. 1263-84.
214. Gutierrez, A., et al., High frequency of PTEN, PI3K, and AKT abnormalities in T-cell acute lymphoblastic leukemia. Blood, 2009. 114(3): p. 647-50.
215. Kharas, M.G., et al., Constitutively active AKT depletes hematopoietic stem cells and induces leukemia in mice. Blood, 2010. 115(7): p. 1406-15.
216. Steelman, L.S., et al., Roles of the Ras/Raf/MEK/ERK pathway in leukemia therapy. Leukemia, 2011. 25(7): p. 1080-94.
217. Blackburn, J.S., et al., Clonal evolution enhances leukemia-propagating cell frequency in T cell acute lymphoblastic leukemia through Akt/mTORC1 pathway activation. Cancer Cell, 2014. 25(3): p. 366-78.
218. Kerkhoff, E., et al., Regulation of c-myc expression by Ras/Raf signalling. Oncogene, 1998. 16(2): p. 211-6.
219. Fauriat, C. and D. Olive, AML drug resistance: c-Myc comes into play. Blood, 2014. 123(23): p. 3528-30.
220. Loosveld, M., et al., Therapeutic targeting of c-Myc in T-cell acute lymphoblastic leukemia, T-ALL. Oncotarget, 2014. 5(10): p. 3168-72.
221. Roderick, J.E., et al., c-Myc inhibition prevents leukemia initiation in mice and impairs the growth of relapsed and induction failure pediatric T-ALL cells. Blood, 2014. 123(7): p. 1040-50.
222. Teachey, D.T., et al., The mTOR inhibitor CCI-779 induces apoptosis and inhibits growth in preclinical models of primary adult human ALL. Blood, 2006. 107(3): p. 1149-55.
223. Teachey, D.T., et al., mTOR inhibitors are synergistic with methotrexate: an effective combination to treat acute lymphoblastic leukemia. Blood, 2008. 112(5): p. 2020-3.
224. Levy, D.S., J.A. Kahana, and R. Kumar, AKT inhibitor, GSK690693, induces growth inhibition and apoptosis in acute lymphoblastic leukemia cell lines. Blood, 2009. 113(8): p. 1723-9.
225. Nishioka, C., et al., Inhibition of MEK signaling enhances the ability of cytarabine to induce growth arrest and apoptosis of acute myelogenous leukemia cells. Apoptosis, 2009. 14(9): p. 1108-20.
226. Chiarini, F., et al., A combination of temsirolimus, an allosteric mTOR inhibitor, with clofarabine as a new therapeutic option for patients with acute myeloid leukemia. Oncotarget, 2012. 3(12): p. 1615-28.
227. Polak, R. and M. Buitenhuis, The PI3K/PKB signaling module as key regulator of hematopoiesis: implications for therapeutic strategies in leukemia. Blood, 2012. 119(4): p. 911-23.
228. Willems, L., et al., The dual mTORC1 and mTORC2 inhibitor AZD8055 has anti-tumor activity in acute myeloid leukemia. Leukemia, 2012. 26(6): p. 1195-202.
229. Schubbert, S., et al., Targeting the MYC and PI3K pathways eliminates leukemia-initiating cells in T-cell acute lymphoblastic leukemia. Cancer Res, 2014. 74(23): p. 7048-59.
230. Cani, A., et al., Triple Akt inhibition as a new therapeutic strategy in T-cell acute lymphoblastic leukemia. Oncotarget, 2015. 6(9): p. 6597-610.
231. Perl, A.E., et al., A phase I study of the mammalian target of rapamycin inhibitor sirolimus and MEC chemotherapy in relapsed and refractory acute myelogenous leukemia. Clin Cancer Res, 2009. 15(21): p. 6732-9.
232. Park, S., et al., A phase Ib GOELAMS study of the mTOR inhibitor RAD001 in association with chemotherapy for AML patients in first relapse. Leukemia, 2013. 27(7): p. 1479-86.
233. Shepherd, C., et al., PI3K/mTOR inhibition upregulates NOTCH-MYC signalling leading to an impaired cytotoxic response. Leukemia, 2013. 27(3): p. 650-60.
234. Chandy, K.G., et al., Altered K+ channel expression in abnormal T lymphocytes from mice with the lpr gene mutation. Science, 1986. 233(4769): p. 1197-200.
235. Leanza, L., et al., Inhibitors of mitochondrial Kv1.3 channels induce Bax/Bak-independent death of cancer cells. EMBO Mol Med, 2012. 4(7): p. 577-93.
236. Comes, N., et al., The voltage-dependent K(+) channels Kv1.3 and Kv1.5 in human cancer. Front Physiol, 2013. 4: p. 283.
237. Szabo, I., et al., Biophysical characterization and expression analysis of Kv1.3 potassium channel in primary human leukemic B cells. Cell Physiol Biochem, 2015. 37(3): p. 965-78.

238. Teisseyre, A., J. Gasiorowska, and K. Michalak, Voltage-Gated Potassium Channels Kv1.3--Potentially New Molecular Target in Cancer Diagnostics and Therapy. Adv Clin Exp Med, 2015. 24(3): p. 517-24.
239. de la Cruz, A., et al., Fludarabine Inhibits KV1.3 Currents in Human B Lymphocytes. Front Pharmacol, 2017. 8: p. 177.
240. Simma, N., et al., NMDA-receptor antagonists block B-cell function but foster IL-10 production in BCR/CD40-activated B cells. Cell Commun Signal, 2014. 12: p. 75.
241. Szabo, S.J., et al., A novel transcription factor, T-bet, directs Th1 lineage commitment. Cell, 2000. 100(6): p. 655-69.
242. Glimcher, L.H., Trawling for treasure: tales of T-bet. Nat Immunol, 2007. 8(5): p. 448-50.
243. Cai, Y.C. and J. Douglass, In vivo and in vitro phosphorylation of the T lymphocyte type n (Kv1.3) potassium channel. J Biol Chem, 1993. 268(31): p. 23720-7.
244. Schwartz, A.B., et al., Margatoxin-bound quantum dots as a novel inhibitor of the voltage-gated ion channel Kv1.3. J Neurochem, 2017. 140(3): p. 404-420.
245. Chou, T.C. and P. Talalay, Quantitative analysis of dose-effect relationships: the combined effects of multiple drugs or enzyme inhibitors. Adv Enzyme Regul, 1984. 22: p. 27-55.
246. Terrisse, A.D., et al., Daunorubicin- and Ara-C-induced interphasic apoptosis of human type II leukemia cells is caspase-8-independent. Biochim Biophys Acta, 2002. 1584(2-3): p. 99-103.
247. Waterhouse, N.J. and J.A. Trapani, A new quantitative assay for cytochrome c release in apoptotic cells. Cell Death Differ, 2003. 10(7): p. 853-5.
248. Lowinus, T., et al., Memantine potentiates cytarabine-induced cell death of acute leukemia correlating with inhibition of Kv1.3 potassium channels, AKT and ERK1/2 signaling. Cell Commun Signal, 2019. 17(1): p. 5.
249. Fung-Leung, W.P., et al., T Cell Subset and Stimulation Strength-Dependent Modulation of T Cell Activation by Kv1.3 Blockers. PLoS One, 2017. 12(1): p. e0170102.
250. Levite, M., et al., Extracellular K(+) and opening of voltage-gated potassium channels activate T cell integrin function: physical and functional association between Kv1.3 channels and beta1 integrins. J Exp Med, 2000. 191(7): p. 1167-76.
251. Tan, J., et al., CD45 isoform alteration in CD4+ T cells as a potential diagnostic marker of Alzheimer's disease. J Neuroimmunol, 2002. 132(1-2): p. 164-72.
252. McCubrey, J.A., et al., Targeting survival cascades induced by activation of Ras/Raf/MEK/ERK, PI3K/PTEN/Akt/mTOR and Jak/STAT pathways for effective leukemia therapy. Leukemia, 2008. 22(4): p. 708-22.
253. Brown, K.K. and A. Toker, The phosphoinositide 3-kinase pathway and therapy resistance in cancer. F1000Prime Rep, 2015. 7: p. 13.
254. Eil, R., et al., Ionic immune suppression within the tumour microenvironment limits T cell effector function. Nature, 2016. 537(7621): p. 539-543.
255. Aliev, G., et al., Link between cancer and Alzheimer disease via oxidative stress induced by nitric oxide-dependent mitochondrial DNA overproliferation and deletion. Oxid Med Cell Longev, 2013. 2013: p. 962984.
256. Driver, J.A., Inverse association between cancer and neurodegenerative disease: review of the epidemiologic and biological evidence. Biogerontology, 2014. 15(6): p. 547-57.
257. Ganguli, M., Cancer and Dementia: It's Complicated. Alzheimer Dis Assoc Disord, 2015. 29(2): p. 177-82.
258. C, O.N., PI3-kinase/Akt/mTOR signaling: impaired on/off switches in aging, cognitive decline and Alzheimer's disease. Exp Gerontol, 2013. 48(7): p. 647-53.
259. Kim, E.K. and E.J. Choi, Compromised MAPK signaling in human diseases: an update. Arch Toxicol, 2015. 89(6): p. 867-82.
260. Driver, J.A., et al., Inverse association between cancer and Alzheimer's disease: results from the Framingham Heart Study. BMJ, 2012. 344: p. e1442.
261. Catala-Lopez, F., et al., Inverse and direct cancer comorbidity in people with central nervous system disorders: a meta-analysis of cancer incidence in 577,013 participants of 50 observational studies. Psychother Psychosom, 2014. 83(2): p. 89-105.
262. Majumder, S., et al., Lifelong rapamycin administration ameliorates age-dependent cognitive deficits by reducing IL-1beta and enhancing NMDA signaling. Aging Cell, 2012. 11(2): p. 326-35.
263. Caccamo, A., et al., mTOR regulates tau phosphorylation and degradation: implications for Alzheimer's disease and other tauopathies. Aging Cell, 2013. 12(3): p. 370-80.
264. Furman, R.R., et al., Idelalisib and rituximab in relapsed chronic lymphocytic leukemia. N Engl J Med, 2014. 370(11): p. 997-1007.
265. von Minckwitz, G., et al., Adjuvant Pertuzumab and Trastuzumab in Early HER2-Positive Breast Cancer. N Engl J Med, 2017. 377(2): p. 122-131.
266. Araki, W., Potential repurposing of oncology drugs for the treatment of Alzheimer's disease. BMC Med, 2013. 11: p. 82.
267. Brunden, K.R., et al., The characterization of microtubule-stabilizing drugs as possible therapeutic agents for Alzheimer's disease and related tauopathies. Pharmacol Res, 2011. 63(4): p. 341-51.
268. Hayes, C.D., et al., Striking reduction of amyloid plaque burden in an Alzheimer's mouse model after chronic administration of carmustine. BMC Med, 2013. 11: p. 81.

Danksagungen

Diese Arbeit wäre ohne die vielgestaltige Unterstützung nachfolgend genannter Personen nicht in ihrer vorliegenden Form realisierbar gewesen. Dafür möchte ich mich an dieser Stelle herzlich bedanken.

Meiner Betreuerin Frau Prof. Ursula Bommhardt gilt ein ganz besonderer Dank: Ich bin Ihnen sehr verbunden für die stets sehr wertvollen Weichenstellungen während des Projektes, Ihr Vertrauen in meine Fähigkeiten und Ideen sowie Ihr ausdauerndes und akribisches Redigieren meiner Texte.

Bei Prof. Burkhart Schraven möchte ich mich bedanken für die Möglichkeit, in seinem Institut arbeiten und wissenschaftliches Grundverständnis erlernen zu dürfen sowie für die Unterstützung des Projektes.

An Prof. Thomas Fischer und Prof. Florian Heidel möchte ich einen speziellen Dank richten: Danke für die anhaltende Begeisterung, die Sie in mir für das Fachgebiet Hämatologie/Onkologie geweckt haben! Daraus ist meine Motivation für das Leukämie-Projekt entstanden, welches ohne Ihre intensive Unterstützung keinesfalls durchführbar gewesen wäre.

Prof. Dirk Reinhold möchte ich recht herzlich danken für die zahlreichen Hilfestellungen von Beginn an meiner Arbeit und den fortwährenden Beistand in schwierigen Situationen, den ich immer sehr geschätzt habe.

Weiterer Dank gilt allen Ko-Autoren meiner Publikationen für die gemeinsame Arbeit und die interessanten Anregungen. Besonders bei Prof. Ingo Schmitz möchte ich mich bedanken für die sehr wertvolle Unterstützung und Zuversicht für das Projekt noch während der Anfänge. Ebenso danken möchte ich PD Dr. Stefan Busse für die engagierte und positive Zusammenarbeit sowie meiner Kollegin Dr. Tanima Bose und ihrem Betreuer Dr. Martin Heine vom Leibniz Institut für Neurobiologie Magdeburg für die eingebrachten relevanten Versuche und Diskussionen.

Ein sehr wichtiger Dank geht an alle Kollegen/Innen des IMKI. Insbesondere danke ich vielmals meinen Kollegen Dr. Varma Reddycherla und Dr. Narasimhulu Simma sowie Gabriele Weitz für die unterschiedlichsten Methoden und Labortätigkeiten, die ich von Euch erlernen durfte.

Letztlich gilt auch meiner Familie und meinen engen Freunden ein großer Dank für ihr Interesse, Verständnis und ihre Zuversicht für meine Arbeit, was mir die fortwährende Beschäftigung damit erst ermöglichte.

Ehrenerklärung

Ich erkläre, dass ich die der Medizinischen Fakultät der Otto-von-Guericke-Universität zur Promotion eingereichte Dissertation mit dem Titel

„Beeinflussung primärer und leukämischer T-Lymphozyten

über K_v1.3-Kanäle mittels Memantin“

im Institut für Molekulare und Klinische Immunologie

mit Unterstützung durch Frau Professor Dr. rer. nat. Ursula Bommhardt

ohne sonstige Hilfe durchgeführt und bei der Abfassung der Dissertation keine anderen als die dort aufgeführten Hilfsmittel benutzt habe.

Bei der Abfassung der Dissertation sind Rechte Dritter nicht verletzt worden.

Ich habe diese Dissertation bisher an keiner in- oder ausländischen Hochschule zur Promotion eingereicht. Ich übertrage der Medizinischen Fakultät das Recht, weitere Kopien meiner Dissertation herzustellen und zu vertreiben.

Magdeburg, den 01. April 2019

Theresa Lowinus

Darstellung des Bildungsweges

Theresa Lowinus *07.02.1989 in Berlin-Pankow

Der Lebenslauf ist in der Version aus Datenschutzgründen nicht enthalten.

Anlagen

Abbildungsverzeichnis

MCB
Journals.ASM.org

Immunosuppression by *N*-Methyl-D-Aspartate Receptor Antagonists Is Mediated through Inhibition of $K_v1.3$ and $K_{Ca}3.1$ Channels in T Cells

Sascha Kahlfuß,[a] Narasimhulu Simma,[a] Judith Mankiewicz,[a] Tanima Bose,[b] Theresa Lowinus,[a] Stefan Klein-Hessling,[c] Rolf Sprengel,[d] Burkhart Schraven,[a] Martin Heine,[b] Ursula Bommhardt[a]

Institute of Molecular and Clinical Immunology, Otto von Guericke University Magdeburg, Magdeburg, Germany[a]; Leibniz Institute for Neurobiology, Magdeburg, Germany[b]; Institute of Pathology, University of Würzburg, Würzburg, Germany[c]; Max Planck Institute for Medical Research, Heidelberg, Germany[d]

***N*-Methyl-D-aspartate receptors (NMDARs) are ligand-gated ion channels that play an important role in neuronal development, plasticity, and excitotoxicity. NMDAR antagonists are neuroprotective in animal models of neuronal diseases, and the NMDAR open-channel blocker memantine is used to treat Alzheimer's disease. In view of the clinical application of these pharmaceuticals and the reported expression of NMDARs in immune cells, we analyzed the drug's effects on T-cell function. NMDAR antagonists inhibited antigen-specific T-cell proliferation and cytotoxicity of T cells and the migration of the cells toward chemokines. These activities correlated with a reduction in T-cell receptor (TCR)-induced Ca^{2+} mobilization and nuclear localization of NFATc1, and they attenuated the activation of Erk1/2 and Akt. In the presence of antagonists, Th1 effector cells produced less interleukin-2 (IL-2) and gamma interferon (IFN-γ), whereas Th2 cells produced more IL-10 and IL-13. However, in NMDAR knockout mice, the presumptive expression of functional NMDARs in wild-type T cells was inconclusive. Instead, inhibition of NMDAR antagonists on the conductivity of $K_v1.3$ and $K_{Ca}3.1$ potassium channels was found. Hence, NMDAR antagonists are potent immunosuppressants with therapeutic potential in the treatment of immune diseases, but their effects on T cells have to be considered in that $K_v1.3$ and $K_{Ca}3.1$ channels are their major effectors.**

N-Methyl-D-aspartate receptors (NMDARs) and α-amino-3-hydroxy-5-methyl-4-isoxazolepropionic acid receptors (AMPARs) are the main ionotropic glutamate receptors involved in glutamatergic neurotransmission in the central nervous system. Their functions in synaptic transmission and plasticity, long-term potentiation/depression, and excitotoxicity are well established (1). Heterotetrameric NMDARs consist of the obligatory dimer of GluN1 subunit and a homodimeric or heterodimeric subunit formed by GluN2A-D, GluN3, or GluN4 (2). Activation of NMDARs requires the binding of glutamate or aspartate, the coagonist glycine or D-serine, and membrane depolarization. The NMDAR opening kinetic depends on the subunit composition and has profound consequences for downstream signaling pathways. NMDARs can sense different activation patterns and trigger specific intracellular signaling cascades through the induction of intracellular Ca^{2+} changes at small domains below the neuronal plasma membrane. Activation of protein kinase C members and the mitogen-activated protein kinase (MAPK) Erk1/2 and phosphatidylinositol 3-kinase (PI3-K)–Akt pathways culminates in the induction of transcription factors that orchestrate specific gene expression programs guiding neuronal homeostasis, death, or plasticity (3). The location and composition of NMDARs in the neuronal membrane are fundamental for the initiation of these intracellular signaling events (4). NMDAR activity is effectively blocked by ifenprodil, a noncompetitive antagonist that binds to the GluN2B subunits of NMDARs, and by the noncompetitive open-channel blockers MK801 and memantine (5). These pharmaceuticals have been neuroprotective in animal models of stroke, epilepsy, and experimental autoimmune encephalomyelitis, and memantine is used to treat Alzheimer's disease (6). NMDARs themselves can be targets of immune attack as in anti-NMDAR encephalitis, which is caused by autoantibodies directed against the GluN1 subunit of NMDARs (7).

In recent years, evidence has emerged that immune cells, including dendritic cells (DCs), release glutamate and can be regulated by glutamate present in the bloodstream, peripheral organs, and central nervous system (8, 9). NMDARs, AMPARs (GluA3 subunit), and metabotropic glutamate receptors (mGluRs) (group 1) were found to be expressed in human peripheral blood lymphocytes and Jurkat T cells and modulate their function (10–14). For murine $CD4^+$ $CD8^+$ thymocytes in contact with antigen-presenting DCs, inhibition of NMDARs regulated T-cell receptor (TCR)-induced Ca^{2+} flux and, thereby, the apoptosis of double-positive cells (9).

For a beneficial therapeutic application of NMDAR antagonists, it is important to understand how they influence T-cell function and, thereby, the adaptive immune response. Here, we show profound inhibition of $CD4^+$ and $CD8^+$ T-cell effector function by NMDAR antagonists. The inhibition correlated with reduced activation of major TCR-induced signaling pathways, including Ca^{2+} mobilization and activation of Erk1/2, Akt, and NFATc1. Consistent with results reported previously (9), we detected mRNA expression and positive immunoreactivity for NMDAR subunits in thymocytes and peripheral T cells. However, GluN1 protein expression was not evident in wild-type (wt) thymocytes

Received 25 September 2013 **Returned for modification** 9 October 2013
Accepted 6 December 2013

Published ahead of print 16 December 2013

Address correspondence to Martin Heine, Martin.Heine@ifn-magdeburg.de, or Ursula Bommhardt, Ursula.Bommhardt@med.ovgu.de.

S.K, N.S., J.M., and T.B. contributed equally to this work.

Supplemental material for this article may be found at http://dx.doi.org/10.1128/MCB.01273-13.

doi:10.1128/MCB.01273-13

compared to control thymocytes from GluN1 knockout (KO) mice. Assuming that the strong influence of NMDAR antagonist pharmacology on Ca^{2+}-mediated signaling involves off-target effects, we demonstrate that NMDAR antagonists inhibit the activity of $K_v1.3$ and $K_{Ca}3.1$ potassium channels. Hence, NMDAR antagonists, which are potent immune modulators/suppressors, seem to act via their inhibitory effects on $K_v1.3$ and $K_{Ca}3.1$ channels.

MATERIALS AND METHODS

Mice. wt C57BL/6 mice, BALB/c mice, OT2 TCR transgenic (tg) mice (15), OT1 TCR tg mice (16), and NFATc1-EGFP mice (17) on a C57BL/6 background, at the age of 6 to 10 weeks, were used. GluN1 KO mice, generated by crossing $GluN1^{flx/flx}$ with Cre deleter mice (18, 19), both on a C57BL/6 background, and littermate mice were used within hours after birth. All animal work was conducted in compliance with the German Guidelines for the Use of Experimental Animals and was approved by the Tierschutzaufsichtsbehörde of the State Saxony-Anhalt.

Antibodies, flow cytometry, and Th-cell differentiation. The following antibodies (Abs) for cell isolation, cell stimulation, and flow cytometry were obtained: CD4-fluorescein isothiocyanate (FITC) (GK1.5), CD8-allophycocyanin (APC)-phycoerythrin (PE) (53-6.7), CD25-PE (7D4), TCR-FITC (H57-597), CD69-PE (H1.2F3), CD44-FITC (IM7), CD3 (145.2C11), and CD28 (37.51), from BD Bioscience (San Jose, CA); CD4-APC (GK1.5), from Biolegend (London, United Kingdom); CD3 (145.2C11), CD28 (37.51), CD127-PE (A7R34), interleukin-2 (IL-2)–PE (JES6-5H4), gamma interferon (IFN-γ)-PE (XMG1.2), IL-4–PE (11B11), IL-10–PE (JES5-16E3), IL-13–PE (eBio13A), B220-FITC-PE (RA3-6B2), and IgG2a-PE-FITC (eBR2a), from eBioscience (San Diego, CA); PE-conjugated $F(ab')_2$ fragment donkey anti-rabbit IgG(H+L), IgG2b (eBMG2b), and IgG2a (pk), from Dianova (Hamburg, Germany); rabbit anti-mouse GluN1 (AGC-001), GluN2A (AGC-002), and GluN2B (AGC-003), from Alomone Laboratories (Jerusalem, Israel); mouse anti-mouse GluN1 (M68), from Synaptic Systems (Göttingen, Germany); and phosphorylated Erk1/2 (pErk1/2) (Thr^{202}/Tyr^{204}), pS6 ($S^{240/244}$), pAkt-Alexa Fluor 488 (S^{473}), and IgG2a-Alexa Fluor 488, from Cell Signaling (Beverly, MA). Intracellular staining of NMDAR subunits, cytokines, or other signaling proteins was performed with the FoxP3 staining kit from eBioscience after surface labeling with CD4, CD8, or B220 Abs. Primary Abs were detected with PE-conjugated $F(ab')_2$ fragment donkey anti-rabbit IgG(H+L). The specificity of GluN1, GluN2A, and GluN2B Abs was controlled with subunit-specific peptides (Alomone Laboratories), which were incubated with Abs for 30 min at room temperature in FoxP3 staining buffer. Ab-peptide conjugates were added to the cells, followed by staining with PE-conjugated $F(ab')_2$ fragment donkey anti-rabbit IgG(H+L) (data not shown). For measurement of intracellular cytokine production, OT2 TCR tg (OT2) $CD4^+$ T cells were stimulated with ovalbumin (OVA) peptide-loaded (amino acids [aa] 323 to 339) (10 μg/ml; a gift of M. Gunzer) bone marrow-derived DCs (BMDCs) (pOVA-DCs) in the cell ratios indicated. Anti-mouse IL-4 (2 μg/ml) (11B11) for evaluation of Th1 polarization and anti-mouse IL-12 (3 μg/ml) (C18.2), anti-mouse IFN-γ (5 μg/ml) (AN-18) (all from Biolegend), and recombinant IL-4 (rIL-4) (20 U/ml; eBioscience) for skewing toward Th2 cells were added to cell cultures on day 0. On day 5, cells were restimulated with phorbol myristate acetate (PMA) and ionomycin (P/IO) (100 ng/ml each; Calbiochem, Darmstadt, Germany) for 4 h in the presence of brefeldin A (2 μg/ml; Calbiochem) and analyzed for the expression of intracellular cytokines by flow cytometry using FACSFortessa and CellQuest Pro software (BD Bioscience).

Generation of bone marrow-derived DCs. Bone marrow (BM) cells were suspended in RPMI 1640 medium (Biochrom, Berlin, Germany) reconstituted with 1% nonessential amino acids (Gibco, Invitrogen, Carlsbad, CA), 5% fetal calf serum (FCS) (PAN Biotech, Aidenbach, Germany), 1% L-glutamine (Gibco), 0.1% gentamicin (Carl Roth, Karlsruhe, Germany), 0.1% 2-mercaptoethanol (Gibco), IL-4 (48 ng/ml), and granulocyte-macrophage colony-stimulating factor (GM-CSF) (10 ng/ml) from a hybridoma supernatant (a gift of M. Gunzer). A total of 3×10^6 BM cells/5 ml BMDC medium were cultured for 7 days. At day 3, 2 ml medium was replaced by fresh BMDC medium, and at day 6, total medium was replaced and cells were stimulated with lipopolysaccharide (LPS) (20 ng/ml; Sigma-Aldrich, Steinheim, Germany) for 24 h. DCs, used at day 9 or 10, were restimulated with LPS 24 h before the start of experiments. Maturation of BMDCs was verified at day 7 by staining of cells with Abs against major histocompatibility complex class II (MHC-II), CD11c, CD80, and CD86 (BD Bioscience).

Cell isolation and proliferation assay. $CD4^+$ or $CD8^+$ T cells were isolated from pooled lymph nodes by negative selection using a cocktail of biotinylated Abs, NK1.1 (PK136), CD8α (53-6.7), CD4 (GK1.5), I-A/I-E (2G9), CD45R/B220 (RA3-6B2), and Ter-119 (all from BD Bioscience), and streptavidin magnetic beads (Miltenyi Biotec, Bergisch Gladbach, Germany). The purity of $CD4^+$ or $CD8^+$ T cells was routinely >90%. Mature BMDCs ($MHC\text{-}II^+$ $CD11c^+$ $CD80^+$ $CD86^+$) were pulsed with OVA peptide (aa 323 to 339 [10 μg/ml] or aa 257 to 264 [SIINFEKL] [5 μg/ml]; AnaSpec, Fremont, CA) for 2 h and cultured with OT2 $CD4^+$ or OT1 TCR tg (OT1) $CD8^+$ T cells, respectively. $CD4^+$ T cells (0.5×10^5 to 1×10^5) were stimulated with plate-bound CD3 Abs (3 or 10 μg/ml) or CD3 and CD28 Abs (3 and 5 μg/ml, respectively). For mixed-lymphocyte reactions, 1×10^5 $CD4^+$ T cells from C57BL/6 mice were cocultured with irradiated (3 Gy) splenocytes from BALB/c mice at 1:3 to 1:5 ratios for 5 days. Cells were cultured in the presence or absence of ifenprodil, MK801, or memantine (diluted in double-distilled water [ddH_2O] or phosphate-buffered saline [PBS]) (Tocris, Bristol, Great Britain), at the concentrations indicated, in complete RPMI 1640 medium–10% FCS. Proliferation was measured by [^{3}H]thymidine incorporation (0.2 μCi/well; MP Biomedicals, Heidelberg, Germany) for 8 to 16 h at 24 or 48 h or after 5 days. For analysis of cell cycle progression, OT1 or OT2 T cells were labeled with carboxyfluorescein succinimidyl ester (CFSE) (5 μM; Invitrogen), cultured with pOVA-loaded DCs for the indicated days, and then analyzed by flow cytometry.

Measurement of apoptosis. Apoptosis was determined with apoptosis detection kit 1 from BD Pharmingen. A total of 1×10^6 OT2 $CD4^+$ T cells were left untreated or were activated with pOVA (aa 323 to 339)-loaded BMDCs in a DC-to-T-cell ratio of 1:10 in the presence or absence of NMDAR inhibitors for the indicated times. After harvest, cells were stained with annexin V-FITC and propidium iodide (PI), according to the manufacturer's protocol, and analyzed by flow cytometry. The percentage of vital cells was determined by gating on annexin V-negative (annexin V^-) PI^- cells.

CTL assay. Lymph node cells from OT1 TCR tg mice were stimulated with rIL-2 (20 ng/ml; Biolegend) and pOVA (1 μg/ml SIINFEKL) in complete RPMI 1640–10% FCS medium for 72 h. Cells were then expanded in the presence of rIL-2 (20 ng/ml) for 1 to 2 days, and killing assays with pOVA-loaded (5 μg/ml SIINFEKL) RMA-S target cells were performed in triplicates in 96-well round-bottom plates. When indicated, cytotoxic T lymphocytes (CTLs) were pretreated with ifenprodil (10 to 30 μM) for 20 min at 37°C. CTL assays were performed for 4 h at 37°C, cells were stained with CD8-APC and annexin V-FITC, and the percentage of apoptotic annexin V-positive (annexin V^+) RMA-S cells was determined with flow cytometry. The relative killing efficiency was calculated by relating the percentage of apoptotic target cells to the ratio of CTLs to target cells.

RNA isolation and PCR. RNA from brain, thymocytes, and peripheral T cells was isolated with TRIzol reagent (Life Technologies, Darmstadt, Germany) and reverse transcribed with a First-Strand cDNA Synthesis kit (Thermo Scientific, Karlsruhe, Germany). Oligonucleotides for reverse transcription-PCR (RT-PCR) and PCR, obtained from Apara Bioscience GmbH, Denzlingen, Germany, were as follows: Fwd-β-actin (5′-CCAGG TCATCACTATTGGCAAGGA-3′), Rev-β-actin (5′-GAGCAGTAATCT CCTTCTGCATCC), Fwd-GAPDH (5′-CAAGGTCATCCATGACAACT TTG), Rev-GAPDH (3′ GTCCACCACCCTGTTGCTGTAG), Fwd-GluN1C1 (5′-TGTGTCCCTGTCCATACTCAAG-3′), Rev-GluN1C1

(5′-GTCGGGCTCTGCTCTACCACTC-3′), Fwd GluN2A (5′-GGAGAA GGGTACTCCAGCGCTGAA-3′), Rev GluN2A (5′-AGTCTGTGAGGA GATAAAATCCAGC-3′), Fwd-GluN2B (5′-GCAAGCTTCTGTCATGC TCAACATC-3′), and Rev-GluN2B (5′-GCTCTGCAGCTTCTTCAGCT GATTC-3′) (20). wt and floxed GluN1 alleles and GluN1 excision were analyzed by PCR using DNA isolated from tail, thymocytes, or brain; primers used were as follows: forward (Fwd) primer 5′-CTGGGACTCA GCTGTGCTGG-3′ and reverse (Rev) primer 5′-AGGGGAGGCAACAC TGTGGAC-3′ for GluN1$^{flox/wt}$ and Fwd primer 5′-GAGAAAGACATGG GGCATTATCC-3′ for GluN1 excision.

Western blot analysis. Isolated CD4$^+$ T cells (5×10^6) were stimulated with plate-bound CD3 Abs (10 μg/ml for short-term and 3 μg/ml for long-term stimulation) or CD3 and CD28 Abs (3 and 5 μg/ml, respectively) in the presence or absence of ifenprodil (30 to 50 μM) for the indicated time points. Cells were lysed to obtain total or cytoplasmic and nuclear protein extracts as described previously (21). The protein lysate obtained from T cells (5 to 15 μg), thymocytes (20 μg), or brain (5 μg) was subjected to 8 to 10% SDS-PAGE. Separated proteins were transferred onto a nitrocellulose membrane and blocked with 5% nonfat milk powder in Tris-buffered saline–Tween (TBST). The expression/activation of signaling proteins was analyzed by using primary Abs specific for pSrc (Y^{416}), phosphorylated phospholipase C-γ1 (pPLC-γ1) (Y^{783}), pErk1/2 (Thr^{202}/Tyr^{204}), pAkt (Ser^{473}) (DE9), pS6 (S$^{240/244}$), pmTOR (S^{2448}), phosphorylated glycogen synthase kinase 3β (pGSK3β) (S^9) (all from Cell Signaling Technology, Frankfurt, Germany), NFATc1 (7A6; Alexis Biochemicals, Lörrach, Germany), GluN1 (Synaptic Systems), β-actin (AC 40; Sigma-Aldrich), and lamin B (Santa Cruz, Biotechnology, Santa Cruz, CA), followed by horseradish peroxidase (HRP)-coupled mouse anti-rabbit, goat anti-mouse, or donkey anti-goat secondary Abs (Jackson ImmunoResearch Laboratories, Dianova) and detection with the ECL system (Thermo Scientific Pierce, Rockford, IL, USA). The immune-reactive bands were scanned and quantified with Kodak software.

Measurement of Ca^{2+} flux. Lymph node cells from wt mice were stained with 4 μM Indo-1 AM (Invitrogen, Molecular Probes) for 45 min at 37°C. After being washed, the cells were stained for CD8 and B220 or CD4 and B220 surface expression for 15 min, washed, and resuspended in Hanks' buffer (Biochrom) supplemented with 1 mM $CaCl_2$. CD3-biotin Abs (145.2C11) (10 μg/ml) plus streptavidin (25 μg/ml) (Dianova) were added to induce Ca^{2+} flux. The NMDAR antagonist ifenprodil (10 or 30 μM) was added for 5 min, followed by CD3 Ab and streptavidin treatment. Toward the end of each measurement, ionomycin (2 μM; Calbiochem) was added as a positive control for cell reactivity. Ca^{2+} flux was measured on an LSRII flow cytometer (BD Biosciences), data files were transferred to FlowJo V3.6.1 (Tree Star, Ashland, OR), mean Ca^{2+} flux was determined for unlabeled CD4$^+$ or CD8$^+$ T cells, and data were further processed with IgorPro5.04B software (WaveMetrics Inc., Portland, OR). For each graph, ΔCa^{2+} flux was defined as the difference between the maximum and minimum values of Ca^{2+} intensity.

Migration assay. Splenocytes (4×10^6), untreated or preincubated with ifenprodil (30 and 50 μM) for 30 min in Dulbecco's modified Eagle's medium (DMEM) (Biochrom) supplemented with 0.1% bovine serum albumin (BSA) and 10 mM HEPES (pH 7.4), were transferred into transwell chambers (6.5-mm diameter and 3.0-μm pore size; Corning Costar, Tewksbury, MA) coated with fibronectin (6.5 μg/ml; Roche Diagnostics, Basel, Switzerland). Cells were allowed to migrate toward SDF1α (100 ng/ml) or CCL21 (300 ng/ml) (both from PeproTech, Hamburg, Germany) for 150 min at 37°C, with migration in the absence of a chemokine serving as the control. Migration was stopped by the addition of 0.1 M EDTA. Migrated cells were stained with CD4 and CD8 Abs and measured for 30 s with the FACSFortessa. Relative migration was calculated by dividing the number of cells that migrated in the presence of chemokine (set as 1.0) by the number of cells that migrated in the absence of chemokine.

Confocal microscopy. CD4$^+$ T cells from OT2 TCR tg mice were incubated for 10 min with LPS-matured and pOVA-loaded (10 μg/ml) (aa 323 to 339) BMDCs in RPMI 1640–10% FCS medium at a DC-to-T-cell ratio of 1:3. Obtained DC–T-cell pairs or freshly isolated thymocytes were transferred onto poly-L-lysine-coated slides (Marienfeld, Königshofen, Germany). Cells were fixed with 2% paraformaldehyde for 15 min at 37°C, permeabilized with 0.1% Triton X-100 for 10 min, blocked with 1% BSA (Carl Roth GmbH) for 30 min at room temperature, and incubated with Abs against GluN1 (Synaptic Systems) and GluN2B (Alomone Labs) subunits or with isotype control Abs overnight at 4°C or for 2 h at room temperature. Thereafter, cells were stained with goat anti-rabbit F(ab′)$_2$–Alexa Fluor 488 (Invitrogen) or donkey anti-mouse antibody–Alexa Fluor 488 Ab (Jackson ImmunoResearch Laboratories, West Grove, PA) for 1 h at room temperature in the presence of phalloidin-Cy5 (Dyomics, Jena, Germany). Confocal settings were the same for NMDAR-specific, isotype, and control stainings with NMDAR subunit-specific peptides. Images show the maximum-intensity projection of 3 planes (5 planes in Fig. S3 in the supplemental material) from a Z-stack. Image acquisition was performed with a Leica TCS SP5 or STED confocal microscope (Leica, Houston, TX), and data were processed with ImageJ software.

Electrophysiology. All experiments were carried out in the whole-cell configuration of the patch-clamp technique with an EPC10 amplifier and PatchMaster v. 2.11 (HEKA Electronic, Lambrecht, Germany) at room temperature (20°C to 24°C) and with CD4$^+$ T cells activated with CD3 and CD28 Abs (3 and 5 μg/ml, respectively) for 48 h (22) or EL-4 lymphoma cells. Patch pipettes from borosilicate glass used for recordings had a resistance of between 3 and 5 MΩ. $K_v1.3$ or $K_{Ca}3.1$ currents were recorded with an external solution of the following composition: 160 mM NaCl, 4.5 mM KCl, 5 mM HEPES, 1 mM $MgCl_2$, and 2 mM $CaCl_2$ or 160 mM Na-aspartate, 4.5 mM KCl, 2 mM $CaCl_2$, 1 mM $MgCl_2$, and 10 mM HEPES, respectively. The pipette solution contained 162 mM KF, 11 mM EGTA, 10 mM HEPES, 1 mM $CaCl_2$, and 2 mM $MgCl_2$ (23) or 145 mM K-aspartate, 8.5 mM $CaCl_2$, 2 mM $MgCl_2$, 10 mM EGTA, and 10 mM HEPES (24, 25), respectively, adjusted to pH 7.4 for the external solution and to pH 7.2 for the internal solution; osmolarity was set to 300 to 340 mOsm for both solutions. $K_v1.3$ currents were measured with depolarizing voltage steps up to +60 mV from a holding potential of −80 mV every 30 s. $K_{Ca}3.1$ currents were elicited by a 200-ms voltage ramp from −120 to +40 mV from a holding potential of −80 mV every 15 s. The sampling rates were 50 kHz for $K_v1.3$ and 20 kHz for $K_{Ca}3.1$. Antagonists [ifenprodil, memantine, MK801, ketamine, and D-(−)-2-amino-5-phosphonopentanoic acid (D-APV) Tocris] at a constant inhibitor concentration were added during the recording. Analysis of transient currents was performed by using HEKA FitMaster v2x53. Amplitude values were transferred to GraphPad Prism 5.0 for analysis of the dose-response curve and Hill slope.

Statistical analysis. Statistical differences in cell number, percentage, mean fluorescence intensity, and proliferation were analyzed by the use of Student's *t* test or, in the case of more than two groups, by one-way analysis of variance (ANOVA) followed by a posttest (Dunnett's test) to analyze individual differences. If not stated otherwise, data are given as mean values ± standard deviations (SD).

RESULTS

NMDAR antagonists inhibit T-cell proliferation. NMDAR expression was determined by the use of RT-PCR. mRNA for GluN1 and GluN2 subunits was detected in thymocytes and naive and activated CD4$^+$ and CD8$^+$ T cells (Fig. 1A). To elucidate the impact of NMDAR antagonists on T-cell activation, CD4$^+$ T cells were stimulated with CD3 Abs at high (10 μg/ml) (Fig. 1B) and lower (3 μg/ml) (Fig. 1C) Ab concentrations in the absence or presence of the GluN2B antagonist ifenprodil or the open-channel blockers MK801 and memantine. Both types of antagonists significantly reduced T-cell proliferation in a concentration-dependent manner. In addition, low concentrations of the antagonists strongly inhibited the proliferative response of CD4$^+$ T cells to

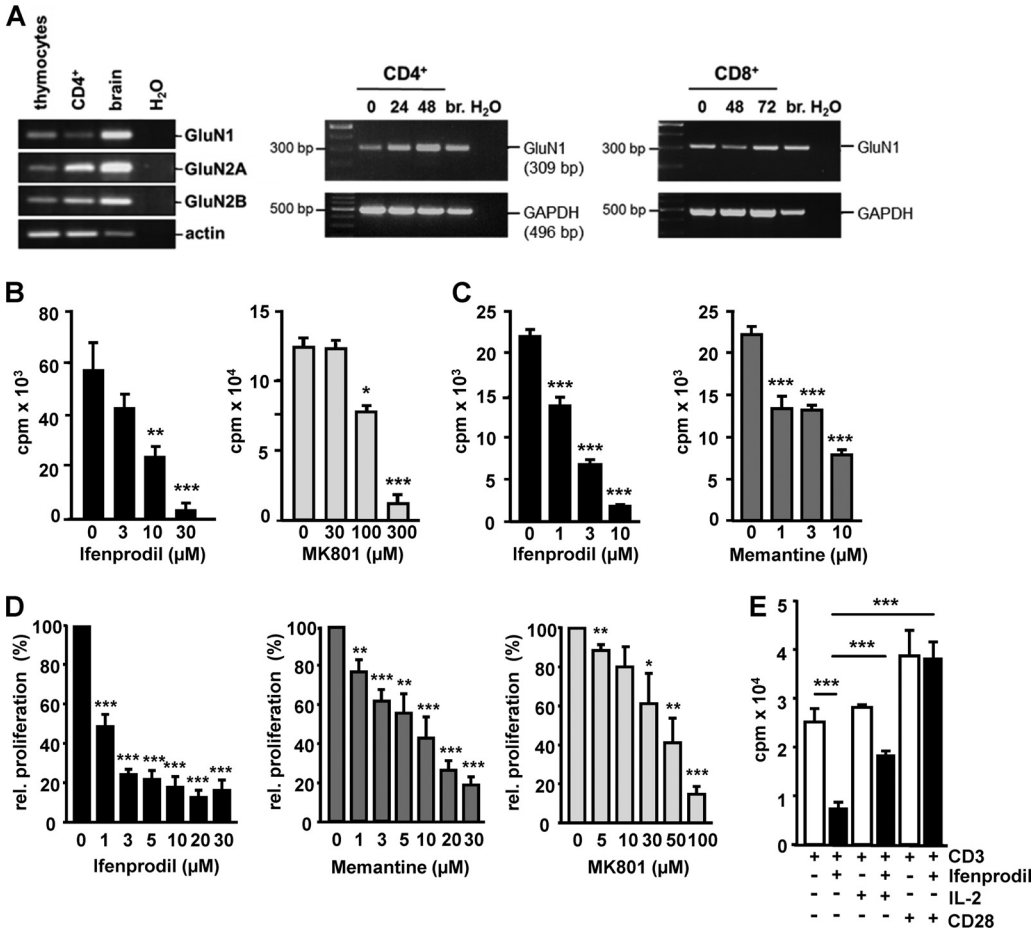

FIG 1 NMDAR antagonists impair T-cell proliferation. (A) RT-PCR analysis of mRNA expression of NMDAR subunits GluN1, GluN2A, and GluN2B in thymocytes, brain (br.), peripheral $CD4^+$ T cells, as well as $CD4^+$ and $CD8^+$ T cells activated with CD3 and CD28 Abs (3 and 5 μg/ml, respectively) for the indicated times. Actin or glyceraldehyde-3-phosphate dehydrogenase (GAPDH) mRNA expression levels served as the RT-PCR control. (B to E) $CD4^+$ T cells were activated in the absence or presence of the NMDAR antagonist ifenprodil, MK801, or memantine at the concentrations indicated. Proliferation was determined by measurement of [^{3}H]thymidine incorporation (cpm) at 24 h or after 5 days (D). (B and C) Cells were activated with CD3 Abs at 10 μg/ml (B) or 3 μg/ml (C). (D) $CD4^+$ T cells were cocultured with irradiated splenocytes from BALB/c mice for 5 days. (E) $CD4^+$ T cells were stimulated with CD3 Abs (3 μg/ml) or CD3 and CD28 Abs (3 and 5 μg/ml, respectively) with or without ifenprodil (50 μM) and IL-2 (20 U/ml). The data in panels B, C, and E show the means and SD of triplicates and are representative of 2 to 3 experiments. Relative proliferation in panel D was calculated from 3 experiments. Significant *P* values were calculated by the use of Student's *t* test (*, $P < 0.05$; **, $P < 0.01$; ***, $P < 0.001$).

alloantigens of BALB/c splenocytes in mixed-lymphocyte reactions (Fig. 1D). Ifenprodil was the most effective of the three agents in inhibiting proliferation. In the presence of IL-2 or upon costimulation with CD28 Abs, ifenprodil had a significantly weaker inhibitory effect on T-cell expansion than that found for T cells stimulated with CD3 Abs only (Fig. 1E), suggesting that ifenprodil impairs TCR signaling and IL-2 production.

NMDAR antagonists lower TCR signaling strength. In order to understand how NMDAR antagonists influence T-cell activation, we analyzed their effects on TCR-induced signaling. $CD4^+$ and $CD8^+$ T cells, loaded with Indo-1 AM to monitor intracellular Ca^{2+} changes by flow cytometry, responded to TCR ligation with a rapid increase in Ca^{2+} concentrations. This effect was significantly reduced by 10 μM ifenprodil and almost entirely blocked by 30 μM (Fig. 2A). To address further signaling effects, $CD4^+$ T cells were stimulated with plate-bound CD3 Abs or CD3 and CD28 Abs in the presence or absence of an NMDAR antagonist, and the activation of signaling mediators was determined by Western blotting (Fig. 2B to D and F). Ifenprodil-treated $CD4^+$ T cells had less activation of several TCR-induced signaling molecules, including activation of the kinases Lck/Fyn, Erk1/2, and Akt, than did untreated cells (Fig. 2B). Speculating that long-lasting signaling from the TCR could be influenced by NMDAR antagonists, we analyzed $CD4^+$ T cells activated for 8, 16, and 24 h. Phosphorylation of PLC-γ1, GSK3β, mTOR, and S6 was reduced at 16 h and 24 h in the presence of ifenprodil compared with the response in untreated cells (Fig. 2C). This finding indicates a lower or, in the case of GSK3β, an enhanced activity of these signaling molecules during later phases of T-cell activation and, thus, a long-ranging effect of ifenprodil on PLC-γ1- and Akt-mediated signaling events. In accordance with the rescued T-cell proliferation, CD3 and CD28 Ab-stimulated T cells had higher levels of pPLC-γ1, pGSK-3β, pmTOR, and pS6 after ifenprodil treatment than did cells activated with CD3 Abs only (Fig. 2D).

The activity of cytosolic NFAT factors is controlled by several serine/threonine protein kinases, intracellular Ca^{2+} concentra-

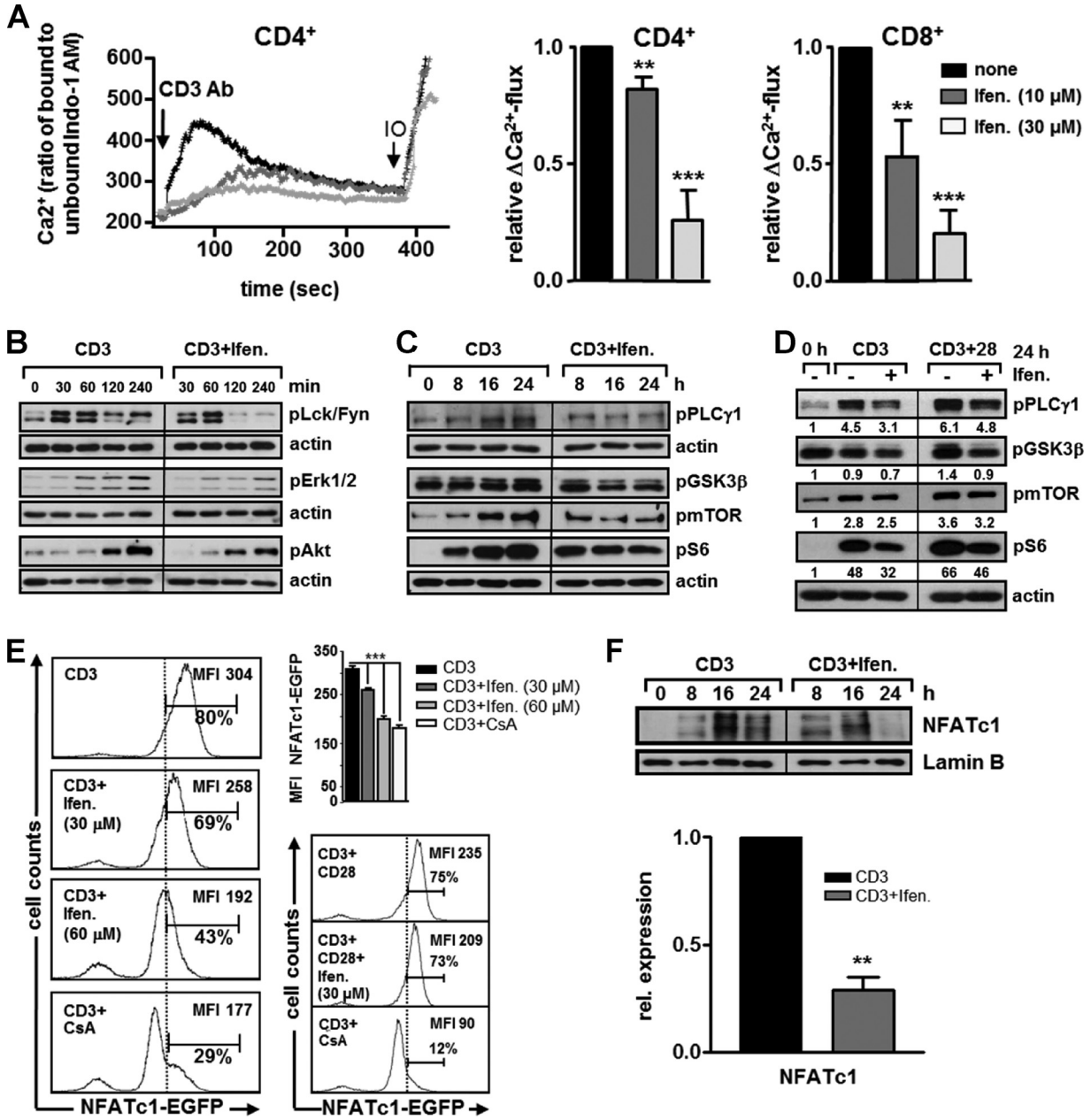

FIG 2 NMDAR antagonists attenuate TCR signaling. (A) Indo-1 AM-loaded $CD4^+$ T cells were activated with CD3 Abs (10 μg/ml) in the absence or presence of ifenprodil. Ca^{2+} flux was determined by flow cytometry. Ionomycin (IO) was added toward the end of each measurement. Data in the graphs show the mean relative ΔCa^{2+} flux and SD for $CD4^+$ and $CD8^+$ T cells, calculated from 3 experiments. ΔCa^{2+} flux from cells activated without ifenprodil (none) was set to a value of 1. (B to D and F) $CD4^+$ T cells were stimulated with 10 μg/ml (B) and 3 μg/ml (C and F) plate-bound CD3 Abs or CD3 and CD28 Abs (3 and 5 μg/ml, respectively) (D) without or with ifenprodil (50 μM [30 μM in panel D]). Total protein lysates (B) and cytoplasmic (C and D) and nuclear (F) protein extracts were analyzed for the indicated signaling molecules by Western blotting, with actin and lamin B expression serving as the controls for protein loading. Data in panels B and C are representative of three experiments, and those in panel D are representative of two experiments. (F) Nuclear protein extracts were analyzed for NFATc1 expression. Data in the graph represent the mean relative expression levels of NFATc1 and SD at 24 h, calculated from two experiments. (E) Splenic cells from NFATc1-EGFP reporter mice were activated with CD3 Abs (3 μg/ml) (2 experiments) (left), or pooled $CD4^+$ T cells isolated from three mice were stimulated with CD3 Abs (3 μg/ml) or CD3 and CD28 Abs (3 and 5 μg/ml, respectively) (one experiment) (right), without or with ifenprodil or cyclosporine A (100 ng/ml) for 24 h. Induction of NFATc1-EGFP was determined by flow cytometry. The percentage of cells with high-level expression of NFATc1-EGFP and the mean fluorescence intensity (MFI) of NFATc1-EGFP are indicated. Data in the graph give the fluorescence intensity of NFATc1-EGFP in the indicated cell populations as means and SD for three mice. Significant *P* values were calculated by the use of Student's *t* test (**, $P < 0.01$; ***, $P < 0.001$).

tion ($[Ca^{2+}]_i$), and the Ca^{2+}/calmodulin-dependent phosphatase calcineurin. Calcineurin dephosphorylates NFAT proteins and controls their nuclear localization, which leads to the transcriptional induction of *Nfatc1* (26, 27), among other genes. Activated $CD4^+$ T cells from NFATc1-enhanced green fluorescent protein (EGFP) reporter mice (17) exhibited a strong transcriptional induction of NFATc1-EGFP (Fig. 2E). Ifenprodil treatment reduced the percentage of cells expressing high levels of NFATc1-EGFP;

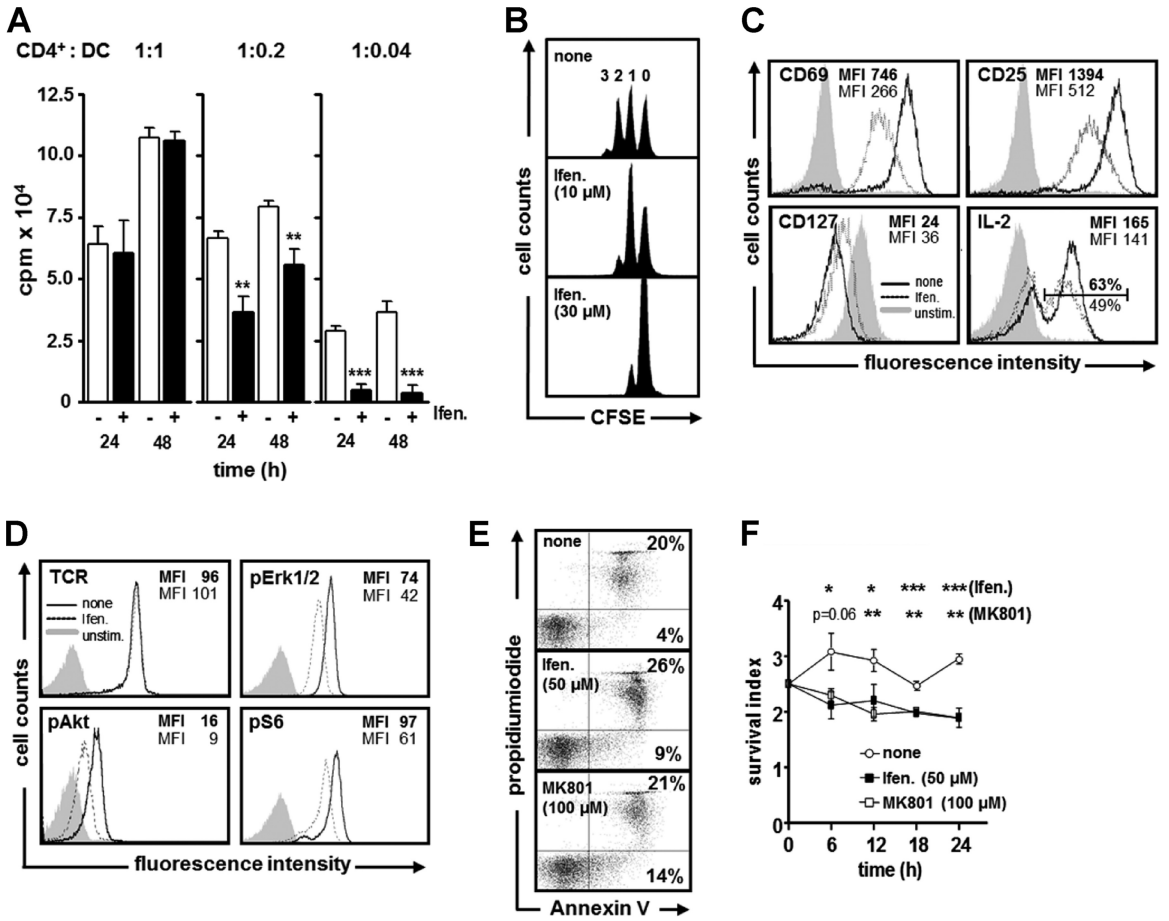

FIG 3 NMDAR antagonists alter antigen-induced T-cell signaling, proliferation, and survival. (A) OT2 CD4$^+$ T cells were activated with pOVA-loaded DCs at the indicated ratios for 24 h or 48 h in the absence or presence of ifenprodil (30 μM). DNA synthesis, measured as [^{3}H]thymidine incorporation (cpm), is shown as means and SD of triplicates. Data in the graph are representative of three experiments. (B) CFSE-labeled OT2 CD4$^+$ T cells were activated with pOVA-loaded DCs (T-cell-to-DC ratio of 1:0.1) in the absence or presence of ifenprodil and analyzed by flow cytometry at day 3. The number of cell divisions is indicated. Data are representative of two experiments. (C and D) OT2 CD4$^+$ T cells, cultured with pOVA-loaded DCs for 24 h (C) or 4 h (D) without or with 30 μM (C) or 50 μM (D) ifenprodil, were analyzed for surface or intracellular expression of the indicated proteins by flow cytometry. The percentage of IL-2-expressing cells and mean fluorescence intensity (MFI) values of the indicated proteins are given for untreated (bold line and boldface type) and ifenprodil-treated (dotted line and lightface type) cells. Shaded histograms represent isotype staining. Data are the representative of two or three experiments. (E and F) OT2 CD4$^+$ T cells were cultured with pOVA-loaded DCs for 24 h (E) or for the indicated time points (F), with or without ifenprodil (50 μM) or MK801 (100 μM), and apoptosis of cells was determined by annexin V and propidium iodide staining. (E) The percentages of early (annexin V$^+$) and late (annexin V$^+$/PI$^+$) apoptotic cells are indicated. (F) Data in the graph show the mean survival indexes ± SD, which were calculated by dividing the percentages of live (annexin V$^-$/PI$^-$) and apoptotic cells determined at the indicated time points of culture. Data are representative of two independent experiments. Significant *P* values were calculated by the use of Student's *t* test (*, $P < 0.05$; **, $P < 0.01$; ***, $P < 0.001$).

indeed, at high concentrations of the inhibitor, NFAT levels approached those found in T cells treated with cyclosporine, which inhibits NFAT activation (28). However, upon CD3 and CD28 Ab stimulation, NFATc1-EGFP induction was only mildly affected by ifenprodil. The effect on prolonged NFAT activation was also evident in Western blot analyses, as CD3 Ab-activated CD4$^+$ T cells had much less nuclear NFATc1 at 24 h in the presence of ifenprodil than the amount in cells not treated with ifenprodil (Fig. 2F). Hence, ifenprodil impairs T-cell activation by attenuating important TCR-induced signaling events, including Ca^{2+} flux and the activation of PLC-γ1, Erk1/2, Akt, and NFATc1, and this inhibition can be compensated for, at least partially, by CD28 signaling (29–32).

NMDAR antagonists increase the threshold for antigen-induced T-cell signaling and proliferation. NMDARs have been shown to accumulate in the synaptic region of antigen-specific thymocyte-DC contacts (9). Thus, we asked how much NMDAR inhibitors influence the proliferation of OT2 CD4$^+$ T cells upon activation by DCs presenting the cognate ovalbumin peptide (pOVA-DCs) for tg OT2 TCR (15). At a T-cell-to-DC ratio of 1:1, ifenprodil treatment had no significant effect on T-cell proliferation (Fig. 3A). However, at T-cell-to-DC ratios of 1:0.2 and 1:0.04, ifenprodil reduced DNA synthesis by 39% and 88% at 24 h and by 23% and 92% at 48 h, respectively, compared with synthesis in untreated cells. Likewise, cell division of OT2 CD4$^+$ T cells cultured with pOVA-DCs at a ratio of 1:0.1 for 3 days was markedly impaired when NMDAR inhibitors were applied (Fig. 3B). In accordance with decreased T-cell expansion, ifenprodil-treated OT2 CD4$^+$ T cells had increased surface expression levels of CD127, a reduction in the expression levels of CD25 and CD69, and less

IL-2 production (Fig. 3C). Experiments performed with MK801 and irradiated pOVA-DCs yielded similar results (see Fig. S1A and B in the supplemental material). As with peripheral T cells, proliferation of OT2 TCR tg thymocytes activated by pOVA-DCs was strongly impaired by ifenprodil, depending on the DC-to-thymocyte ratio (see Fig. S1C in the supplemental material).

Next, we assessed whether NMDAR antagonists affect antigen-induced signaling in a way similar to that of stimulation with CD3 Abs (Fig. 2). OT2 $CD4^+$ T cells, cultured with pOVA-DCs for 4 h in the presence of ifenprodil, had similar TCR surface expression levels but much less pErk1/2, pAkt, and pS6 than found in untreated cells (Fig. 3D). Thus, NMDAR antagonists dampen TCR signaling and thereby alter the activation threshold needed for T-cell proliferation.

The effect of NMDAR inhibitors on the survival of peripheral antigen-specific T cells is unknown. Thus, we cultured OT2 $CD4^+$ T cells with pOVA-DCs and analyzed induction of apoptosis. When applied at high doses, ifenprodil (50 μM) or MK801 (100 μM) increased the percentage of cells undergoing early (annexin V^+/PI^-) and late (annexin V^+/PI^+) apoptosis from 4% and 20% in untreated cells to 9% and 26% at 24 h, respectively (Fig. 3E). In time course experiments, the survival index of antagonist-treated OT2 $CD4^+$ T cells was found to be reduced 6 h after the onset of stimulation (Fig. 3F), suggesting that NMDAR antagonists slightly affect the survival of activated $CD4^+$ T cells.

NMDAR antagonists modulate the cytokine secretion profile of antigen-differentiated Th cells. Next, we addressed whether NMDAR inhibitors influence cytokine secretion by Th1 and Th2 cells. Since proliferation was strongly blocked when NMDAR antagonists were added at the beginning of T-cell–DC coculture, we applied a low concentration (7 μM) of ifenprodil at 12 to 16 h after activation of T cells (Fig. 4A and B). Under these conditions, cell division of ifenprodil-treated OT2 $CD4^+$ T cells resembled that of untreated cells (see Fig. S2A and B in the supplemental material), an effect that enabled analysis of cytokines in cycling cell populations. In T-cell–DC cocultures skewed toward Th1 differentiation (see Fig. S2C in the supplemental material) and treated with ifenprodil, the percentage of IL-2- or IFN-γ-producing cells initially was the same, but it was diminished by 20 to 30% in cells that had undergone 5 to 6 cell cycles compared with the response in untreated cells (Fig. 4A). In T-cell–DC cocultures skewed toward Th2 differentiation (see Fig. S2D in the supplemental material), the addition of ifenprodil caused a marked reduction of IL-4-producing cells in all cycling populations (Fig. 4B), but the percentage of OT2 $CD4^+$ T cells producing IL-10 or IL-13 was increased 2- to 3-fold. Hence, NMDAR antagonists diminish cytokine production of expanded Th1 effector cells and foster IL-10 and IL-13 production by Th2 cells.

NMDAR antagonists decrease CTL activity and chemokine-induced T-cell migration. The impact of NMDAR inhibitors on $CD8^+$ T-cell activation is unknown. Thus, we monitored cell division of CFSE-labeled $CD8^+$ T cells from OT1 TCR tg mice (OT1 $CD8^+$) activated by DCs presenting the SIINFEKL peptide from ovalbumin, the cognate antigen for the OT1 TCR (16). Ifenprodil impaired cell cycling, as 30% of OT1 $CD8^+$ T cells had undergone 5 cell divisions after 3 days, whereas only 11% of cells had done so in the presence of the antagonist (Fig. 4C). To determine the killing capacity of CTLs in the presence of NMDAR antagonists, OT1 $CD8^+$ T-cell blasts were cultured with SIINFEKL-loaded RMA-S T-lymphoma target cells. Annexin V staining of RMA-S target cells revealed an average of 44% apoptotic cells within 4 h. Upon addition of ifenprodil, the percentage of apoptotic RMA-S cells declined by 18 to 34% (Fig. 4D), thus revealing an inhibitory effect of NMDAR antagonists on CTL activity.

The chemokines SDF1α and CCL21 induce a migratory response in naive T cells upon binding to their respective receptors, CXCR4 and CCR7. Since T-cell migration to sites of inflammation is fundamental for effective immune responses, we asked whether chemokine-induced migration, which is a T-cell response independent of TCR engagement, is also affected by ifenprodil. We found 60 to 90% and 50 to 70% reductions in SDF1α- and CCL21-induced T-cell migration, respectively (Fig. 4E). Therefore, NMDAR antagonists attenuate/inhibit multiple effector functions of T cells, including their migratory response to chemokines.

GluN1 protein expression in murine T cells is elusive. In previous work (9), GluN1 protein expression was detected in thymocytes by intracellular staining and flow cytometry, and localization of GluN1 subunits in the thymocyte-DC contact zone was shown by confocal microscopy. Inspired by this work, we performed similar experiments and apparently confirmed the results for NMDAR subunit expression in thymocytes: we found expression of GluN1, GluN2B, and GluN2A subunits in peripheral T cells (see Fig. S3A and B in the supplemental material). Upon coculture of OT2 $CD4^+$ T cells with pOVA-DCs, GluN1 and GluN2B subunits were detected in the immunological synapse, as shown by confocal microscopy (see Fig. S3C and D in the supplemental material). In Western blot analyses, GluN1 protein in thymocytes and $CD4^+$ T cells (data not shown) appeared at a lower molecular weight than GluN1 protein of brain lysate (Fig. 5C, lanes 1 to 3). To prove that the detected protein is GluN1, we performed analyses on thymocytes obtained from newborn GluN1 KO mice. PCR and RT-PCR analyses showed the deletion of GluN1 at the DNA and mRNA levels in thymocytes (Fig. 5A and B), and GluN1 protein was absent in brain samples (Fig. 5C, brain, lanes 4 and 5) but not in thymocytes. These observations strongly suggest that the GluN1 Ab does not detect GluN1 protein in thymocytes (Fig. 5C, thymocytes, lanes 4 and 5). Intracellular fluorescence-activated cell sorter (FACS) staining with two different GluN1 Abs and immunohistochemistry also showed identical staining for wt and GluN1 KO thymocytes (Fig. 5D and E). Hence, on the protein level, there is no evidence for expression of the obligatory GluN1 subunit of NMDARs in murine thymocytes and T cells. In addition, ifenprodil (10 to 30 μM) inhibited the proliferation of GluN1 KO thymocytes in a way similar to that of wt thymocytes (data not shown).

NMDAR antagonists inhibit $K_v1.3$ and $K_{Ca}3.1$ potassium channels. In view of the above-described findings and the strong effects of NMDAR pharmacology on Ca^{2+}-dependent signaling, we hypothesized that the effects of NMDAR antagonists on the TCR-induced Ca^{2+} signal involve $K_v1.3$ and $K_{Ca}3.1$ potassium channels. These channels regulate T-cell activation by controlling membrane potential and, hence, Ca^{2+} flux into T cells (9, 33–35). Indeed, current-clamp recordings of CD3 plus CD28 Ab-activated $CD4^+$ T cells showed that ifenprodil (30 μM) and memantine (50 μM) depolarized the membrane potential from ~−50 mV to ~−15 mV and ~−20 mV, respectively (data not shown). We then recorded $K_v1.3$ and $K_{Ca}3.1$ channel-mediated currents in activated $CD4^+$ T cells in the absence or presence of NMDAR antagonists and constructed dose-response curves from the transient maximal current amplitude. The obtained Hill slopes and 50% inhibitory concentrations (IC_{50}s)

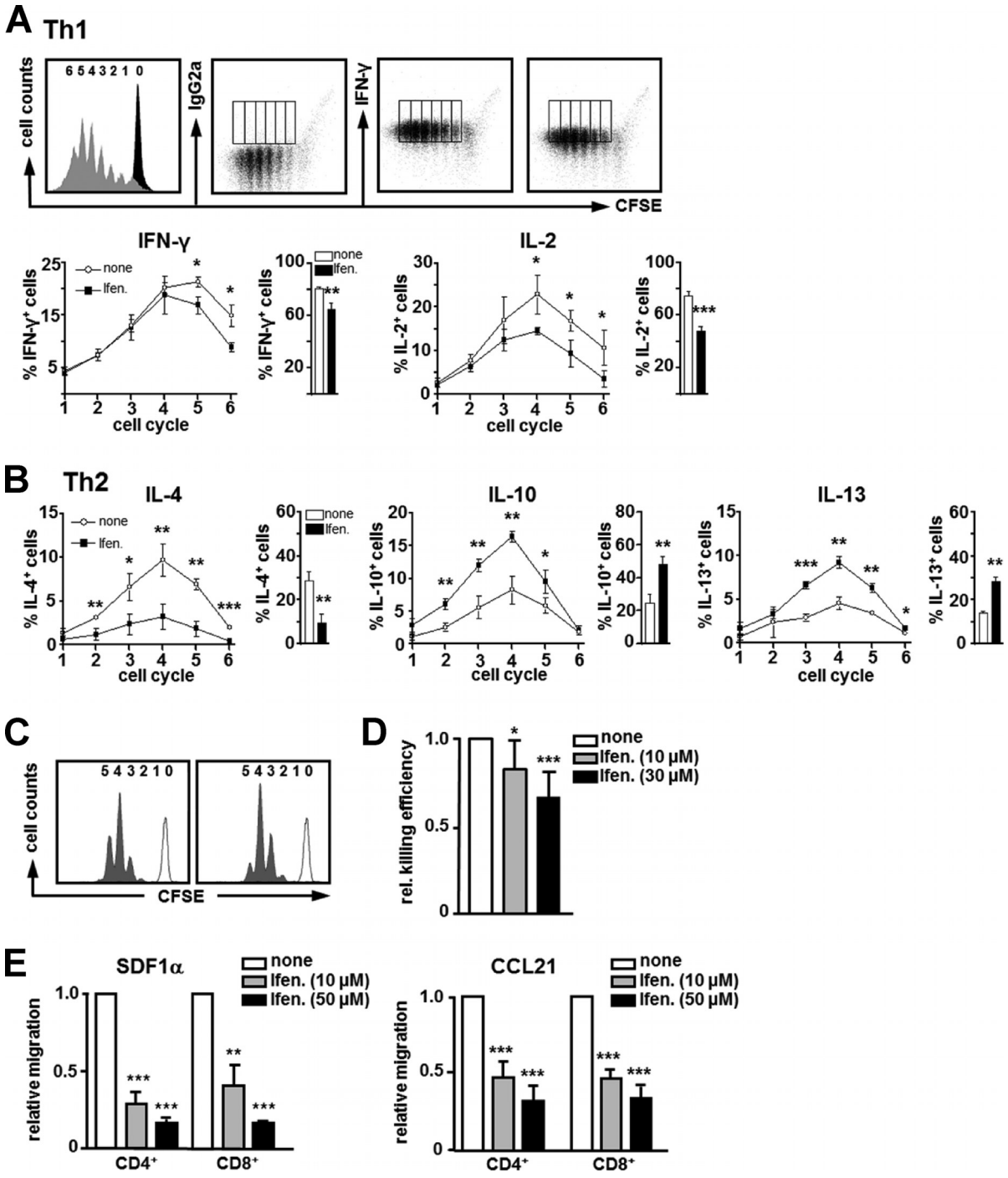

FIG 4 NDMAR antagonists modulate cytokine secretion and CTL activity and migration. (A and B) CFSE-labeled OT2 $CD4^+$ T cells were cultured with pOVA-loaded DCs (T-cell-to-DC ratio of 1:0.1) for 5 days under Th1-skewing (A) and Th2-skewing (B) conditions. Ifenprodil (7 μM) was added daily from days 2 to 4. The left histogram in panel A shows cell cycle progression, as determined by flow cytometry. The number of cell divisions is indicated; the black histogram represents unstimulated cells. The production of the indicated cytokines in each cycling population in the absence (middle dot plot) or presence (right dot plot) of ifenprodil was determined by intracellular staining and flow cytometry (dot plots). Cells were considered positive for cytokine expression on the basis of isotype staining (left dot plot). In panels A and B, the data in the corresponding graphs show the mean percentages ± SD of cytokine-producing cells in each dividing population and in the total T-cell population. (C) CFSE-labeled OT1 $CD8^+$ T cells were stimulated by SIINFEKL-pulsed DCs (T-cell-to-DC ratio of 1:0.1), without (left) or with (right) ifenprodil (30 μM). Cell cycle progression of T cells was analyzed after 72 h by flow cytometry. The number of cell divisions is indicated. The white histograms represent nonstimulated cells. (D) OT1 effector T cells were cultured with SIINFEKL-loaded RMA-S target cells for 4 h. The percentage of apoptotic RMA-S cells was determined by annexin V staining and flow cytometry. Data in the graph give the mean relative killing efficiencies and SD of CTLs in the presence of ifenprodil or in its absence, which was set to a value of 1. (E) The migration of $CD4^+$ and $CD8^+$ T cells toward SDF1α or CCL21 was determined in the absence or presence of ifenprodil. Data represent relative migration as means and SD. Except for panel C ($n = 2$), all data were calculated from three experiments. Significant P values were calculated by the use of Student's t test (*, $P < 0.05$; **, $P < 0.01$; ***, $P < 0.001$).

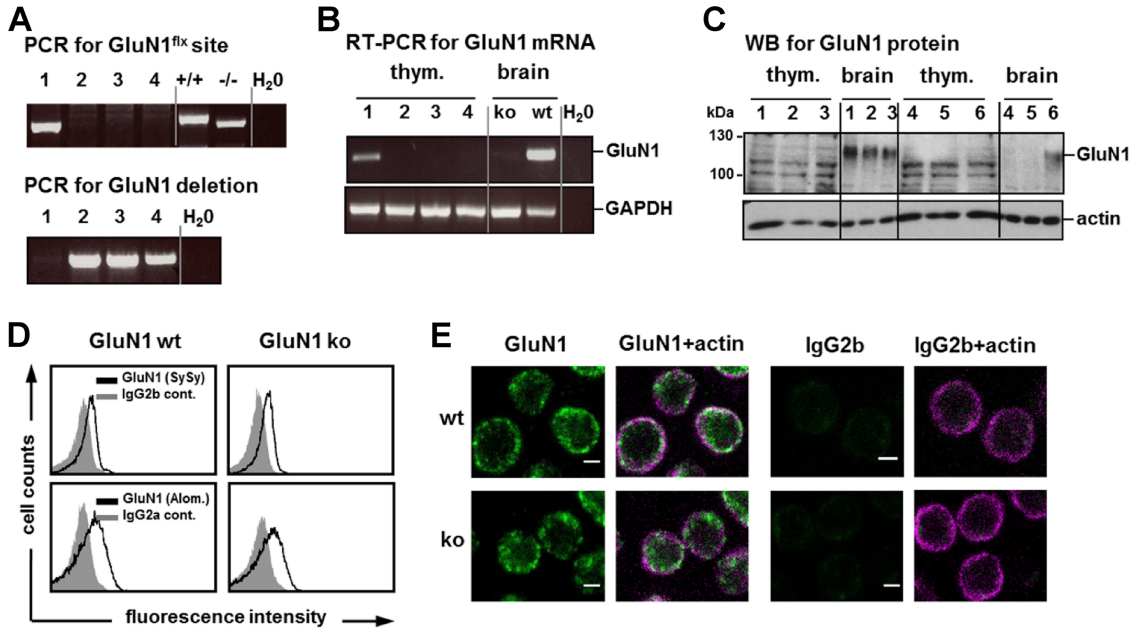

FIG 5 Assessment of GluN1 protein expression in thymocytes. Thymocytes and brain, isolated from newborn littermates of GluN1$^{flx/flx}$ × Cre deleter mice, were analyzed for GluN1 on the DNA (A), RNA (B), and protein (C to E) levels. (A) PCR analysis of thymocyte DNA for floxed (+) and wt (−) GluN1 alleles (top) and excision of floxed GluN1 sequence (bottom). (B) RT-PCR analysis of GluN1 and glyceraldehyde-3-phosphate dehydrogenase (GAPDH) mRNA expression in thymocytes and brain from wt and GluN1 KO mice. In panels A and B, lane 1 represents thymocytes from a GluN1 wt mouse, and lanes 2 to 4 represent thymocytes from GluN1 KO mice. (C) Western blot (WB) analysis of GluN1 protein expression (GluN1 Ab from Synaptic Systems) in protein extracts of thymocytes and brain of the same mice. Actin expression was used as the control for protein loading. Lanes 4 and 5 represent GluN1 KO mice, lanes 1 to 3 represent GluN1 heterozygous mice, and lane 6 represent a GluN1 wt mouse. (D) Thymocytes from GluN1 wt and GluN1 KO mice were analyzed for GluN1 protein expression by intracellular FACS staining and flow cytometry. GluN1 Abs were obtained from Synaptic Systems (SySy) or Alomone Labs (Alom.). Shaded histograms show isotype control staining. (E) Thymocytes from the indicated mice were analyzed for GluN1 (Synaptic Systems) (in green) and actin (in magenta) expression by use of confocal microscopy. Data are representative of two to three experiments and three to four GluN1 KO mice; scale bars represent 2 μm.

for $K_v1.3$ channels in the presence of ifenprodil and memantine were ~1.5 and ~1.9 and ~35 μM and ~45 μM, respectively (Fig. 6). For $K_{Ca}3.1$ channels, Hill slopes and IC_{50}s were ~1.2 and ~15 μM for ifenprodil and ~1.6 and ~30 μM for memantine, respectively (Fig. 6). We also tested the effect of D-APV, a competitive NMDAR antagonist, on $K_v1.3$ channels in activated $CD4^+$ T cells (see Fig. S4A in the supplemental material) and the effects of the NMDAR antagonists ifenprodil, MK801, memantine, ketamine, and D-APV on $K_v1.3$ channel activity in EL-4 lymphoma cells (see Fig. S4B in the supplemental material). All inhibitors strongly blocked $K_v1.3$ channel currents, but in the case of D-APV, about 10-fold-higher concentrations were needed to obtain inhibition similar to that with ifenprodil. Thus, the employed concentrations of NMDAR antagonists, which were similar to those used previously by others (9), nonspecifically inhibited two potassium channels expressed on T cells, which reportedly modulate many Ca^{2+}-mediated processes in T cells (34).

DISCUSSION

NMDAR antagonists are in use and are promising candidates for therapy of various neuronal diseases, including Alzheimer's disease, Parkinson's disease, depression, and other neuropsychiatric disorders (6). The use of these pharmaceuticals necessitates thorough evaluation of their possible effects on lymphocytes, for which NMDAR expression has been reported (13). Here, we affirm that NMDAR antagonists have profound effects on T-cell function. CTL activity, T-cell proliferation, cytokine secretion, and migration were significantly impaired or altered by the open-channel blockers MK801 and memantine and by the GluN2B subunit-specific antagonist ifenprodil. These NMDAR antagonists either inhibited or attenuated TCR signaling and T-cell activation, depending on the strength of the TCR stimulus. Notably, this inhibition was partially compensated for by CD28 signaling, suggesting that the antagonists have different effects on T-cell subsets, depending on the activation status of the T cell, the antigen dose, and provision of costimulation (32, 36). Indeed, at a DC-to-T-cell ratio of 1:1, the antagonists only mildly affected proliferation, but at lower DC-to-T-cell ratios, T-cell activation was markedly reduced. In mixed-lymphocyte reactions, proliferation was effectively inhibited by 3 to 5 μM ifenprodil and memantine and by 30 μM MK801, suggesting that NMDAR antagonists could be useful therapeutics for preventing allograft rejection in transplantation settings. Interestingly, repetitive application of a low-dose NMDAR antagonist to differentiating Th cells did not inhibit their antigen-induced proliferation but did diminish IL-2 and IFN-γ production in Th1 cells as well as increased the production of IL-10 and IL-13 in Th2 cells; IL-10 and IL-13 are two cytokines associated with immunosuppressive functions (37, 38). As IL-13 also exerts proinflammatory effects (as, for example, in asthma) (39), NMDAR antagonists *in vivo* may polarize the local environment toward either inflammation or immune suppression, depending on the cell type and disease setting (40).

Our study also found novel effects of NMDAR antagonists on $CD8^+$ T-cell responses. In the presence of ifenprodil, antigen-induced cell cycle progression of OT1 $CD8^+$ T cells was retarded, and killing of RMS-A tumor cells was significantly reduced. The

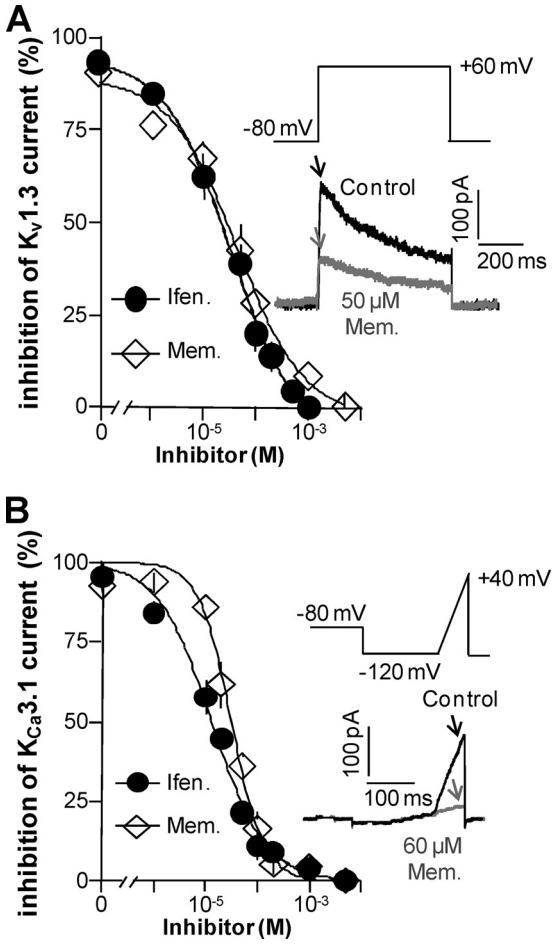

FIG 6 NDMAR antagonists inhibit K_v1.3 and K_{Ca}3.1 potassium channels. Dose-response relationships for the indicated NMDAR antagonists were measured for isolated K_v1.3 (A) and K_{Ca}3.1 (B) channel-mediated currents with the patch-clamp technique in $CD4^+$ T cells activated with CD3 and CD28 Abs. Insets show voltage ramp protocols and examples of current traces under control conditions and in the presence of memantine. Data are normalized to the current measured under control conditions and are represented as relative inhibition. Data points in the dose-response relationships represent mean values ± standard errors of the means calculated from 5 to 7 cells each.

mechanisms of these effects have to be defined, but TCR-induced activation of Ca^{2+}-dependent signaling molecules, such as protein kinase C and calcineurin, which participate in granule exocytosis (41–43), or synapse formation between CTLs and target cells could be impaired by NMDAR antagonists. By targeting $CD8^+$ T-cell function, NMDAR antagonists may either limit antiviral and antitumor CTL responses (44) or be beneficial by ameliorating pathological CTL responses, as in multiple sclerosis (45). Furthermore, ifenprodil significantly reduced SDF1α- and CCL21-induced migration of $CD4^+$ and $CD8^+$ T cells, an effect that may foster immunosuppression by limiting T-cell migration to sites of inflammation in physiological or pathological immune responses.

NMDAR expression has been described for human T cells and murine thymocytes (9, 13, 14, 46), but, as mentioned by Affaticati et al. (9), experiments using the patch-clamp technique or the competitive antagonist D-APV failed to prove the existence of surface-expressed NMDARs. Hence, Affaticati et al., aware that NMDARs in neuronal synapses are few (often <10 per synapse) (47), proposed that although few NMDARs may be expressed on the cell surface, they are functionally important. Also, a single NMDAR would conduct much more Ca^{2+} than a single Stim-Orai complex (27, 48), and hence, NMDAR surface expression should be under tight control. In our experiments, we also could not reliably detect NMDAR expression on live resting or activated T cells or on thymocytes by the use of two different Abs binding to extracellular epitopes of GluN1 by routine FACS staining and flow cytometry. Western blot analysis revealed GluN1 protein expression in thymocytes, and confocal microscopy revealed subunit labeling of GluN1, GluN2B, and GluN2A in peripheral T cells, similar to what others have reported (9). However, expression and functional studies in thymocytes from NMDAR KO mice contradicted these results. Hence, there is no proof that NMDARs are expressed at the protein level in T cells. Instead, we provide evidence that all applied NMDAR antagonists reduce K_v1.3 and K_{Ca}3.1 channel conductivity in activated $CD4^+$ T cells and EL-4 lymphoma cells. In addition, the competitive NMDAR antagonist D-APV had effects only at much higher concentrations, 0.5 to 1 mM, than reported for neuronal NMDARs (IC_{50} for NMDAR of ~0.7 µM) (49).

K_v1.3 and K_{Ca}3.1 channels provide the counterbalancing K^+ efflux needed for Ca^{2+} influx upon TCR ligation (34, 35, 50). Their blockade inhibits T-cell function and ameliorates various diseases, including experimental autoimmune encephalitis and allergic inflammatory lung diseases (42, 45, 51). As K_{Ca}3.1 is the functionally dominant K^+ channel in naive and early memory T cells, and K_v1.3 is the dominant channel in effector memory T cells, NMDAR antagonists may target both populations (51). Similar to our results with ifenprodil, inhibition of T-cell function by K_v1.3 and K_{Ca}3.1 channel blockers could be rescued by CD28 costimulation (52, 53), which supports our results that NMDAR antagonists act primarily via inhibition of these potassium channels. Furthermore, as T-regulatory (Treg) cells express similar numbers of K_v1.3 and K_{Ca}3.1 channels as naive T cells (54, 55), NMDAR antagonists may also modulate Treg cell function. Besides K_v1.3 and K_{Ca}3.1 channels, NMDAR antagonist-induced membrane depolarization could also impair the function of L-type or CRAC channels. Both channel types are voltage-gated Ca^{2+} channels that will be affected by steady-state changes in the membrane potential, as reported here. In particular, membrane depolarization of T cells to −30 to −20 mV will nearly completely inactivate all expressed L-type channels, besides a possible direct blockade of the channel, as reported for ifenprodil at concentrations of >10 µM (56). Although CRAC channels can be activated at low membrane potential, the changed membrane potential will alter open probability and conductivity compared to the normal resting membrane potential. Therefore, the reduced Ca^{2+} response in the presence of NMDAR antagonists is, at least partially, caused by lowering the Ca^{2+} influx and by inhibition of the positive feedback function of Ca^{2+}-induced activation of K_{Ca}3.1 channels during T-cell activation (56–60).

In conclusion, NMDAR antagonists target TCR signaling, cytotoxic T-cell function, cytokine secretion, and T-cell migration. We propose that the potent effects of NMDAR antagonists on T-cell function are due to their inhibitory side effects on K_v1.3 and K_{Ca}3.1 channels. Hence, when these antagonists are used to treat neuronal diseases, their immunosuppressive effects have to be considered. In addition, NMDAR antagonists like memantine

may be suitable drugs to modulate T-cell function and T-cell migration in inflammatory and autoimmune diseases.

ACKNOWLEDGMENTS

We thank G. Weitz for technical assistance, M. Gunzer for DC culture reagents and mice, and E. Serfling for mice and discussion.

N.S. and T.B. were supported by grant SFB854-TP9 from the Deutsche Forschungsgemeinschaft (DFG) to M.H. and U.B.

U.B. and M.H. designed the study and analyzed and discussed the data. S.K., N.S., J.M., T.L., T.B., and U.B. performed experiments and analyzed data. S.K.-H. provided NFATc1-EGFP mice, and R.S. provided GluN1$^{flx/flx}$ × Cre deleter mice. B.S. contributed reagents and discussion. M.H. and U.B. wrote the manuscript.

We declare that we have no conflicts of interest.

REFERENCES

1. **Gladding CM, Raymond LA.** 2011. Mechanisms underlying NMDA receptor synaptic/extrasynaptic distribution and function. Mol. Cell. Neurosci. **48:**308–320. http://dx.doi.org/10.1016/j.mcn.2011.05.001.
2. **Collingridge GL, Olsen RW, Peters J, Spedding M.** 2009. A nomenclature for ligand-gated ion channels. Neuropharmacology **56:**2–5. http://dx.doi.org/10.1016/j.neuropharm.2008.06.063.
3. **Salter MW, Dong Y, Kalia LV, Liu XJ, Pitcher G.** 2009. Regulation of NMDA receptors by kinases and phosphatases, p 123–148. *In* Van Dongen AM (ed), Biology of the NMDA receptor. CRC Press, Boca Raton, FL.
4. **Groc L, Heine M, Cousins SL, Stephenson FA, Lounis B, Cognet L, Choquet D.** 2006. NMDA receptor surface mobility depends on NR2A-2B subunits. Proc. Natl. Acad. Sci. U. S. A. **103:**18769–18774. http://dx.doi.org/10.1073/pnas.0605238103.
5. **Paoletti P, Neyton J.** 2007. NMDA receptor subunits: function and pharmacology. Curr. Opin. Pharmacol. **7:**39–47. http://dx.doi.org/10.1016/j.coph.2006.08.011.
6. **Olivares D, Deshpande VK, Shi Y, Lahiri DK, Greig NH, Rogers JT, Huang X.** 2012. N-Methyl D-aspartate (NMDA) receptor antagonists and memantine treatment for Alzheimer's disease, vascular dementia and Parkinson's disease. Curr. Alzheimer Res. **9:**746–758. http://dx.doi.org/10.2174/156720512801322564.
7. **Peery HE, Day GS, Dunn S, Fritzler MJ, Pruss H, De Souza C, Doja A, Mossman K, Resch L, Xia C, Sakic B, Belbeck L, Foster WG.** 2012. Anti-NMDA receptor encephalitis. The disorder, the diagnosis and the immunobiology. Autoimmun. Rev. **11:**863–872. http://dx.doi.org/10.1016/j.autrev.2012.03.001.
8. **Pacheco R, Oliva H, Martinez-Navio JM, Climent N, Ciruela F, Gatell JM, Gallart T, Mallol J, Lluis C, Franco R.** 2006. Glutamate released by dendritic cells as a novel modulator of T cell activation. J. Immunol. **177:**6695–6704. http://www.jimmunol.org/content/177/10/6695.long.
9. **Affaticati P, Mignen O, Jambou F, Potier MC, Klingel-Schmitt I, Degrouard J, Peineau S, Gouadon E, Collingridge GL, Liblau R, Capiod T, Cohen-Kaminsky S.** 2011. Sustained calcium signalling and caspase-3 activation involve NMDA receptors in thymocytes in contact with dendritic cells. Cell Death Differ. **18:**99–108. http://dx.doi.org/10.1038/cdd.2010.79.
10. **Lombardi G, Dianzani C, Miglio G, Canonico PL, Fantozzi R.** 2001. Characterization of ionotropic glutamate receptors in human lymphocytes. Br. J. Pharmacol. **133:**936–944. http://dx.doi.org/10.1038/sj.bjp.0704134.
11. **Nedergaard M, Takano T, Hansen AJ.** 2002. Beyond the role of glutamate as a neurotransmitter. Nat. Rev. Neurosci. **3:**748–755. http://dx.doi.org/10.1038/nrn916.
12. **Boldyrev AA.** 2005. Homocysteinic acid causes oxidative stress in lymphocytes by potentiating toxic effect of NMDA. Bull. Exp. Biol. Med. **140:**33–37. http://dx.doi.org/10.1007/s10517-005-0404-1.
13. **Pacheco R, Gallart T, Lluis C, Franco R.** 2007. Role of glutamate on T-cell mediated immunity. J. Neuroimmunol. **185:**9–19. http://dx.doi.org/10.1016/j.jneuroim.2007.01.003.
14. **Levite M.** 2008. Neurotransmitters activate T-cells and elicit crucial functions via neurotransmitter receptors. Curr. Opin. Pharmacol. **8:**460–471. http://dx.doi.org/10.1016/j.coph.2008.05.001.
15. **Barnden MJ, Allison J, Heath WR, Carbone FR.** 1998. Defective TCR expression in transgenic mice constructed using cDNA-based alpha- and beta-chain genes under the control of heterologous regulatory elements. Immunol. Cell Biol. **76:**34–40. http://dx.doi.org/10.1046/j.1440-1711.1998.00709.x.
16. **Hogquist KA, Jameson SC, Heath WR, Howard JL, Bevan MJ, Carbone FR.** 1994. T cell receptor antagonist peptides induce positive selection. Cell **76:**17–27. http://dx.doi.org/10.1016/0092-8674(94)90169-4.
17. **Hock M, Vaeth M, Rudolf R, Patra AK, Pham DA, Muhammad K, Pusch T, Bopp T, Schmitt E, Rost R, Berberich-Siebelt F, Tyrsin D, Chuvpilo S, Avots A, Serfling E, Klein-Hessling S.** 2013. NFATc1 induction in peripheral T and B lymphocytes. J. Immunol. **190:**2345–2353. http://dx.doi.org/10.4049/jimmunol.1201591.
18. **Sprengel R, Single FN.** 1999. Mice with genetically modified NMDA and AMPA receptors. Ann. N. Y. Acad. Sci. **868:**494–501. http://dx.doi.org/10.1111/j.1749-6632.1999.tb11318.x.
19. **Schwenk F, Baron U, Rajewsky K.** 1995. A cre-transgenic mouse strain for the ubiquitous deletion of loxP-flanked gene segments including deletion in germ cells. Nucleic Acids Res. **23:**5080–5081. http://dx.doi.org/10.1093/nar/23.24.5080.
20. **Jelitai M, Schlett K, Varju P, Eisel U, Madarasz E.** 2002. Regulated appearance of NMDA receptor subunits and channel functions during in vitro neuronal differentiation. J. Neurobiol. **51:**54–65. http://dx.doi.org/10.1002/neu.10049.
21. **Pierau M, Engelmann S, Reinhold D, Lapp T, Schraven B, Bommhardt UH.** 2009. Protein kinase B/Akt signals impair Th17 differentiation and support natural regulatory T cell function and induced regulatory T cell formation. J. Immunol. **183:**6124–6134. http://dx.doi.org/10.4049/jimmunol.0900246.
22. **Di L, Srivastava S, Zhdanova O, Ding Y, Li Z, Wulff H, Lafaille M, Skolnik EY.** 2010. Inhibition of the K+ channel KCa3.1 ameliorates T cell-mediated colitis. Proc. Natl. Acad. Sci. U. S. A. **107:**1541–1546. http://dx.doi.org/10.1073/pnas.0910133107.
23. **Cahalan MD, Chandy KG, DeCoursey TE, Gupta S.** 1985. A voltage-gated potassium channel in human T lymphocytes. J. Physiol. **358:**197–237.
24. **Kuras Z, Kucher V, Gordon SM, Neumeier LM, Chimote AA, Filipovich AH, Conforti L.** 2012. Modulation of Kv1.3 channels by protein kinase A I in T lymphocytes is mediated by the disc large 1-tyrosine kinase Lck complex. Am. J. Physiol. Cell Physiol. **302:**C1504–C1512. http://dx.doi.org/10.1152/ajpcell.00263.2011.
25. **Wulff H, Miller MJ, Hansel W, Grissmer S, Cahalan MD, Chandy KG.** 2000. Design of a potent and selective inhibitor of the intermediate-conductance Ca2+-activated K+ channel, IKCa1: a potential immunosuppressant. Proc. Natl. Acad. Sci. U. S. A. **97:**8151–8156. http://dx.doi.org/10.1073/pnas.97.14.8151.
26. **Chuvpilo S, Jankevics E, Tyrsin D, Akimzhanov A, Moroz D, Jha MK, Schulze-Luehrmann J, Santner-Nanan B, Feoktistova E, Konig T, Avots A, Schmitt E, Berberich-Siebelt F, Schimpl A, Serfling E.** 2002. Autoregulation of NFATc1/A expression facilitates effector T cells to escape from rapid apoptosis. Immunity **16:**881–895. http://dx.doi.org/10.1016/S1074-7613(02)00329-1.
27. **Hogan PG, Lewis RS, Rao A.** 2010. Molecular basis of calcium signaling in lymphocytes: STIM and ORAI. Annu. Rev. Immunol. **28:**491–533. http://dx.doi.org/10.1146/annurev.immunol.021908.132550.
28. **Brabletz T, Pietrowski I, Serfling E.** 1991. The immunosuppressives FK 506 and cyclosporin A inhibit the generation of protein factors binding to the two purine boxes of the interleukin 2 enhancer. Nucleic Acids Res. **19:**61–67. http://dx.doi.org/10.1093/nar/19.1.61.
29. **Na SY, Patra A, Scheuring Y, Marx A, Tolaini M, Kioussis D, Hemmings BA, Hunig T, Bommhardt U.** 2003. Constitutively active protein kinase B enhances Lck and Erk activities and influences thymocyte selection and activation. J. Immunol. **171:**1285–1296. http://www.jimmunol.org/content/171/3/1285.long.
30. **Kane LP, Weiss A.** 2003. The PI-3 kinase/Akt pathway and T cell activation: pleiotropic pathways downstream of PIP3. Immunol. Rev. **192:**7–20. http://dx.doi.org/10.1034/j.1600-065X.2003.00008.x.
31. **Riha P, Rudd CE.** 2010. CD28 co-signaling in the adaptive immune response. Self Nonself **1:**231–240. http://dx.doi.org/10.4161/self.1.3.12968.
32. **Boomer JS, Green JM.** 2010. An enigmatic tail of CD28 signaling. Cold Spring Harb. Perspect. Biol. **2:**a002436. http://dx.doi.org/10.1101/cshperspect.a002436.
33. **Desai R, Peretz A, Idelson H, Lazarovici P, Attali B.** 2000. Ca2+-activated K+ channels in human leukemic Jurkat T cells. Molecular clon-

ing, biochemical and functional characterization. J. Biol. Chem. **275:** 39954–39963. http://dx.doi.org/10.1074/jbc.M001562200.
34. **Lam J, Wulff H.** 2011. The lymphocyte potassium channels Kv1.3 and KCa3.1 as targets for immunosuppression. Drug Dev. Res. **72:**573–584. http://dx.doi.org/10.1002/ddr.20467.
35. **Conforti L.** 2012. The ion channel network in T lymphocytes, a target for immunotherapy. Clin. Immunol. **142:**105–106. http://dx.doi.org/10.1016/j.clim.2011.11.009.
36. **Wakamatsu E, Mathis D, Benoist C.** 2013. Convergent and divergent effects of costimulatory molecules in conventional and regulatory CD4+ T cells. Proc. Natl. Acad. Sci. U. S. A. **110:**1023–1028. http://dx.doi.org/10.1073/pnas.1220688110.
37. **Newcomb DC, Boswell MG, Zhou W, Huckabee MM, Goleniewska K, Sevin CM, Hershey GK, Kolls JK, Peebles RS, Jr.** 2011. Human TH17 cells express a functional IL-13 receptor and IL-13 attenuates IL-17A production. J. Allergy Clin. Immunol. **127:**1006–1013.e4. http://dx.doi.org/10.1016/j.jaci.2010.11.043.
38. **Ozdemir C, Akdis M, Akdis CA.** 2009. T regulatory cells and their counterparts: masters of immune regulation. Clin. Exp. Allergy **39:**626–639. http://dx.doi.org/10.1111/j.1365-2222.2009.03242.x.
39. **Van Dyken SJ, Locksley RM.** 2013. Interleukin-4- and interleukin-13-mediated alternatively activated macrophages: roles in homeostasis and disease. Annu. Rev. Immunol. **31:**317–343. http://dx.doi.org/10.1146/annurev-immunol-032712-095906.
40. **Lindblad SS, Mydel P, Hellvard A, Jonsson IM, Bokarewa MI.** 2012. The N-methyl-d-aspartic acid receptor antagonist memantine ameliorates and delays the development of arthritis by enhancing regulatory T cells. Neurosignals **20:**61–71. http://dx.doi.org/10.1159/000329551.
41. **Pores-Fernando AT, Zweifach A.** 2009. Calcium influx and signaling in cytotoxic T-lymphocyte lytic granule exocytosis. Immunol. Rev. **231:**160–173. http://dx.doi.org/10.1111/j.1600-065X.2009.00809.x.
42. **Quintana A, Pasche M, Junker C, Al-Ansary D, Rieger H, Kummerow C, Nunez L, Villalobos C, Meraner P, Becherer U, Rettig J, Niemeyer BA, Hoth M.** 2011. Calcium microdomains at the immunological synapse: how ORAI channels, mitochondria and calcium pumps generate local calcium signals for efficient T-cell activation. EMBO J. **30:**3895–3912. http://dx.doi.org/10.1038/emboj.2011.289.
43. **Schwarz EC, Qu B, Hoth M.** 2013. Calcium, cancer and killing: the role of calcium in killing cancer cells by cytotoxic T lymphocytes and natural killer cells. Biochim. Biophys. Acta **1833:**1603–1611. http://dx.doi.org/10.1016/j.bbamcr.2012.11.016.
44. **Weidinger C, Shaw PJ, Feske S.** 2013. STIM1 and STIM2-mediated Ca(2+) influx regulates antitumour immunity by CD8(+) T cells. EMBO Mol. Med. **5:**1311–1321. http://dx.doi.org/10.1002/emmm.201302989.
45. **Melzer N, Meuth SG, Wiendl H.** 2009. CD8+ T cells and neuronal damage: direct and collateral mechanisms of cytotoxicity and impaired electrical excitability. FASEB J. **23:**3659–3673. http://dx.doi.org/10.1096/fj.09-136200.
46. **Boldyrev AA, Carpenter DO, Johnson P.** 2005. Emerging evidence for a similar role of glutamate receptors in the nervous and immune systems. J. Neurochem. **95:**913–918. http://dx.doi.org/10.1111/j.1471-4159.2005.03456.x.
47. **Racca C, Stephenson FA, Streit P, Roberts JD, Somogyi P.** 2000. NMDA receptor content of synapses in stratum radiatum of the hippocampal CA1 area. J. Neurosci. **20:**2512–2522. http://www.jneurosci.org/content/20/7/2512.long.
48. **Feske S.** 2007. Calcium signalling in lymphocyte activation and disease. Nat. Rev. Immunol. **7:**690–702. http://dx.doi.org/10.1038/nri2152.
49. **Dingledine R, Hynes MA, King GL.** 1986. Involvement of N-methyl-D-aspartate receptors in epileptiform bursting in the rat hippocampal slice. J. Physiol. **380:**175–189.
50. **Cahalan MD, Chandy KG.** 2009. The functional network of ion channels in T lymphocytes. Immunol. Rev. **231:**59–87. http://dx.doi.org/10.1111/j.1600-065X.2009.00816.x.
51. **Wulff H, Zhorov BS.** 2008. K+ channel modulators for the treatment of neurological disorders and autoimmune diseases. Chem. Rev. **108:**1744–1773. http://dx.doi.org/10.1021/cr078234p.
52. **Hu L, Pennington M, Jiang Q, Whartenby KA, Calabresi PA.** 2007. Characterization of the functional properties of the voltage-gated potassium channel Kv1.3 in human CD4+ T lymphocytes. J. Immunol. **179:**4563–4570. http://www.jimmunol.org/content/179/7/4563.long.
53. **Hu L, Wang T, Gocke AR, Nath A, Zhang H, Margolick JB, Whartenby KA, Calabresi PA.** 2013. Blockade of Kv1.3 potassium channels inhibits differentiation and granzyme B secretion of human CD8+ T effector memory lymphocytes. PLoS One **8:**e54267. http://dx.doi.org/10.1371/journal.pone.0054267.
54. **Varga Z, Csepany T, Papp F, Fabian A, Gogolak P, Toth A, Panyi G.** 2009. Potassium channel expression in human CD4+ regulatory and naive T cells from healthy subjects and multiple sclerosis patients. Immunol. Lett. **124:**95–101. http://dx.doi.org/10.1016/j.imlet.2009.04.008.
55. **Reneer MC, Estes DJ, Velez-Ortega AC, Norris A, Mayer M, Marti F.** 2011. Peripherally induced human regulatory T cells uncouple Kv1.3 activation from TCR-associated signaling. Eur. J. Immunol. **41:**3170–3175. http://dx.doi.org/10.1002/eji.201141492.
56. **Delaney AJ, Power JM, Sah P.** 2012. Ifenprodil reduces excitatory synaptic transmission by blocking presynaptic P/Q type calcium channels. J. Neurophysiol. **107:**1571–1575. http://dx.doi.org/10.1152/jn.01066.2011.
57. **Omilusik K, Priatel JJ, Chen X, Wang YT, Xu H, Choi KB, Gopaul R, McIntyre-Smith A, Teh HS, Tan R, Bech-Hansen NT, Waterfield D, Fedida D, Hunt SV, Jefferies WA.** 2011. The Ca(v)1.4 calcium channel is a critical regulator of T cell receptor signaling and naive T cell homeostasis. Immunity **35:**349–360. http://dx.doi.org/10.1016/j.immuni.2011.07.011.
58. **Zainullina LF, Yamidanov RS, Vakhitov VA, Vakhitova YV.** 2011. NMDA receptors as a possible component of store-operated Ca(2)(+) entry in human T-lymphocytes. Biochemistry (Mosc.) **76:**1220–1226. http://dx.doi.org/10.1134/S0006297911110034.
59. **Shaw PJ, Qu B, Hoth M, Feske S.** 2013. Molecular regulation of CRAC channels and their role in lymphocyte function. Cell. Mol. Life Sci. **70:**2637–2656. http://dx.doi.org/10.1007/s00018-012-1175-2.
60. **Feske S.** 2013. Ca(2+) influx in T cells: how many Ca(2+) channels? Front. Immunol. **4:**99. http://dx.doi.org/10.3389/fimmu.2013.00099.

Research Paper

Immunomodulation by memantine in therapy of Alzheimer's disease is mediated through inhibition of K_v1.3 channels and T cell responsiveness

Theresa Lowinus[1], Tanima Bose[2,6], Stefan Busse[3], Mandy Busse[4], Dirk Reinhold[1], Burkhart Schraven[1,5], Ursula H.H. Bommhardt[1]

[1]Institute of Molecular and Clinical Immunology, Otto-von-Guericke-University Magdeburg, Magdeburg, Germany

[2]Molecular Physiology, Leibniz Institute for Neurobiology, Magdeburg, Germany

[3]Department of Psychiatry, Otto-von-Guericke-University Magdeburg, Magdeburg, Germany

[4]Department of Pediatric Pulmonology & Allergology, Medical University of Hannover, Hannover, Germany

[5]Department of Immune Control, Helmholtz Centre for Infection Research, Braunschweig, Germany

[6]Current address: Lee Kong Chian School of Medicine, Singapore

Correspondence to: *Ursula H.H. Bommhardt,* ***email:*** *Ursula.Bommhardt@med.ovgu.de*

Keywords: *human T cells, memantine, K_v1.3 potassium channel, NMDA receptor antagonist, Alzheimer´s disease*

Received: *February 04, 2016* ***Accepted:*** *July 09, 2016* ***Published:*** *July 22, 2016*

ABSTRACT

Memantine is approved for the treatment of advanced Alzheimer´s disease (AD) and reduces glutamate-mediated neuronal excitotoxicity by antagonism of N-methyl-D-aspartate receptors. In the pathophysiology of AD immune responses deviate and infectious side effects are observed during memantine therapy. However, the particular effects of memantine on human T lymphocytes are unresolved. Here, we provide evidence that memantine blocks K_v1.3 potassium channels, inhibits CD3-antibody- and alloantigen-induced proliferation and suppresses chemokine-induced migration of peripheral blood T cells of healthy donors. Concurrent with the *in vitro* data, $CD4^+$ T cells from AD patients receiving therapeutic doses of memantine show a transient decline of K_v1.3 channel activity and a long-lasting reduced proliferative response to alloantigens in mixed lymphocyte reactions. Furthermore, memantine treatment provokes a profound depletion of peripheral blood memory $CD45RO^+$ $CD4^+$ T cells. Thus, standard doses of memantine profoundly reduce T cell responses in treated patients through blockade of K_v1.3 channels. This may normalize deviant immunopathology in AD and contribute to the beneficial effects of memantine, but may also account for the enhanced infection rate.

INTRODUCTION

The non-competitive N-methyl-D-aspartate (NMDA) receptor antagonist memantine (Axura®, Ebixa®, Namenda®) is approved for the treatment of moderate to severe Alzheimer´s disease (AD). Memantine is clinically well tolerated; it facilitates normal neuronal function due to its low affinity and fast off-rate and seems to be efficacious only under pathological conditions [1, 2]. Undesired neuronal side effects include somnolence, confusion and headache [3, 4]. Side effects on the hematopoietic and immune system have been reported with regard to infections of the respiratory and urinary tract and pancytopenia, and fungi infections were observed in 1-10 out of 1000 treated patients during post-marketing experience [5, 6].

Emerging evidence suggests that altered immune responses contribute to the pathophysiology of AD. For instance, T cell proliferation induced by amyloid beta (A-beta) or alloantigens in mixed lymphocyte reactions (MLRs) and transendothelial migration of T cells via the blood brain barrier are enhanced in AD patients compared to age-matched controls [7–13]. It was also demonstrated that an aberrant, glutamate-dependent modulation increases the activity of K_v1.3 potassium channels on T lymphocytes of AD patients [14]. The key targets of memantine are NMDA receptors and the reduction of glutamate-mediated NMDA receptor excitotoxicity is the major mechanism whereby memantine confers neuroprotection in the treatment of advanced AD. However, NMDA receptors seem also to be expressed on non-neuronal cells,

including human peripheral blood lymphocytes (PBLs) and leukemic Jurkat T cells [15–20]. In addition, memantine cross-targets other ligand-gated ion channels like $K_{ir}2.1$ channels expressed on macrophages and microglia [21] and suppresses murine lymphocyte function through cross-inhibition of $K_v1.3$ and $K_{Ca}3.1$ potassium channels [22, 23]. The particular effects of memantine on human T cells, however, are unresolved.

Here, we provide first evidence that application of memantine blocks $K_v1.3$ channel conductivity, inhibits proliferation and migration of human peripheral blood T cells and induces a strong depletion of the memory $CD45RO^+$ $CD4^+$ T cell pool. The data suggest that memantine's effect on human T cells suppresses adaptive immune responses and, thereby, contributes to the drug's beneficial and unwanted side effects in AD therapy.

RESULTS

Memantine blocks $K_v1.3$ channels and suppresses the proliferation and migration of primary human T cells

To assess the impact of memantine on the proliferation of human T cells, DNA synthesis of $CD3^+$ cells isolated from peripheral blood mononuclear cells (PBMCs) of healthy donors was evaluated by ^{3}[H]-Thymidine incorporation in the presence or absence of memantine. Memantine inhibited CD3 Ab-induced T cell proliferation in a concentration dependent manner with an IC_{50} of ~40 μM (Figure 1A, left panel), whereas PMA/IO-activated T cells were hardly affected (Figure 1A, middle panel). Memantine doses up to 100 μM did not significantly impair the viability of human T cells (data not shown). Furthermore, we co-cultured T cells with CD3-depleted PBMCs of HLA incompatible healthy donors in MLRs. Under these more physiological stimulatory conditions, 1-10 μM memantine reduced T cell proliferation by 10-30% with an IC_{50} of ~20 μM (Figure 1A, right panel). Above results indicate that memantine's inhibitory effect on T cell proliferation inversely correlates with the strength of T cell activation.

T-bet is the critical transcription factor induced in differentiating T_H1 cells which are responsive in alloreactive settings [24]. Using intracellular FACS staining and flow cytometry, we found that the percentage of T-bet^+ T cells reacting to alloantigens in MLRs was profoundly diminished upon memantine treatment (Figure 1B), which substantiates memantine's suppressive effect on human T cell activation and T_H1 cell formation.

Since memory T cells display a lower activation threshold than naïve T cells [25], we analyzed whether memantine has differential effects on those T cell subsets. In MLRs, naïve $CD45RO^-$ $CD4^+$ T cells were more sensitive to inhibition at lower memantine concentrations than memory $CD45RO^+$ $CD4^+$ T cells, which showed a significant proliferative inhibition only at 30-50 μM memantine (Figure 1C).

In murine lymphocytes memantine cross-inhibits voltage-gated $K_v1.3$ potassium channels, which regulate the membrane potential and represent the driving force for Ca^{2+}-influx and lymphocyte activation [22, 23, 26]. Using voltage-clamp recordings, we show here that memantine dose-dependently blocks maximal transient $K_v1.3$ channel currents of primary human $CD3^+$ T cells. The obtained IC_{50} values for memantine were 20 μM and 40 μM for resting and CD3 Ab-activated human T cells, and Hill slope values were 1.2 and 1.6, respectively (Figure 2A). Memory T cells express higher levels of $K_v1.3$ channels than naïve T cells [27] and are less dependent on $K_v1.3$ activity for IL-2 production [28]. Accordingly, memory $CD45RO^+$ $CD4^+$ T cells were less sensitive to inhibition of $K_v1.3$ channel currents by memantine than naïve $CD45RO^-$ $CD4^+$ T cells, but only at lower drug concentrations (Figure 2B). Thus, memantine blocks $K_v1.3$ channel currents and proliferation of both naïve and memory $CD4^+$ T cells, but in line with a lower activation threshold memory $CD4^+$ T cells require higher drug concentrations.

Effective immune responses depend on the migration of T cells to the sites of inflammation which is driven by chemokines like SDF-1α (CXCL12), which binds to its receptor CXCR4 expressed on T cells. Pre-treatment of human $CD3^+$ cells from healthy donors with 20 μM memantine reduced SDF-1α-induced migration of $CD4^+$ and $CD8^+$ T cells through fibronectin-coated as well as uncoated transwells by 50% (Figure 3). The latter suggests that memantine´s inhibitory effect on T cell migration is not due to a grossly altered adhesive capacity of T cells upon drug treatment. Hence, *in vitro* application of memantine inhibits $K_v1.3$ channels and two important T cell responses, proliferation and migration.

Memantine treatment of AD patients depletes memory T cells and suppresses T cell reactivity by inactivation of $K_v1.3$ channels

To elucidate possible side effects of memantine on adaptive immune responses during therapeutic drug administration, we studied T cell function of AD patients being treated with memantine (Axura®). Patients were neuro-physiologically evaluated, diagnosed, treated, and accompanied by physicians of the psychiatric department. Peripheral blood of AD patients was taken after informed consent at three time points: at Z1 before the onset of drug treatment, at Z2 after 1 week of treatment with memantine (Axura®, 10 mg/d) and at Z3 after additional 11 weeks of treatment with memantine (Axura®, 20 mg/d, i.e. in total after 12 weeks of daily drug treatment) (Figure 4A). The effect of memantine therapy on AD patients' T cell responsiveness was analyzed by alloantigen-specific T cell proliferation in MLRs. $CD4^+$ T cells were isolated

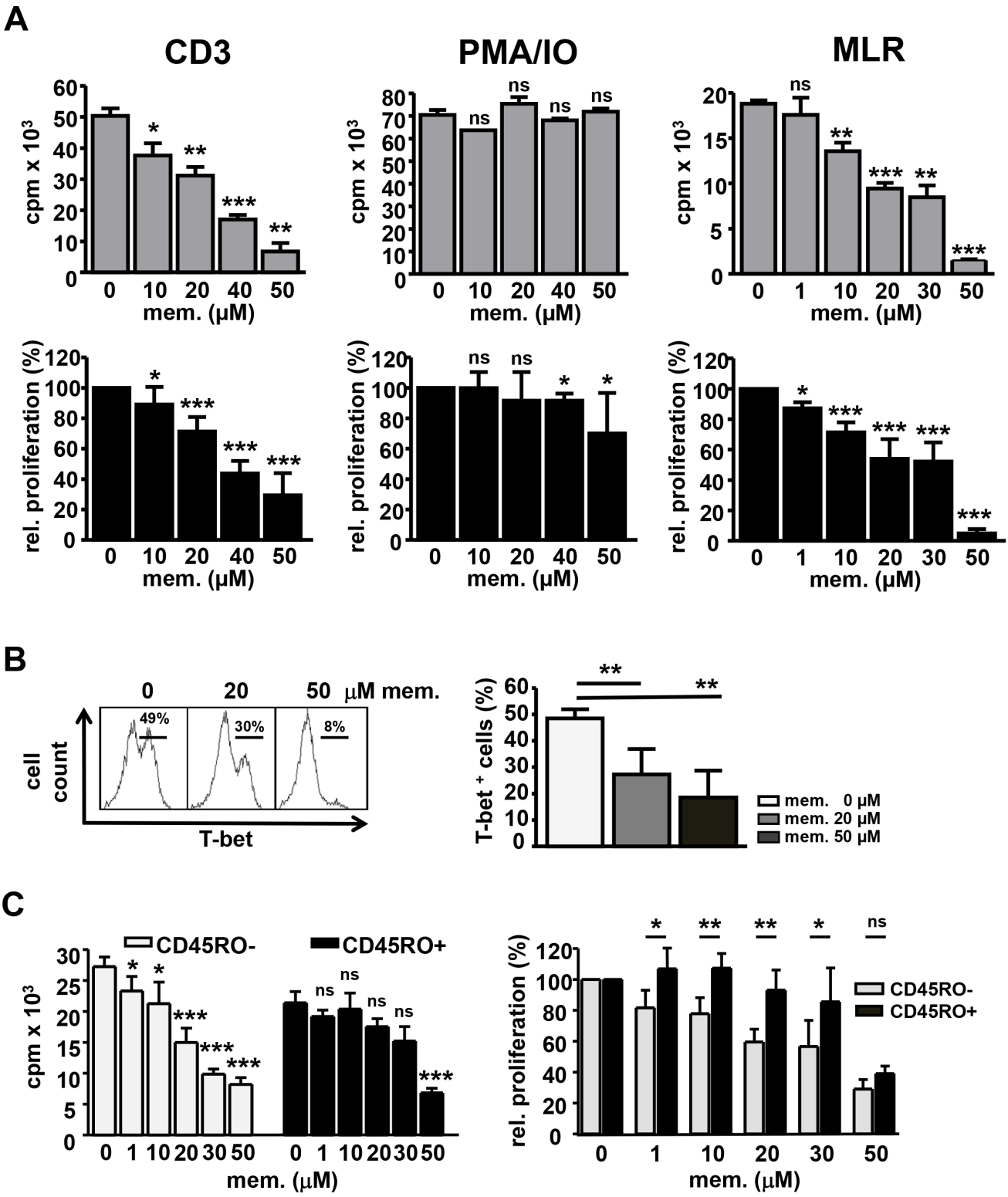

Figure 1: Memantine abrogates T-bet expression and proliferation of human T cells. A. Human peripheral blood $CD3^+$ T cells were stimulated with CD3 Abs (left), PMA/IO (middle) or irradiated, CD3-depleted PBMCs from another healthy donor in MLRs (right) +/- memantine. DNA synthesis was determined by ^{3}[H]-Thymidine incorporation (cpm). Upper graphs represent a single experiment and lower graphs the mean relative proliferation + SD; n=4-6 and MLR n=3. **B.** T-bet expression in T cells reacting in MLRs +/- memantine was determined by flow cytometry. The histogram displays a representative experiment and data in the graph the mean + SD percentage of $T\text{-bet}^+$ cells; n=5. **C.** The proliferation of naïve $CD45RO^-$ and memory $CD45RO^+$ $CD4^+$ human T cells was analyzed in MLRs +/- memantine. Graphs show the data of a representative experiment (left) and the mean relative proliferation + SD of 5 experiments (right). The significance of data was determined with Student´s *t* test; p*<0.05, p**<0.01, and p***<0.001.

from the same AD individual at Z1-Z3 and co-cultured with HLA-incompatible irradiated PBMCs from the same respective healthy donor to evaluate $CD4^+$ T cell reactivity of the same person to the same alloantigens before and during memantine therapy. At time point Z2, $CD4^+$ T cells of most AD patients proliferated less well (10 out of 13 patients, group 1) showing a 46% reduction in DNA synthesis compared to their respective individual proliferation at Z1. For three patients $CD4^+$ T cell proliferation was enhanced at Z2 (group 2). At time point Z3, alloresponses of $CD4^+$ T cells from patient group 1 were further inhibited showing a 5-fold reduction of DNA synthesis compared to Z1 values. $CD4^+$ T cells of patient group 2 now also showed a proliferative inhibition, but it was not significant. Considering all patients, memantine treatment led to a substantial inhibition of T cell alloreactivity with DNA

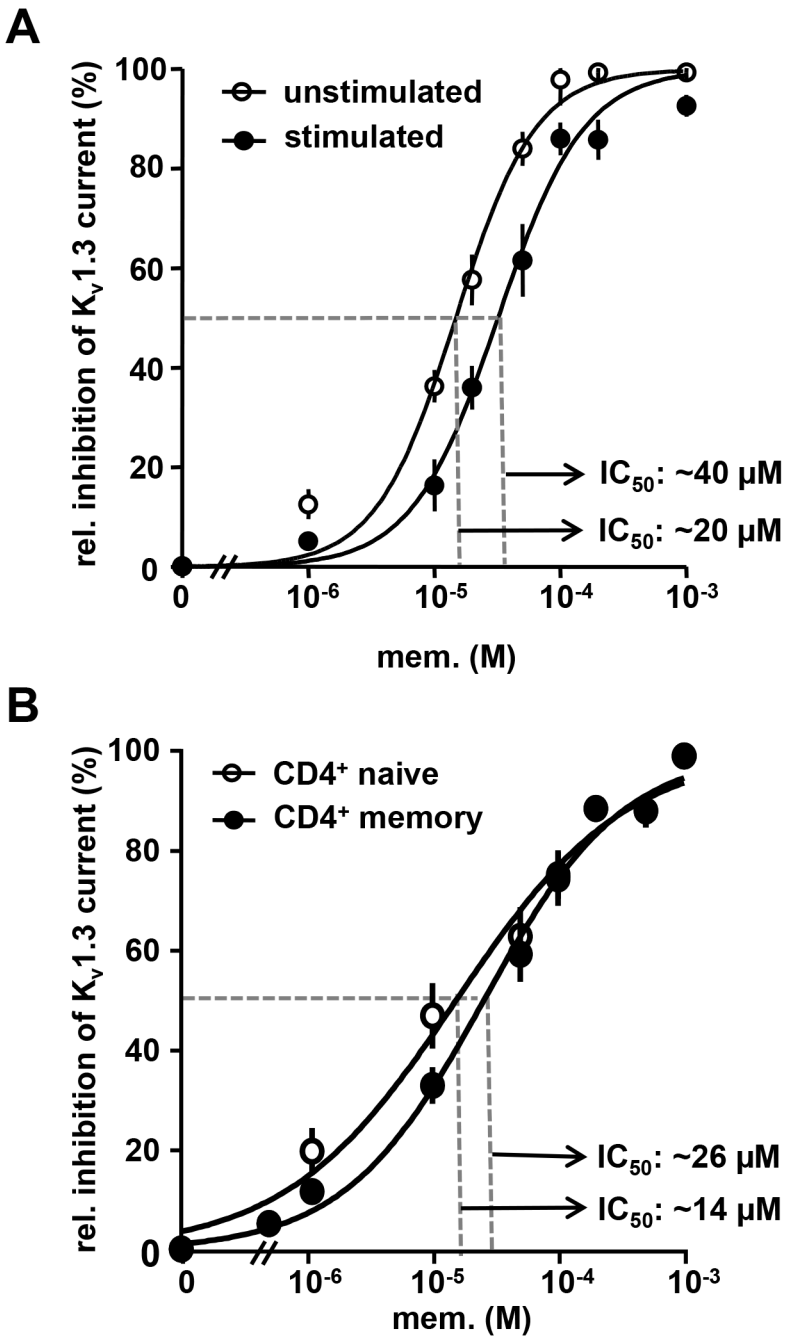

Figure 2: Memantine inhibits K_v1.3 channel currents of human T cells. A. and **B.** The dose response relationship for memantine is shown for isolated K_v1.3 currents recorded from A. resting and CD3 Ab-activated (24 h) human $CD3^+$ cells and B. naïve and memory $CD4^+$ T cells isolated from peripheral blood of healthy donors. Data points represent mean values ± SEM calculated from 4-5 cells per experiment. A, n=5; B, n=4 experiments.

synthesis being suppressed to 32% of pre-therapy values at Z3 (Figure 4B).

Since immune-pathological studies in AD patients found an increase in memory T cells compared to age-matched controls [29–31], we determined the distribution of CD45RO$^+$ CD4$^+$ T cells within PBMCs of AD patients at time points Z1-Z3. Whereas the percentage of total CD4$^+$ T cells within PBMCs was stable, CD4$^+$ T cells were significantly depleted of CD45RO$^+$ cells by 22% at Z2 and by 56% at Z3 compared to Z1 pre-treatment conditions (Figure 4C). This suggests that memantine mainly affects the CD45RO$^+$ T cell pool and may 'normalize' the pathological CD4$^+$ subset composition found in AD.

Given that memantine inhibits K_v1.3 channels of human T cells of healthy donors *in vitro* (Figure 2) and a possible role of those channels in AD immune-pathogenesis [14, 21], we determined K_v1.3 channel currents of CD4$^+$ T cells from AD patients at time points Z1-Z3. Interestingly, K_v1.3 currents at Z2 were 40% lower than those recorded at Z1, i.e. before memantine treatment, whereas at Z3 recorded K_v1.3 currents were only reduced by 7% (Figure 5A). Thus, therapeutic application of memantine suppresses T cell function in AD patients through blockade of K_v1.3 channel activity. Furthermore, analyzing CD4$^+$ T cells of the same AD patient at Z1-Z3, we found an increased K_v1.3 surface expression on naïve and memory CD4$^+$ T cells at Z2 (60% and 55%, respectively) compared to Z1. At Z3, K_v1.3 expression was also enhanced (by 29% and 18%), but it was not significant (Figure 5B). Thus, blockade of K_v1.3 channel activity by memantine provokes a transient compensatory

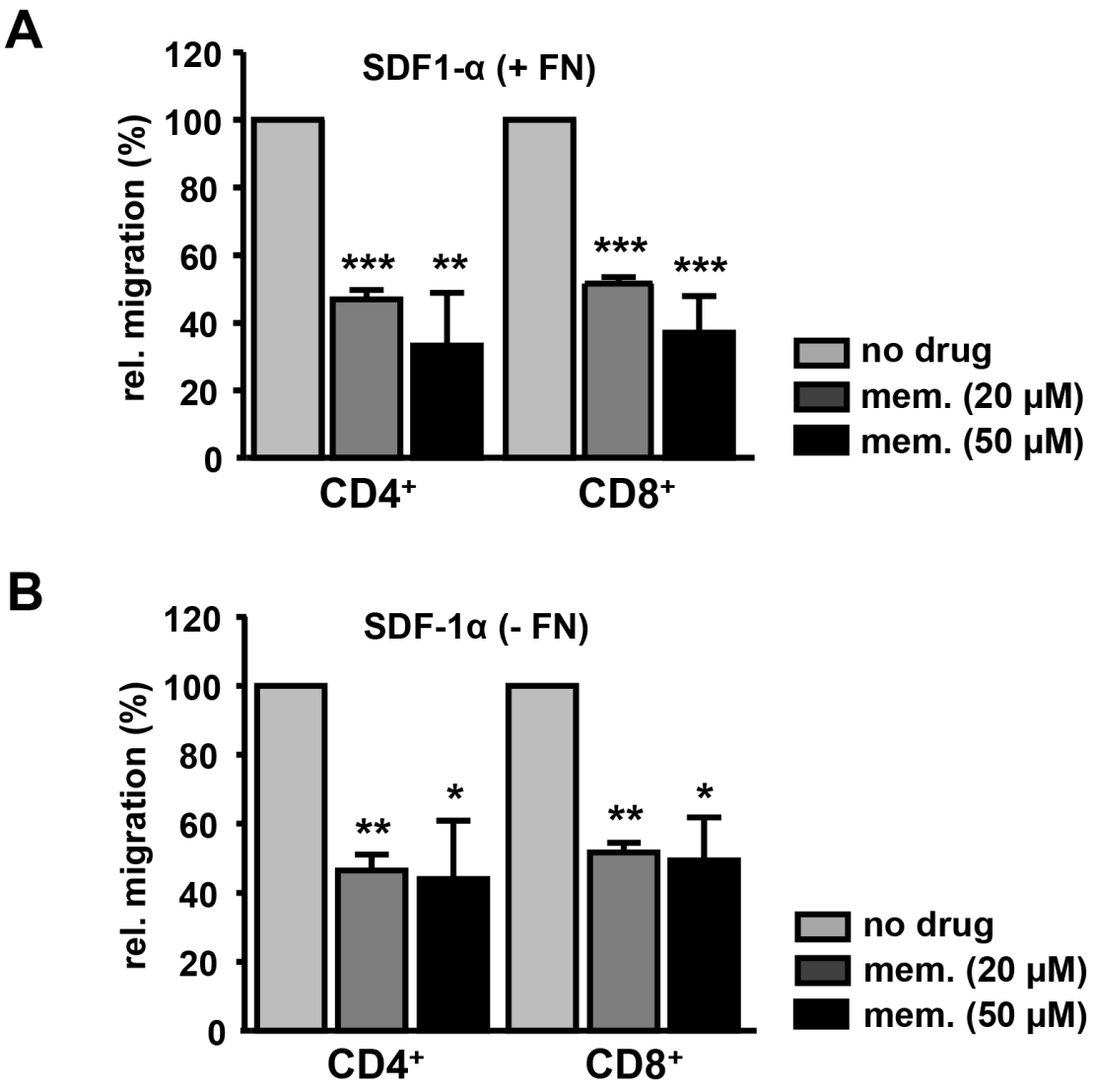

Figure 3: Memantine suppresses the migration of primary human T cells towards SDF-1α. Isolated CD3$^+$ T cells of healthy donors were left untreated or pre-incubated with memantine and their migration through **A.** fibronectin-coated (+ FN) and **B.** uncoated (- FN) transwells was induced by SDF-1α. The number of transmigrated CD4$^+$ and CD8$^+$ T cells was determined by flow cytometry. The graphs represent the data as mean + SD of A. 3 and B. 2 experiments. The significance of data was determined with Student´s *t* test; p*<0.05, p**<0.01, and p***<0.001.

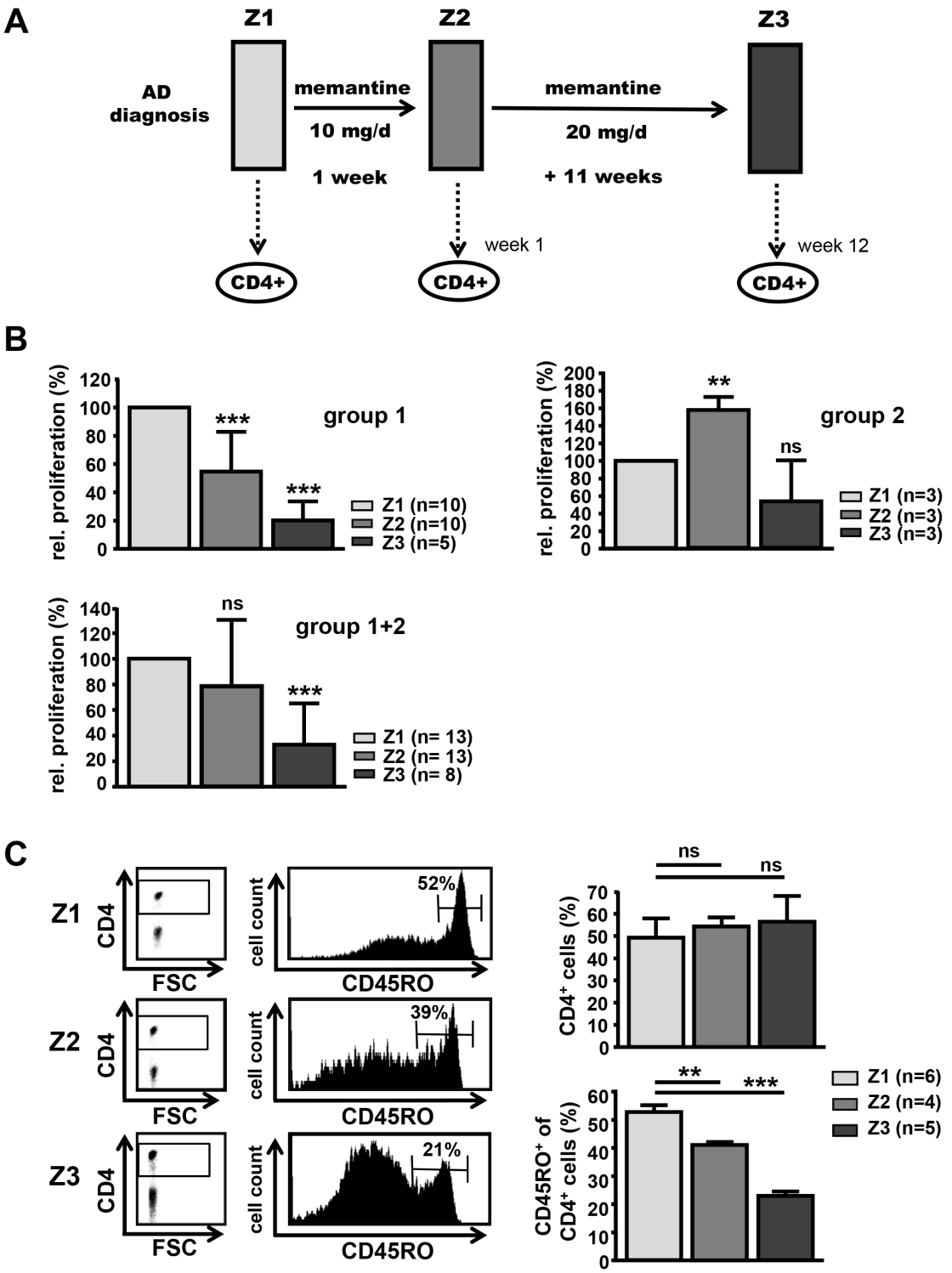

Figure 4: Treatment of AD patients with memantine depletes CD45RO$^+$ CD4$^+$ T cells and suppresses T cell responsiveness. A. Scheme for treatment of AD patients with memantine (Axura®). CD4$^+$ T cells of AD patients undergoing memantine therapy were analyzed at time points Z1 (after initial diagnosis and before treatment), Z2 (after one week) and Z3 (after a total of 12 weeks of daily memantine treatment). **B.** The alloresponse of CD4$^+$ T cells isolated from AD patients at Z1-Z3 was determined in MLRs by ^{3}[H]-Thymidine incorporation; cpm values at Z1 were set as 100%. The graphs show the mean relative proliferation + SD of T cells from two groups of patients (group 1: 5-10 patients, group 2: 3 patients) responding to memantine treatment in a different manner, and for all (8-13) patients. **C.** PBMCs of memantine-treated patients were isolated at Z1-Z3 and analyzed for the content of CD45RO$^+$ CD4$^+$ T cells by flow cytometry. The left panel shows representative dot plots for CD4 expression and histograms for CD45RO levels on gated CD4$^+$ T cells. The right graphs display the mean percentage + SD of CD4$^+$ and CD45RO$^+$ cells and the number of analyzed patients. The significance of data was determined with Student´s *t* test with p*<0.05, p**<0.01, and p***<0.001.

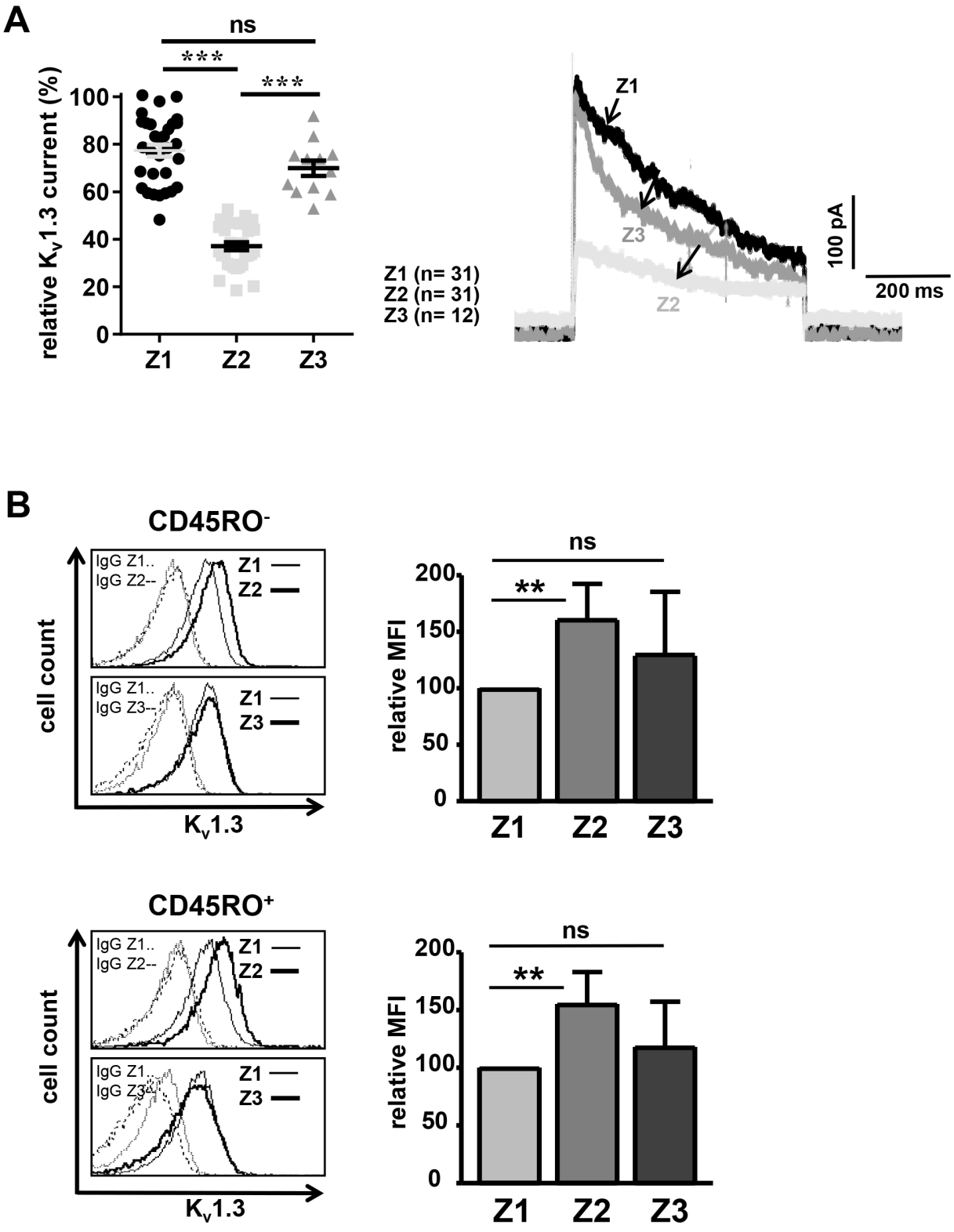

Figure 5: Memantine therapy transiently reduces K_v1.3 channel conductivity of CD4$^+$ T cells. A. K_v1.3 channel currents of CD4$^+$ T cells from AD patients were recorded at time points Z1-Z3 by patch-clamp. Relative maximal transient currents are represented as mean ± SEM (left panel). The number of analyzed T cells is indicated. The right panel displays representative current traces at Z1-Z3. **B.** K_v1.3 surface expression was determined on naïve (upper panel) and memory (lower panel) CD4$^+$ T cells of AD patients at time points Z1-Z3 using flow cytometry; n=5 patients. Histograms show K_v1.3 expression and IgG control staining on CD4$^+$ T cells of one representative AD patient at time points Z2 and Z3 in overlay with Z1. The data in graphs give the relative mean + SD mean fluorescence intensity (MFI). MFI values at Z1 were set as 100. The significance of data was determined with Student´s *t* test with p*<0.05, p**<0.01, and p***<0.001.

increase of K_v1.3 channel surface expression in naïve and memory $CD4^+$ T cells.

DISCUSSION

In this report, we show that memantine suppresses the reactivity of human T lymphocytes of healthy individuals *in vitro* and of AD patients undergoing memantine (Axura®) therapy. The inhibitory effect of memantine on T cell proliferation directly correlated with the drug concentration and inversely with the strength of TCR stimulation, in line with the co-localization of CD3 and K_v1.3 channels in the immunological synapse [32]. A significant inhibition of alloreactive T cell responses *in vitro* was observed with 1 µM memantine and naïve $CD45RO^-$ T cells were more responsive to low memantine concentrations than memory $CD45RO^+$ cells or CD3Ab-activated T cells. As memantine inhibited the induction of T-bet, which plays a pivotal role in graft rejection [24] and T_H1 migratory programs [33], memantine may also exert potent immunosuppressive function in the prevention of transplant rejection [34, 35]. The used standard dose of memantine in the treatment of AD (10-20 mg/d) correlates with memantine serum concentrations below 1 µM [5]. T cells required much higher memantine concentrations for inhibition *in vitro*. However, standard doses of memantine given to AD patients profoundly reduced *ex vivo* T cell proliferation to 32% of initial values after 12 weeks of treatment. Thus, even low steady-state doses of memantine have substantial inhibitory side effects on T cell reactivity *in vivo* as found for higher drug concentration *in vitro*. It has also to be taken into account that in our experiments memantine was applied only once at the beginning of culture, whereas AD patients received daily medication. For immunosuppressive therapies higher drug doses of memantine may be needed, but memantine doses up to 200 mg/d seem to be tolerated concerning severe central nervous effects [5].

In line with the reported mechanism for NMDA receptor antagonists on murine T cells [22], it is conclusive that memantine significantly reduced K_v1.3 potassium channel currents in human T cells. Compared to resting $CD3^+$ and naïve $CD4^+$ T cells, blockade of K_v1.3 channels on CD3 Ab-stimulated $CD3^+$ and memory T cells required higher memantine concentrations, probably due to an up-regulation of K_v1.3 channels upon T cell activation and on memory T cells [27, 36, 37]. Memantine also suppressed T cell migration towards the chemokine SDF1-α. In view that T cell migration across the blood brain barrier is enhanced in AD patients [8], it is tempting to speculate that memantine's beneficial effect in AD treatment involves a reduced migration of inflammatory or A-beta-reactive T cells into the brain [38]. Deregulated T cell responses in the immune-pathogenesis of AD were reported to include an increased percentage of memory versus naïve T cells [29–31]. Notably, memantine given in the standard dose to newly diagnosed AD patients, substantially reduced $CD45RO^+$ $CD4^+$ T cells. In agreement with reports showing that K_v1.3 channels associate with beta1 integrins [39] and are needed for effector memory T cell migration [40], the depletion of $CD45RO^+$ $CD4^+$ T cells may result from a reduced migration of memory cells into the blood stream or an enhanced egression.

Consistent with the *in vitro* results, K_v1.3 potassium channel currents were significantly lower in $CD4^+$ T cells of AD patients being treated with memantine for 7 days (Z2). However, the inhibition was transient as K_v1.3 channel activity was very similar to untreated cells at 12 weeks of medication (Z3). This correlated with an enhanced surface expression of K_v1.3 channels at Z2, probably representing a compensatory up-regulation of channel expression as a mechanism of tolerance [41]. It is important to emphasize that despite 'restoration' of K_v1.3 channel activity and surface expression of K_v1.3 channels to pre-treatment conditions at Z3, $CD4^+$ T cells of most AD patients displayed progressively attenuated alloresponses at Z2 and Z3. Therefore, a transient inactivation of K_v1.3 channel activity can correlate with a prolonged T cell unresponsiveness.

In conclusion, our data show that memantine has profound inhibitory effects on human T cells and imply that the beneficial effects of memantine in the treatment of AD may involve immunomodulation of T cells and a normalization of deviant immune functions. The drug's inhibitory side effects on T cells may also account for the enhanced infection rate during memantine application [5]. Since K_v1.3 channel inhibitors are still quested for clinical use [42, 43], it seems worthwhile to further evaluate memantine´s potential as an immune-modulating drug in the treatment of AD, autoimmune diseases or transplant rejection [44, 45].

MATERIALS AND METHODS

Ethics statement

Investigation has been conducted in accordance with the ethical standards and according to the Declaration of Helsinki and German guidelines and has been approved by the authors' local institutional review board (MD133/13). Written consent was obtained from all AD patients.

Isolation of human T cells and proliferation assay

PBMCs were isolated with Biocoll Separating Solution (Biochrom AG, Berlin, Germany) and density gradient centrifugation. Isolation of $CD3^+$ cells from PBMCs was performed with the human Pan T Cell Isolation Kit 2 and AutoMACS (Miltenyi Biotec, Bergisch-Gladbach, Germany). Naïve and memory $CD4^+$ T cells were isolated from PBMCs with human Naïve $CD4^+$ T Cell

Isolation Kit 2 and human Memory $CD4^+$ T Cell Isolation Kit (both Miltenyi Biotec). For patch-clamp analyses, isolation of naïve and memory $CD4^+$ T cells was performed with EasySep™ Human Naïve and Human Memory CD4+ T Cell Enrichment Kits (STEMCELL, Vancouver, Canada). Purity of isolated naïve or memory $CD4^+$ T cells was 80-90%. For proliferation assays, isolated T cells were cultured in AIM-V medium (Gibco, Life Technologies, Darmstadt, Germany) and stimulated with MEM92 (CD3 IgM Ab supernatant) or PMA and ionomycin (IO; each 100 ng/ml, Sigma-Aldrich, Hamburg, Germany) in the presence or absence of memantine (R&D Systems, Minneapolis, USA; Tocris Bioscience, Wiesbaden-Nordenstadt, Germany) in the indicated concentrations. 96-well plates were pre-coated with AffiniPure goat anti-mouse IgG+IgM (H+L) (Jackson ImmunoResearch Europe Ltd., Suffolk, UK) over night at 4°C, washed and incubated with MEM92 supernatant. DNA synthesis was determined in triplicates at 72 h of culture by ^{3}[H]-Thymidine incorporation (0.2 µCi/ well, MP Biomedicals Europe, Heidelberg, Germany) for 16 h. For MLRs, isolated $CD4^+$ T cells were stimulated with T cell-depleted and irradiated (30 Gy) PBMCs from another healthy donor in 1:3 ratios. Cells were co-cultured for 120 h and DNA synthesis was determined by ^{3}[H]-Thymidine incorporation for 16 h. In MLRs, the expression of T-bet in responding T cells of healthy donors was analyzed with the intracellular staining kit (Foxp3 Staining Buffer Set, eBioscience, San Diego, USA) using T-bet-PE Ab (clone 4B10, eBioscience) and flow cytometry.

Migration assay

Isolated $CD3^+$ cells ($4x10^6$) remained untreated or were pre-incubated with memantine (20 and 50 µM) for 30 min in AIM-V medium (Gibco®, Life Technologies) supplemented with 0.1% bovine serum albumin and 10 mM HEPES (pH 7.4) and then transferred unto uncoated or fibronectin-coated (6.5 µg/ml; Roche Diagnostics, Basel, Switzerland) transwell chambers (6.5 mm diameter and 3.0 µm pore; Corning Costar, Tewksbury, MA). Cells were allowed to migrate towards human SDF-1α (100 ng/ml; PeproTech, Hamburg, Germany) for 150 min at 37°C. Migration in the absence of chemokine served as a control. Migration was stopped by the addition of 0.1 M EDTA. Migrated cells were stained with CD4-PE and CD8-FITC Abs (BD Pharmingen, Heidelberg, Germany) and acquired for 30 sec at a FACSFortessa™ (BD Bioscience, Heidelberg, Germany). Relative migration was determined by defining the number of cells that migrated in the absence of memantine (mem. 0 µM) as 100%.

Patch-clamp analysis

Whole-cell configuration patch-clamp analysis of human peripheral blood T cells was performed as described (22). In brief, $K_v1.3$ currents were recorded with an external solution containing 160 mM NaCl, 4.5 mM KCl, 5 mM HEPES, 1 mM $MgCl_2$, 2 mM $CaCl_2$, pH 7.4. The pipette solution was 162 mM KF, 11 mM EGTA, 10 mM HEPES, 1 mM $CaCl_2$, 2 mM $MgCl_2$, pH 7.2. Osmolarity was set to 300-340 mOsm. $K_v1.3$ currents were measured every 30 s with depolarizing voltage steps up to +60 mV from a holding potential of -80 mV. Sampling rate during the measurement of $K_v1.3$ currents was 50 kHz. The analysis of transient currents was done with HEKA FitMaster v2x53 and dose-response curves and Hill slopes were determined from amplitude values in GraphPad Prism 5.0.

Analysis of T cells from AD patients

18 ml of blood, with heparin as anti-coagulant, was collected from AD patients for T cell proliferation and FACS analyses. In addition, routine blood analyses were performed, including determination of differential blood cell counts, levels of C-reactive protein, glucose, lipids, liver enzymes, and thyroid hormones. None of the subjects was excluded due to changes in these routine blood parameters. Also, no person had a history of autoimmune disorders, immuno-modulating treatment, cancer, chronic terminal disease, severe cardiovascular disorder, substance abuse or severe trauma. Peripheral blood samples were taken at three time points: before drug treatment (Z1), after 1 week of treatment with memantine (Axura®, 10 mg/d, Z2) and after 12 weeks of drug treatment (Z2 plus Axura®, 20 mg/d for another 11 weeks, Z3). Isolation of $CD4^+$ T cells from PBMCs of patients was performed with the human $CD4^+$ T Cell Isolation Kit (Miltenyi Biotec) and AutoMACS. Cells were cultured in AIM-V medium. For MLR experiments at Z1-Z3, isolated $CD4^+$ T cells were co-cultured with irradiated (30 Gy) total PBMCs from healthy donors for 5 days. Proliferation of $CD4^+$ T cells from the same AD patient was analyzed at Z1-Z3 to compare individual proliferation values before and after drug treatment. PBMCs from the same healthy donor were used as stimulator cells at time points Z1-Z3. DNA synthesis was determined by ^{3}[H]-Thymidine incorporation at 120 h. For FACS analyses, patients' PBMCs were stained with $K_v1.3$ (extracellular)-FITC (polyclonal, Sigma-Aldrich), CD45RO-PE (clone UCHL1, eBioscience) and CD4-APC Abs (clone OKT4, BioLegend, San Diego, USA) and analyzed on a FACSFortessa™. $K_v1.3$ expression on T cells was analyzed for the same patient at Z1-Z3. The percentage of total $CD4^+$ and $CD45RO^+$ $CD4^+$ T cells and patch-clamp analyses at Z1-Z3 were determined on blood samples taken from different patients as drug pre-treatment values at Z1 did not significantly differ between individuals.

Statistical analysis

Flow cytometry data were analyzed with Cell Quest Pro (Becton Dickinson, San Jose, CA, USA) or Flow Jo V3.6.1 (Tree Star, Ashland, OR, USA) software.

Graphs were compiled with Graph-Pad Prism 3.0 and 5.0. Significance of data was determined with Student´s *t* test with p*<0.05, p**<0.01, and p***<0.001.

ACKNOWLEDGMENTS

We thank our colleagues for discussion and support and G. Weitz for technical assistance.

CONFLICTS OF INTEREST

The authors declare having no conflicts of interest.

FUNDING

This work was supported by grants of the SFB854-1/2 of the Deutsche Forschungsgemeinschaft (DFG) to B.S. (B19) and T. B. and U. B. (B9). T. L. was supported by a stipend of the Medical Faculty.

REFERENCES

1. Chen HS, Lipton SA. The chemical biology of clinically tolerated NMDA receptor antagonists. J Neurochem. 2006; 97:1611-1626.
2. Parsons CG, Danysz W, Quack G. Memantine is a clinically well tolerated N-methyl-D-aspartate (NMDA) receptor antagonist—a review of preclinical data. Neuropharmacology. 1999; 38:735-767.
3. Yang Z, Zhou X, Zhang Q. Effectiveness and safety of memantine treatment for Alzheimer's disease. J Alzheimers Dis. 2013; 36:445-458.
4. Thomas SJ, Grossberg GT. Memantine: a review of studies into its safety and efficacy in treating Alzheimer's disease and other dementias. Clin Interv Aging. 2009; 4:367-377.
5. Merz Pharmaceuticals GmbH. Axura: EPAR-Product Information: Summary of Product Characteristics. European Medicines Agency. Last updated January 2016.
6. Merz Pharmaceuticals GmbH. Prescribing information for memantine (Namenda®). U.S. Food and Drug Administration. Revised October 2013. Reference ID: 3394954.
7. Busse S, Steiner J, Glorius S, Dobrowolny H, Greiner-Bohl S, Mawrin C, Bommhardt U, Hartig R, Bogerts B, Busse M. VGF expression by T lymphocytes in patients with Alzheimer's disease. Oncotarget. 2015; 6:14843-14851. doi: 10.18632/oncotarget.3569.
8. Man SM, Ma YR, Shang DS, Zhao WD, Li B, Guo DW, Fang WG, Zhu L, Chen YH. Peripheral T cells overexpress MIP-1alpha to enhance its transendothelial migration in Alzheimer's disease. Neurobiol Aging. 2007; 28:485-496.
9. Schindowski K, Eckert A, Peters J, Gorriz C, Schramm U, Weinandi T, Maurer K, Frolich L, Muller WE. Increased T-cell reactivity and elevated levels of CD8+ memory T-cells in Alzheimer's disease-patients and T-cell hyporeactivity in an Alzheimer's disease-mouse model: implications for immunotherapy. Neuromolecular Med. 2007; 9:340-354.
10. Sulger J, Dumais-Huber C, Zerfass R, Henn FA, Aldenhoff JB. The calcium response of human T lymphocytes is decreased in aging but increased in Alzheimer's dementia. Biol Psychiatry. 1999; 45:737-742.
11. Singh VK1, Guthikonda P. Circulating cytokines in Alzheimer's disease. J Psychiatr Res. 1997; 31:657-60.
12. Leonardi A, Arata L, Bino G, Caria M, Farinelli M, Parodi C, Scudeletti M, Canonica GW. Functional study of T lymphocyte responsiveness in patients with dementia of the Alzheimer type. J Neuroimmunol. 1989; 22:19-22.
13. Monsonego A, Zota V, Karni A, Krieger JI, Bar-Or A, Bitan G, Budson AE, Sperling R, Selkoe DJ, Weiner HL. Increased T cell reactivity to amyloid beta protein in older humans and patients with Alzheimer disease. J Clin Invest. 2003; 112:415-422.
14. Poulopoulou C, Markakis I, Davaki P, Tsaltas E, Rombos A, Hatzimanolis A, Vassilopoulos D. Aberrant modulation of a delayed rectifier potassium channel by glutamate in Alzheimer's disease. Neurobiol Dis. 2010; 37:339-348.
15. Miglio G, Varsaldi F, Lombardi G. Human T lymphocytes express N-methyl-D-aspartate receptors functionally active in controlling T cell activation. Biochem Biophys Res Commun. 2005; 338:1875-1883.
16. Kvaratskhelia E, Maisuradze E, Dabrundashvili NG, Natsvlishvili N, Zhuravliova E, Mikeladze DG. N-methyl-D-aspartate and sigma-ligands change the production of interleukins 8 and 10 in lymphocytes through modulation of the NMDA glutamate receptor. Neuroimmunomodulation. 2009; 16:201-7.
17. Mashkina AP, Cizkova D, Vanicky I, Boldyrev AA. NMDA receptors are expressed in lymphocytes activated both in vitro and in vivo. Cell Mol Neurobiol. 2010; 30:901-7.
18. Zainullina LF, Yamidanov RS, Vakhitov VA, Vakhitova YV. NMDA receptors as a possible component of store-operated Ca(2)(+) entry in human T-lymphocytes. Biochemistry (Mosc). 2011; 76:1220-1226.
19. Mashkina AP, Tyulina OV, Solovyova TI, Kovalenko EI, Kanevski LM, Johnson P, Boldyrev AA. The excitotoxic effect of NMDA on human lymphocyte immune function. Neurochem Int. 2007; 51:356-360.
20. Lombardi G, Dianzani C, Miglio G, Canonico PL, Fantozzi R. Characterization of ionotropic glutamate receptors in human lymphocytes. Br J Pharmacol. 2001; 133:936-944.
21. Tsai KL, Chang HF, Wu SN. The inhibition of inwardly rectifying K+ channels by memantine in macrophages and microglial cells. Cell Physiol Biochem. 2013; 31:938-951.
22. Kahlfuss S, Simma N, Mankiewicz J, Bose T, Lowinus T, Klein-Hessling S, Sprengel R, Schraven B, Heine M, Bommhardt U. Immunosuppression by N-methyl-D-aspartate receptor antagonists is mediated through inhibition

of Kv1.3 and KCa3.1 channels in T cells. Mol Cell Bio. 2014; 34:820-831.

23. Simma N, Bose T, Kahlfuss S, Mankiewicz J, Lowinus T, Luehder F, Schueler T, Schraven B, Heine M, Bommhardt U. NMDA-receptor antagonists block B-cell function but foster IL-10 production in BCR/CD40-activated B cells. Cell Commun Signal. 2014; 12:75.
24. Fu J, Wang D, Yu Y, Heinrichs J, Wu Y, Schutt S, Kaosaard K, Liu C, Haarberg K, Bastian D, McDonald DG, Anasetti C, Yu XZ. T-bet is critical for the development of acute graft-versus-host disease through controlling T cell differentiation and function. J Immunol. 2015; 194:388-397.
25. Zamoyska R. Why is there so much CD45 on T cells? Immunity. 2007; 27:421-3.
26. Chandy KG, DeCoursey TE, Cahalan MD, McLaughlin C, Gupta S. Voltage-gated potassium channels are required for human T lymphocyte activation. J Exp Med. 1984; 160:369-85.
27. Wulff H, Calabresi PA, Allie R, Yun S, Pennington M, Beeton C, Chandy KG. The voltage-gated Kv1.3 K(+) channel in effector memory T cells as new target for MS. J Clin Invest. 2003; 111:1703-1713.
28. Liu QH, Fleischmann BK, Hondowicz B, Maier CC, Turka LA, Yui K, Kotlikoff MI, Wells AD, Freedman BD. Modulation of Kv channel expression and function by TCR and costimulatory signals during peripheral CD4(+) lymphocyte differentiation. J Exp Med. 2002; 196:897-909.
29. Pellicano M, Larbi A, Goldeck D, Colonna-Romano G, Buffa S, Bulati M, Rubino G, Iemolo F, Candore G, Caruso C, Derhovanessian E, Pawelec G. Immune profiling of Alzheimer patients. J Neuroimmunol. 2012; 242:52-59.
30. Larbi A, Pawelec G, Witkowski JM, Schipper HM, Derhovanessian E, Goldeck D, Fulop T. Dramatic shifts in circulating CD4 but not CD8 T cell subsets in mild Alzheimer's disease. J Alzheimers Dis. 2009; 17:91-103.
31. Tan J, Town T, Abdullah L, Wu Y, Placzek A, Small B, Kroeger J, Crawford F, Richards D, Mullan M. CD45 isoform alteration in CD4+ T cells as a potential diagnostic marker of Alzheimer's disease. J Neuroimmunol. 2002; 132:164-172.
32. Panyi G, Bagdány M, Bodnár A, Vámosi G, Szentesi G, Jenei A, Mátyus L, Varga S, Waldmann TA, Gáspar R, Damjanovich S. Colocalization and nonrandom distribution of Kv1.3 potassium channels and CD3 molecules in the plasma membrane of human T lymphocytes. Proc Natl Acad Sci U S A. 2003; 100:2592-7.
33. Lazarevic V1, Glimcher LH. T-bet in disease. Nat Immunol. 2011; 12:597-606.
34. Grgic I, Wulff H, Eichler I, Flothmann C, Köhler R, Hoyer J. Blockade of T-lymphocyte KCa3.1 and Kv1.3 channels as novel immunosuppression strategy to prevent kidney allograft rejection. Transplant Proc. 2009; 41:2601-6.
35. Lam J, Wulff H. The Lymphocyte Potassium Channels Kv1.3 and KCa3.1 as Targets for Immunosuppression. Drug Dev Res. 2011; 72:573-584.
36. Cahalan MD, Wulff H, Chandy KG. Molecular properties and physiological roles of ion channels in the immune system. J Clin Immunol. 2001; 21:235-52.
37. Cahalan MD, Chandy KG. The functional network of ion channels in T lymphocytes. Immunol Rev. 2009; 231:59-87.
38. Gocke AR, Lebson LA, Grishkan IV, Hu L, Nguyen HM, Whartenby KA, Chandy KG, Calabresi PA. Kv1.3 deletion biases T cells toward an immunoregulatory phenotype and renders mice resistant to autoimmune encephalomyelitis. J Immunol. 2012; 188:5877-86.
39. Levite M, Cahalon L, Peretz A, Hershkoviz R, Sobko A, Ariel A, Desai R, Attali B, Lider O. Extracellular K(+) and opening of voltage-gated potassium channels activate T cell integrin function: physical and functional association between Kv1.3 channels and beta1 integrins. J Exp Med. 2000; 191:1167-76.
40. Matheu MP, Beeton C, Garcia A, Chi V, Rangaraju S, Safrina O, Monaghan K, Uemura MI, Li D, Pal S, de la Maza LM, Monuki E, Flügel A, Pennington MW,Parker I, Chandy KG, Cahalan MD. Imaging of effector memory T cells during a delayed-type hypersensitivity reaction and suppression by Kv1.3channel block. Immunity. 2008; 29:602-14.
41. Alfredo Ghezzi, Jascha B. Pohl, Yan Wang, Nigel S. Atkinson. BK channels play a counter-adaptive role in drug tolerance and dependence. Proc Natl Acad Sci U S A. 2010; 107: 16360–16365.
42. Pennington MW, Beeton C, Galea CA, Smith BJ, Chi V, Monaghan KP, Garcia A, Rangaraju S, Giuffrida A, Plank D, Crossley G, Nugent D, Khaytin I et al. Engineering a stable and selective peptide blocker of the Kv1.3 channel in T lymphocytes. Mol Pharmacol. 2009; 75:762-773.
43. Lange A, Giller K, Hornig S, Martin-Eauclaire MF, Pongs O, Becker S, Baldus M. Toxin-induced conformational changes in a potassium channel revealed by solid-state NMR. Nature. 2006; 440:959-962.
44. Conforti L. The ion channel network in T lymphocytes, a target for immunotherapy. Clin Immunol. 2012; 142:105-6.
45. Varga Z, Hajdu P, Panyi G. Ion channels in T lymphocytes: an update on facts, mechanisms and therapeutic targeting in autoimmune diseases. Immunol Lett. 2010; 130:19-25.

Lowinus et al. Cell Communication and Signaling (2019) 17:5
https://doi.org/10.1186/s12964-018-0317-z

Cell Communication and Signaling

RESEARCH Open Access

Memantine potentiates cytarabine-induced cell death of acute leukemia correlating with inhibition of $K_v1.3$ potassium channels, AKT and ERK1/2 signaling

Theresa Lowinus[1,9], Florian H. Heidel[2,3,4], Tanima Bose[5,10], Subbaiah Chary Nimmagadda[2], Tina Schnöder[2,3,4], Clemens Cammann[6], Ingo Schmitz[1,7], Ulrike Seifert[1,6], Thomas Fischer[2], Burkhart Schraven[1,8] and Ursula Bommhardt[1*]

Abstract

Background: Treatment of acute leukemia is challenging and long-lasting remissions are difficult to induce. Innovative therapy approaches aim to complement standard chemotherapy to improve drug efficacy and decrease toxicity. Promising new therapeutic targets in cancer therapy include voltage-gated $K_v1.3$ potassium channels, but their role in acute leukemia is unclear. We reported that $K_v1.3$ channels of lymphocytes are blocked by memantine, which is known as an antagonist of neuronal N-methyl-D-aspartate type glutamate receptors and clinically applied in therapy of advanced Alzheimer disease. Here we evaluated whether pharmacological targeting of $K_v1.3$ channels by memantine promotes cell death of acute leukemia cells induced by chemotherapeutic cytarabine.

Methods: We analyzed acute lymphoid (Jurkat, CEM) and myeloid (HL-60, Molm-13, OCI-AML-3) leukemia cell lines and patients' acute leukemic blasts after treatment with either drug alone or the combination of cytarabine and memantine. Patch-clamp analysis was performed to evaluate inhibition of $K_v1.3$ channels and membrane depolarization by memantine. Cell death was determined with propidium iodide, Annexin V and SYTOX staining and cytochrome C release assay. Molecular effects of memantine co-treatment on activation of Caspases, AKT, ERK1/2, and JNK signaling were analysed by Western blot. $K_v1.3$ channel expression in Jurkat cells was downregulated by shRNA.

Results: Our study demonstrates that memantine inhibits $K_v1.3$ channels of acute leukemia cells and in combination with cytarabine potentiates cell death of acute lymphoid and myeloid leukemia cell lines as well as primary leukemic blasts from acute leukemia patients. At molecular level, memantine co-application fosters concurrent inhibition of AKT, S6 and ERK1/2 and reinforces nuclear down-regulation of MYC, a common target of AKT and ERK1/2 signaling. In addition, it augments mitochondrial dysfunction resulting in enhanced cytochrome C release and activation of Caspase-9 and Caspase-3 leading to amplified apoptosis.

Conclusions: Our study underlines inhibition of $K_v1.3$ channels as a therapeutic strategy in acute leukemia and proposes co-treatment with memantine, a licensed and safe drug, as a potential approach to promote cytarabine-based cell death of various subtypes of acute leukemia.

Keywords: Memantine, Acute leukemia, Cell death, Cytarabine, Signaling

* Correspondence: Ursula.Bommhardt@med.ovgu.de
[1]Institute of Molecular and Clinical Immunology, Health Campus Immunology, Infectiology and Inflammation (GC-I3), Otto-von-Guericke-University Magdeburg, Leipziger Str. 44, 39120 Magdeburg, Germany
Full list of author information is available at the end of the article

Background

Therapy of acute leukemia demands high dose chemotherapy and often stem cell transplantation, which is not feasible in elderly leukemia patients due to severe toxic side effects. For those patients, prognosis remains poor and even palliative treatment options are limited. In addition, older patients show a more heterogeneous clinical biology with induction of aberrant signaling pathways. Therefore, to complement standard chemotherapy and to improve drug efficacy, multi-targeting approaches with potential drug combinations are being investigated [1, 2]. The PI3K-AKT-mTOR and MAPK/ERK1/2 pathways are major signaling cascades deregulated in acute leukemia [3–7] and contribute to an aggressive phenotype and enhanced chemo-resistance. An important target of ERK1/2 [8] and AKT [9] signaling is the transcription factor MYC, which is involved in cell growth, proliferation and apoptosis [10]. Since MYC is a central oncogene inducing leukemic transformation in T cell acute lymphoid leukemia (T-ALL) and acute myeloid leukemia (AML) [11, 12], influencing AKT, ERK1/2 and MYC signaling may enhance the efficacy of chemotherapy in ALL and AML [13–20].

In search of novel treatment options, voltage-gated $K_v1.3$ potassium channels have become promising drug targets. $K_v1.3$ channels localize in the plasma membrane and participate in controlling the membrane potential, proliferation and effector function of lymphocytes [21]. In addition, inactivation of $K_v1.3$ channels expressed in the inner mitochondrial membrane [22] induces intrinsic apoptosis of lymphocytes via mitochondrial cytochrome C (CytC) release and production of reactive oxygen species (ROS) [23–25]. $K_v1.3$ channels on lymphoid and myeloid leukemia cells have been proposed as diagnostic biomarkers [26, 27] and druggable targets for therapy in chronic lymphocytic leukemia [25, 28], lymphoma [29], and solid cancers [30–34]. However, the role of $K_v1.3$ channels in acute leukemia is unclear and there are no licensed drugs for specific inhibition of $K_v1.3$ channels in cancer treatment.

Memantine (3,5-Dimethyltricyclo [3.3.1.1] decanamin) is a registered drug known to inhibit N-methyl-D-aspartate type glutamate receptors (NMDARs) in neurons and has been used for many years in the treatment of moderate-to-severe Alzheimer disease [35, 36]. We reported that in lymphocytes memantine blocks $K_v1.3$ channel activity and diminishes lymphocyte effector function [37, 38]. Furthermore, standard doses of memantine applied in Alzheimer therapy inhibit $K_v1.3$ channels on patients' peripheral blood T cells and alter T cell reactivity in vivo [39]. Thus, we asked whether pharmacological inhibition of $K_v1.3$ channels by memantine could be an option to enhance cell death of acute leukemia cells induced by the chemotherapeutic drug cytarabine (AraC). Analyzing acute lymphoid and myeloid leukemia cell lines and patients' acute leukemic blasts, our data highlight the importance of $K_v1.3$ channels for the survival of acute leukemia cells and provide initial evidence that memantine and cytarabine co-treatment may be a potential therapeutic strategy to enhance the efficacy in acute leukemia treatment.

Methods

Cell culture and determination of cell death

Jurkat (JE6–1), F9, JMR [40], A3, C8 (I.9.2) [41], CEM, HL-60, Molm-13, OCI-AML-3 cells, primary cells from healthy donors, and primary leukemic cells were cultured in RPMI 1640 medium (Biochrom AG, Berlin, Germany) supplemented with 10% fetal calf serum. JE6–1 and CEM cells were bought from ATCC and AML cell lines from DSMZ or ATCC. Cell lines were tested for mycoplasma with PCR or Mycoplasma Detection Kit from Lonza (Basle, Switzerland). Peripheral blood was obtained from healthy donors and a newly diagnosed T-ALL patient, and bone marrow (BM) samples of AML patients were obtained from the Tumor Bank of the Medical Faculty Magdeburg. Peripheral blood mononuclear cells (PBMC) were isolated with Biocoll (Biochrom AG) and $CD3^+$ T cells with Pan-T-Cell-Isolation Kit-2 (Miltenyi, Bergisch-Gladbach, Germany). In each experiment, cell lines or primary cells were cultured without drug, with memantine (Tocris Biosciences, Bristol, Great Britain), AraC (Department of Pharmacy, Medical Faculty Magdeburg), and a combination of memantine plus AraC. AraC concentrations were titrated for each ALL and AML cell line to cover 10–90% cell death. Cell death (with gating on all cells or specific subpopulations when indicated) was determined with SYTOX-Pacific Blue™ (Molecular Probes, Thermo Fisher Scientific, Darmstadt, Germany) ± Annexin V-FITC (BD Pharmingen, Heidelberg, Germany), propidium iodide (PI) (Sigma-Aldrich, St. Louis, USA) or LIVE/DEAD™ Fixable Aqua Dead Cell Stain Kit (Invitrogen, Thermo Fisher Scientific). Percentage of T-ALL cells in sub-$G_{0/1}$-phase of cell cycle was determined with PI. $K_v1.3$ surface expression was analysed with $K_v1.3$-FITC antibodies (Alomone, Jerusalem, Israel; Sigma-Aldrich) using IgG isotype-FITC (BD Pharmingen) or unstained cells as controls. CEM and AML cell lines were incubated with human FcR block (Miltenyi) before staining with $K_v1.3$ antibodies. BM samples from AML patients were thawed and cultured for 3 or 24 h. Cells were stained with LIVE/DEAD Aqua Blue to discriminate live cells, incubated with human FcR block and then labeled with CD117 (104D2, BioLegend) and $K_v1.3$ antibodies. $K_v1.3$ expression is shown for viable $CD117^+$ leukemic blasts. Flow cytometry was performed with a FACSFortessa™ (BD Bioscience, Mountain View, USA).

Determination of ATP content and cytochrome c (CytC) release

Intracellular ATP content, as a measure of viable cells, was determined with CellTiter-Glo® Luminescent Cell Viability Assay (Promega, Mannheim, Germany) according to the manufacturer's protocol. Mitochondrial CytC release was determined as described [42]. In brief, plasma membranes of cultured cells were permeabilized with the mild detergent saponin. Cells were washed to remove cytosolic CytC released from mitochondria during apoptosis. Then the outer mitochondrial membrane was permeabilized with digitonin (50 μg/ml) in 50 μM EDTA, 100 mM KCl for 5 min on ice. Cells were fixed in 4% paraformaldehyde for 20 min, washed and incubated for 1 h in blocking buffer (3% BSA, 0.05% saponin in PBS). Cells were incubated overnight with CytC-AlexaFluor 488 monoclonal antibodies (6H2.B4, BD Pharmingen) and analyzed by flow cytometry. Cells having released mitochondrial CytC, i.e. apoptotic cells, had a lower fluorescence signal.

Proliferation assay

DNA synthesis was determined in triplicates by ^{3}[H]-Thymidine incorporation (0.2 μCi/ well, MP Biomedicals, Heidelberg, Germany) at day 3 for 16 h.

Electrophysiology

Patch-clamp experiments were performed as described [37]. $K_v1.3$ currents were measured every 30 s with depolarizing voltage steps up to + 60 mV from a holding potential of − 80 mV. Sampling rate was 50 kHz during the measurement of $K_v1.3$ currents. Number of $K_v1.3$ channels per cell was determined by dividing the whole-cell $K_v1.3$ conductance by the single-channel conductance value ($K_v1.3$:12 pS) [43, 44]. For membrane potential experiments, JE6−1 cells were recorded in the current clamp mode with zero pA holding current immediately after establishment of the whole-cell configuration. Memantine was kept in a constant concentration during recording in the fixed holding potential (− 80 mV) and the amplitude of the current was measured to determine membrane depolarization. KCl treatment served as a positive control for cell integrity.

Immunoblotting

Cells were cultured without drug, with memantine, AraC (60 nM for Jurkat, 250 nM for Molm-13), and memantine plus AraC. Cytoplasmic and nuclear protein extracts were prepared as described [37]. Antibodies used in Western blots were: p-AKT(S473), AKT, pS6(S240/244), p-ERK1/2(T202/Y204), ERK1/2, pJNK1/2(Thr183/Tyr185), c-JUN (60A8), human Caspase-9, active Caspase-3 (5A1E, only detects cleaved active Caspase-3), Caspase-8 (all Cell Signaling, Leiden, The Netherlands), c-MYC (9E10, BD Pharmingen), β-Actin (AC-74, Sigma-Aldrich), Lamin B (sc-6217, Santa Cruz Biotechnology Europe). Primary antibodies were detected with species-specific secondary antibodies (Dianova, Hamburg, Germany) and chemiluminescence. Nitrocellulose membranes were reprobed for several proteins.

Lentiviral transduction

Lentiviral transduction was performed as described [45]. Lentivirus was generated in 293 T cells by transfection of pLKO.1-$K_v1.3$ shRNA or pLKO.1-scrambled (scr) shRNA (Sigma-Aldrich). JE6−1 cells were infected twice with lentivirus. Puromycin was kept at 0.25 μM for 4 days. RNA was extracted at day 3–4 post infection using Trizol® (Invitrogen, Thermo Fisher Scientific) and reverse transcribed (Quiagen, Düsseldorf, Germany). Knockdown was confirmed by PCR: forward $K_v1.3$: 5′-GGT CAT CAA CAT CTC CGG CGT GCG CT-3′ and reverse $K_v1.3$: 5′-AGG GCC GCT CCT CCT CCC GC-3′ (Apara Bioscience, Denzlingen, Germany), SYBR Green II (Thermo Fisher Scientific) and the CFX96 Real-Time System (BIO-RAD, Munich, Germany).

Statistical analysis

Statistics were performed with Cell Quest Pro software (BD Bioscience), HEKA FitMaster v2x53 and IgorPro for patch-clamp transient currents and GraphPad Prism for analysis of dose-response curves and Student's *t*-test, with $P^{*} < 0.05$, $P^{**} < 0.01$, and $P^{***} < 0.001$. The combination index (CI) and dose reduction index (DRI) were determined with CompuSyn1.0 software using the Chou-Talalay method [46]. For primary AML cells, the coefficient of drug interaction (CDI) was calculated to assess the synergistic inhibitory effect of the drug combination (CDI = AB/(A × B)) [47].

Results

Inactivation of $K_v1.3$ channels promotes cell death of acute leukemia T cells

$K_v1.3$ channels play a key role in setting the resting potential, proliferation and apoptosis of T cells and are expressed in healthy human T cells and the T-lymphoblastic leukemia cell line Jurkat [21, 48, 49] (Additional file 1: Figure S1a). Given that specific $K_v1.3$ channel blockers for clinical therapy are not licensed, we used memantine, an approved drug shown to block $K_v1.3$ channels in vivo [39], and analyzed its effect on Jurkat cells. In voltage-clamp recordings, memantine blocked $K_v1.3$ channel currents of Jurkat cells in a dose-dependent manner with an IC_{50} value of ~ 40 μM (Fig. 1a). Memantine depolarized the membrane potential (Fig. 1b) and induced substantial cell death of Jurkat cells at concentrations above 200 μM (Fig. 1c). To support a role of $K_v1.3$ channels in survival of acute leukemia cells, we knocked down $K_v1.3$ channels in Jurkat cells. Lentiviral

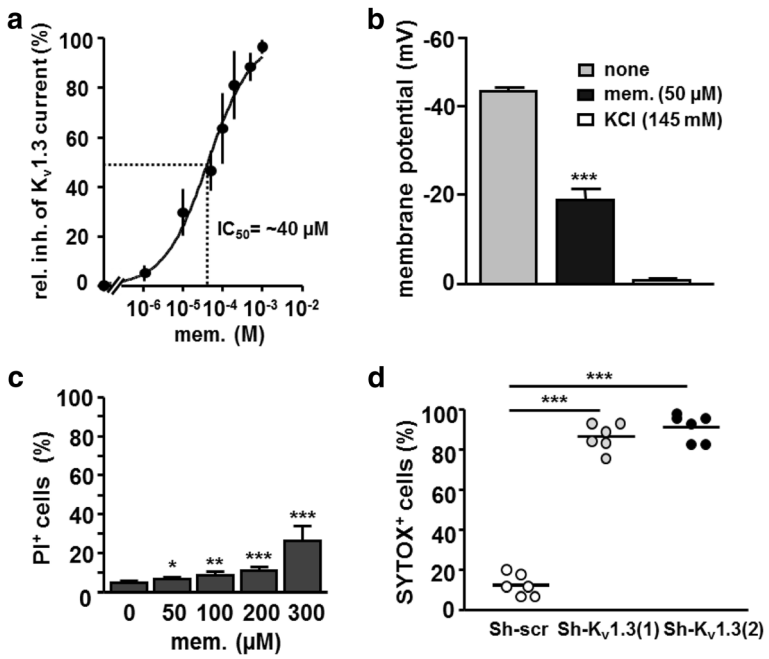

Fig. 1 Pharmacological inhibition by memantine and genetic downregulation of $K_v1.3$ channels promote cell death of acute lymphoblastic leukemia cells. **a** The graph shows the dose response relationship for memantine of isolated $K_v1.3$ currents from Jurkat (JE6–1) cells. Each data point represents the mean ± SD of 5–7 cells from $n = 3$ independent experiments. **b** The membrane potential of untreated and memantine-treated Jurkat cells was determined by current clamp. KCl treatment served as a positive control; the mean + SD was calculated from 5 to 6 cells of $n = 3$ independent experiments. **c** Jurkat cells were treated with the indicated concentrations of memantine for 72 h and cell death was determined with propidium iodide (PI) staining and flow cytometry. Data gives the mean + SD percentage of PI^+ cells from $n = 5$ independent experiments. **d** Jurkat cells were infected with lentivirus harboring shRNA against $K_v1.3$ channels (Sh-$K_v1.3$ (1) and Sh-$K_v1.3$ (2)) or scrambled sequence (Sh-scr). SYTOX staining was performed at day 7. Percentage and mean of $SYTOX^+$ cells is shown for $n = 6$ independent experiments

transduction of Jurkat cells resulted in a 40–50% reduction of $K_v1.3$ mRNA (Additional file 1: Figure S1b). Partial knockdown of $K_v1.3$ mRNA in Jurkat cells by both shRNAs (1 and 2) resulted in pronounced cell death in comparison to cells treated with nonspecific shRNA (Sh-scr) (Fig. 1d). Taken together, pharmacological inhibition using memantine or genetic inactivation of $K_v1.3$ channels impairs survival of Jurkat acute lymphoblastic leukemia cells.

Memantine potentiates AraC-induced cell death of acute lymphoblastic leukemia cells

To evaluate whether pharmacological inhibition of $K_v1.3$ channels on acute leukemia cells could be a valuable approach to enhance chemotherapeutic efficacy, we assessed the effect of $K_v1.3$ channel blockade by memantine in combination with AraC (one of the frontline chemotherapeutic drugs in acute myeloid leukemia treatment). Memantine increased AraC-induced cell death of Jurkat cells in a dose-dependent manner (Fig. 2a). For evaluation of the nature of drug interaction, we used fixed drug ratio design and the Chou-Talalay method [46]. Combination index (CI) values < 1, $=1$, > 1 indicate synergistic, additive and antagonistic effects. CI values for memantine ranged from 0.99 at the affected fraction (Fa) of 0.25 to 0.44 at Fa 0.97 (97% dead cells) indicating varied effects ranging from additive to synergistic (Fig. 2b). The dose reduction index (DRI) at the Fa of 0.97 was 2.4 (Fig. 2b), i.e. memantine co-treatment allows a 2.4-fold dose reduction of AraC to kill 97% of cells. To complement this data, Jurkat cells with $K_v1.3$ channel knockdown were simultaneously treated with AraC. Genetic inactivation of $K_v1.3$ channels induced 70–80% cell death (on day 5). Interestingly, addition of AraC (20 nM) further augmented cell death to 95% (Fig. 2c), supporting a cooperative action of AraC and $K_v1.3$ channel inhibition in inducing cell death. AraC/memantine co-treatment of Jurkat cells also induced a decline in intracellular ATP level and DNA synthesis compared to cells treated with AraC alone (Fig. 2d and e). To exclude the possibility of a Jurkat cell-specific effect, we analysed AraC-induced cell death of the human acute lymphoblastic leukemia cell line CEM. As in Jurkat cells, K_v current in CEM cells is exclusively mediated by $K_v1.3$ channels [50]. Again, AraC/memantine co-treatment enhanced cell death of CEM cells compared to cells treated with AraC alone (Fig. 2f). Further, we examined the effect of memantine co-treatment on primary ALL blasts. PBMC from a newly diagnosed T-ALL patient responded to memantine co-treatment with a 2–3-fold increase in the

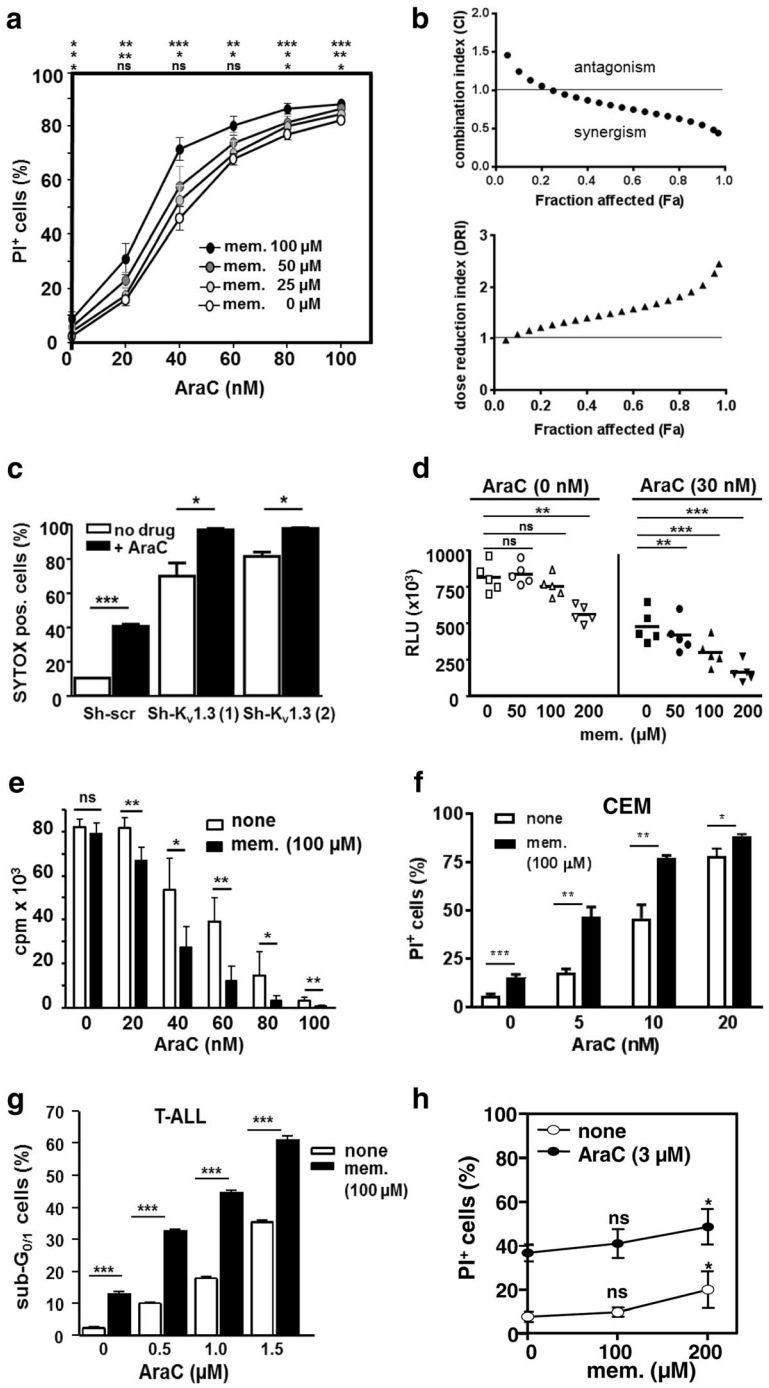

Fig. 2 (See legend on next page.)

(See figure on previous page.)
Fig. 2 Memantine potentiates AraC-induced cell death and decline of ATP content and cell proliferation. **a** Jurkat cells were cultured with AraC ±memantine for 72 h and cell death was determined with PI staining and flow cytometry. The mean ± SD percentage of PI^+ cells was calculated from $n = 4$ independent experiments. **b** Jurkat cells were cultured with AraC and memantine in constant drug ratios for 72 h. The combination index (CI) for AraC+memantine treatment and the dose reduction index (DRI) for AraC was calculated from $n = 5$ independent experiments with the Chou-Talalay method. **c** Jurkat cells, cultured in duplicates, were infected with lentivirus harboring shRNA against $K_v1.3$ channels (Sh-$K_v1.3$ (1) and Sh-$K_v1.3$ (2)) or scrambled sequence (Sh-scr). 48 h post lentiviral infection, part of Jurkat cells were treated with 20 nM AraC. SYTOX staining was performed at day 5. The mean + SD percentage of $SYTOX^+$ cells from duplicate cultures is shown for one out of two experiments. **d** Jurkat cells were cultured without drug, with memantine and AraC±memantine for 72 h and intracellular ATP content was determined with CellTiter-Glo® luminescent assay. Data shows relative light units (RLU) and mean of $n = 5$ independent experiments. **e** DNA synthesis of Jurkat cells treated with AraC±memantine was determined by ^{3}[H]-Thymidine incorporation at 72 h; data show mean + SD cpm values of triplicates of one representative experiment (out of 5). **f** CEM cells were cultured in triplicates with the indicated concentrations of AraC±memantine (100 μM) for 72 h. PI staining was used to determine cell death. The graph shows the mean + SD percentage of PI^+ cells. Data is representative for $n = 3$ independent experiments. **g** PBMC isolated from a newly diagnosed T-ALL patient (78 years of age, 83% blasts) were cultured in triplicates for 72 h with the indicated concentrations of AraC±memantine. The percentage + SD of sub-$G_{0/1}$ cells (indicative of dead cells) was determined with PI staining and flow cytometry. **h** $CD3^+$ T cells were isolated from healthy donors and cultured in triplicates with AraC (3 μM) ± memantine for 72 h. Data show the percentage ± SD of PI^+ cells calculated from $n = 3$ donors. Significance in a-h was determined with Student's *t*-test with $P^* < 0.05$, $P^{**} < 0.01$, $P^{***} < 0.001$, and ns = not significant

percentage of cells in sub-$G_{0/1}$-phase of cell cycle, representing dead cells, compared to AraC application alone (Fig. 2g). In contrast, memantine co-treatment of peripheral blood T cells of healthy donors increased cell death in combination with AraC only at concentrations beyond 100 μM (Fig. 2h), indicating that primary human T cells are less sensitive to memantine co-treatment than acute leukemic T cells. Hence, pharmacological inhibition of $K_v1.3$ channels by memantine potentiates AraC-induced proliferative arrest and cell death in acute lymphoid leukemia cells.

Pharmacological blockade of $K_v1.3$ channels by memantine fosters inhibition of AKT, ERK1/2 and MYC

Hyper-activation of signaling cascades, including AKT and ERK1/2, promotes the development of leukemia. Therefore, simultaneous targeting of these signaling cascades might enhance chemotherapeutic efficacy [51, 52]. To delineate molecular events affected by memantine, AraC alone or in combination, we analyzed the activation of AKT, ribosomal component S6, ERK1/2, and JNK1/2 in Jurkat cells. We also monitored nuclear accumulation of MYC, a target of ERK1/2 and AKT signaling (Fig. 3). While co-application of memantine and AraC reduced the level of p-AKT and p-S6 to 42 and 27% of untreated controls, respectively, AraC treatment had no major effect. Memantine treatment alone enhanced the expression of p-ERK1/2, however, concomitant drug treatment reduced p-ERK1/2 by 54% compared to AraC monotherapy. Neither AraC nor AraC/memantine treatment significantly altered the expression of p-JNK1/2 (Fig. 3a), indicating a selective inhibition of signaling molecules by AraC and AraC/memantine. Furthermore, AraC treatment resulted in decreased nuclear MYC and this effect was even stronger upon memantine co-treatment (a further 4-fold decrease) (Fig. 3b). In contrast, AraC and AraC/memantine co-treatment showed a similar nuclear accumulation of the transcription factor JUN, suggesting that JUN induced by AraC is not significantly affected by memantine (Fig. 3b). Thus, in combination with AraC, memantine fosters inhibition of AKT, ERK1/2 and MYC signaling in Jurkat cells, key regulators of proliferation and survival in acute leukemia.

Memantine enhances CytC release and Caspase-9 activation

Since memantine potentiated AraC-induced cell death, we investigated distinct apoptosis mechanisms. Analyzing the extrinsic apoptotic pathway, Caspase-8 levels in AraC- and AraC/memantine-treated Jurkat cells were similar (Additional file 1: Figure S2a) consistent with a previous report on AraC-induced apoptosis [53]. In addition, in Caspase-8-deficient (C8) and parental (A3) Jurkat cells memantine co-treatment led to a similar enhancement of AraC-induced cell death (Additional file 1: Figure S2b), indicating that the effects of memantine are independent of Caspase-8 activity. We next studied whether memantine acts on the intrinsic apoptotic pathway. Memantine co-treatment augmented the percentage of $CytC^{low}$ Jurkat cells, representing apoptotic cells having released mitochondrial CytC, by 10–40% (Fig. 4a). Furthermore, expression of Caspase-9 fragments, which are indicative of active Caspase-9 induced by mitochondrial CytC release, was elevated in Jurkat cells upon co-treatment in comparison to AraC monotherapy (Fig. 4b). Combined drug treatment also resulted in a 4-fold increase in the expression of the cleaved active form of Caspase-3 (Fig. 4b). The important contribution of Caspase-9 activation for cell death potentiated by memantine was supported by analysis of Caspase-9-deficient (JMR) and Caspase 9-reconstituted (F9) cells. Memantine significantly enhanced AraC-induced cell death in F9, but not in JMR cells, which were less sensitive to AraC treatment than F9 cells (Fig. 4c). Overall, the

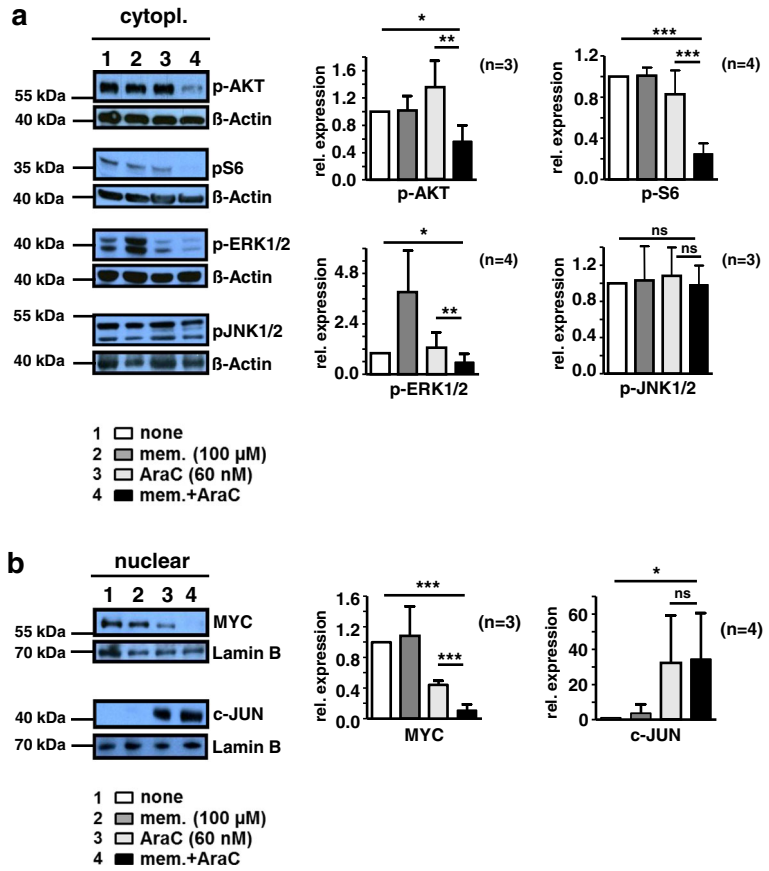

Fig. 3 Memantine co-treatment augments inhibition of AKT, ERK1/2 and MYC signaling. **a.** and **b.** Jurkat cells were cultured without drug, with 100 µM memantine, 60 nM AraC, and memantine+AraC for 72 h (lanes 1–4, respectively). **a** Cytoplasmic and **b** nuclear protein samples were immunoblotted for expression of the indicated proteins; ß-Actin and Lamin B expression served as control for protein loading. A representative Western blot is shown for each indicated protein. The data in bar graphs provide the mean + SD relative expression of the indicated protein calculated from densitometric quantifications of $n = 3–4$ independent experiments for each indicated protein

results allow the conclusion that memantine enhances AraC-induced cell death by promoting CytC release and activation of Caspase-9 and Caspase-3, thus amplifying intrinsic apoptosis.

Memantine potentiates AraC cytotoxicity in AML cell lines and primary AML blasts

Since in adults acute leukemia mainly comprises myeloid differentiation, we asked whether AraC/memantine co-treatment could be an option in therapy of AML. Therefore, we analyzed the human myeloid leukemia cell lines HL-60, Molm-13 and OCI-AML-3. Surface expression of $K_v1.3$ channels on these AML cell lines was verified by flow cytometry (Additional file 1: Figure S3a) [54]. Patch-clamp studies confirmed their functionality and the average expression number could be calculated to 505, 431 and 464 $K_v1.3$ channels per cell for HL-60, Molm-13 and OCI-AML-3, respectively (Additional file 1: Figure S3b). Memantine blocked $K_v1.3$ channel activity with IC_{50} values of 25, 45 and 15 µM for HL-60, Molm-13 and OCI-AML-3 cells (Fig. 5a). In combination with AraC, 25–100 µM memantine further enhanced AraC-induced cell death in the AML cell lines investigated (Fig. 5b). CI values calculated from constant drug ratio experiments showed synergistic effects with CI values at Fa 0.97 of 0.46, 0.76 and 0.71 for HL-60, Molm-13 and OCI-AML-3 cells, respectively, and DRI values at Fa 0.97 of 7.7, 1.8 and 5.4 (Additional file 1: Figure S3c). Co-application of memantine also significantly raised the percentage of $CytC^{low}$ cells in each AraC-treated AML cell line (Fig. 5c), indicating enhanced mitochondrial dysfunction. Immunoblotting of Molm-13 cells revealed that combined AraC/memantine treatment enhances the decline of p-AKT and p-ERK1/2 compared to AraC application alone (Additional file 1: Figure S3d). Altogether, these results suggest that memantine potentiates AraC cytotoxicity through similar mechanisms in acute lymphoid and myeloid leukemia cell lines.

To validate memantine's therapeutic potential in AML, we analyzed leukemic blasts from bone marrow of 10

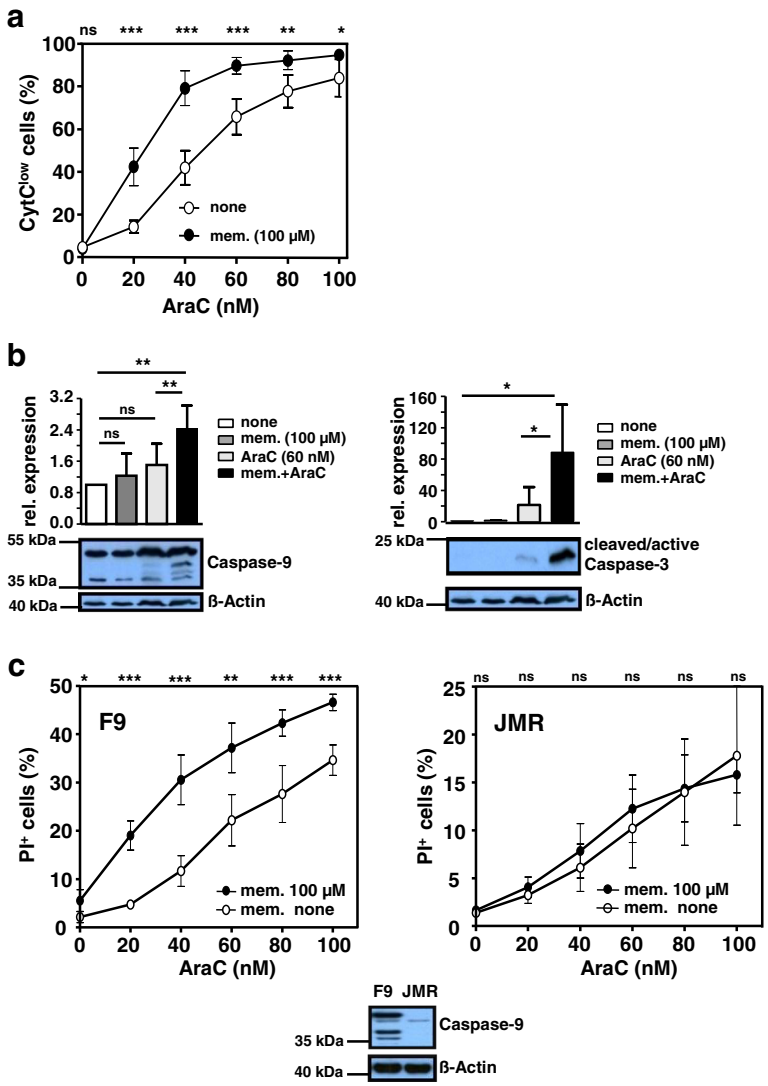

Fig. 4 Memantine co-treatment results in increased CytC release and activation of Caspase-9 and Caspase-3. **a** Jurkat cells were cultured with memantine and AraC±memantine as indicated. After 72 h intracellular CytC level was determined with flow cytometry. $CytC^{low}$ cells represent apoptotic cells having released mitochondrial CytC. Data of $n = 5$ independent experiments is shown as mean ± SD. **b** Expression of Caspase-9 and the cleaved active form of Caspase-3 in Jurkat cells treated without and with drug as indicated was analyzed by Western blot. The data in bar graphs give the mean + SD relative expression of each indicated protein calculated from densitometric quantifications of $n = 4$ independent experiments. **c** Cell death of F9 and JMR cells cultured without or with AraC±memantine for 72 h was determined with PI staining. The percentage of PI^+ cells of $n = 5$ independent experiments is shown as mean ± SD. Western blot shows Caspase-9 and ß-Actin expression in F9 and JMR cells

AML patients (Additional file 1: Table S1). Low surface expression of $K_v1.3$ was detectable on all analysed viable $CD117^+$ AML blasts (Fig. 6a). Although sensitivity of AML cells towards AraC and memantine varied between individuals, co-treatment with memantine (100 and 50 µM) further increased cell death of AraC-treated AML samples (Fig. 6b and c). Nature of memantine and AraC interaction was evaluated by calculating coefficient of drug interaction (CDI) values. Interestingly, CDI values were less than one indicating synergism when the cells were simultaneously treated with memantine and AraC. Compared to cell lines, patients' primary leukemic cells were more sensitive to memantine monotherapy as it induced pronounced cell death in the absence of AraC. The results from primary acute leukemic blasts suggest that combined AraC/memantine treatment could be a therapeutic strategy to enhance cell death in acute leukemia.

Discussion

In line with reports underscoring the importance of $K_v1.3$ channels in survival of leukemic B cells [28, 55]

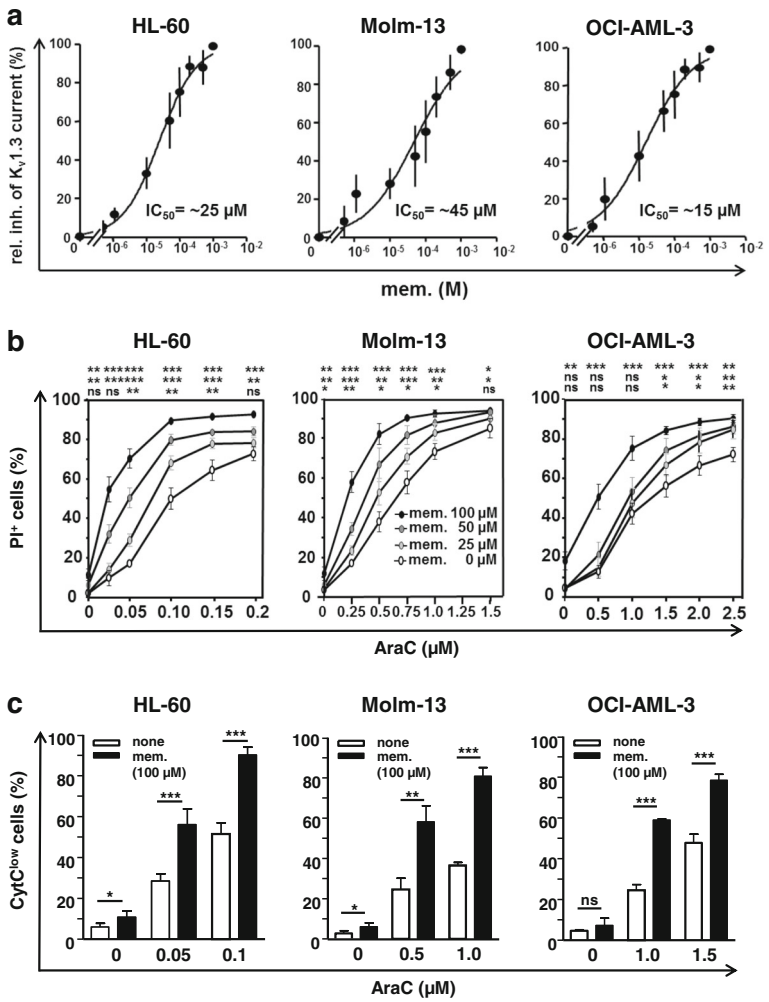

Fig. 5 Memantine potentiates AraC-induced cell death of AML cell lines. **a** Dose response relationship for memantine is shown for isolated $K_v1.3$ currents recorded from the acute myeloid leukemia cell lines HL-60, Molm-13 and OCI-AML-3. Each data point represents the mean ± SD of 5–7 cells from $n = 3$ experiments. **b** HL-60 and Molm-13 cells were treated with AraC±memantine for 3 days and OCI-AML3 cells for 5 days. Cell death was determined with PI staining and flow cytometry. For each cell line the percentage ± SD of PI^+ cells was calculated from $n = 4$ independent experiments. **c** Graphs show the percentage + SD of $CytC^{low}$ AML cells at day 3 (day 5 for OCI-AML-3 cells); for each cell line data was calculated from $n = 4$ independent experiments

and various cancer cell lines [54], our data provide initial evidence that $K_v1.3$ channels are druggable targets in chemotherapy of T-ALL and AML. To address the clinical need for a pharmacological $K_v1.3$ channel inhibitor, we used memantine, which shows an excellent safety profile and is licensed for NMDAR antagonism in advanced Alzheimer disease [35]. Memantine inhibited $K_v1.3$ channels and potentiated AraC-induced cell death of acute lymphoid (Jurkat, CEM) and myeloid (HL-60, Molm-13, OCI-AML-3) leukemia cell lines (representing highly chemoresistant aggressive clones) as well as primary acute leukemic blasts. Synergistic drug effects were observed for the analyzed cell lines and AML blasts. Jurkat and Molm-13 cells showed enhanced reduction of ERK1/2 and AKT signaling upon drug co-treatment and enhanced cell death of Jurkat and AML cell lines was connected with increased CytC release. Since mitochondrial $K_v1.3$ channels contribute to the intrinsic apoptotic pathway upon a pre-existing apoptotic stimulus [23, 25], AraC may act as a sensitizer for inhibition of $K_v1.3$ channels. Thus, addition of memantine to AraC results in enhanced CytC release and activation of Caspase-9 and Caspase-3. In primary ALL and AML blasts memantine monotherapy already induced cell death, but combination of memantine and AraC was most effective in cell death induction of leukemic blasts. In contrast to acute leukemic cells, primary non-malignant T lymphocytes did not show a relevant potentiation of AraC by memantine. This may relate to the enhanced susceptibility of malignant cells to reactive oxygen species

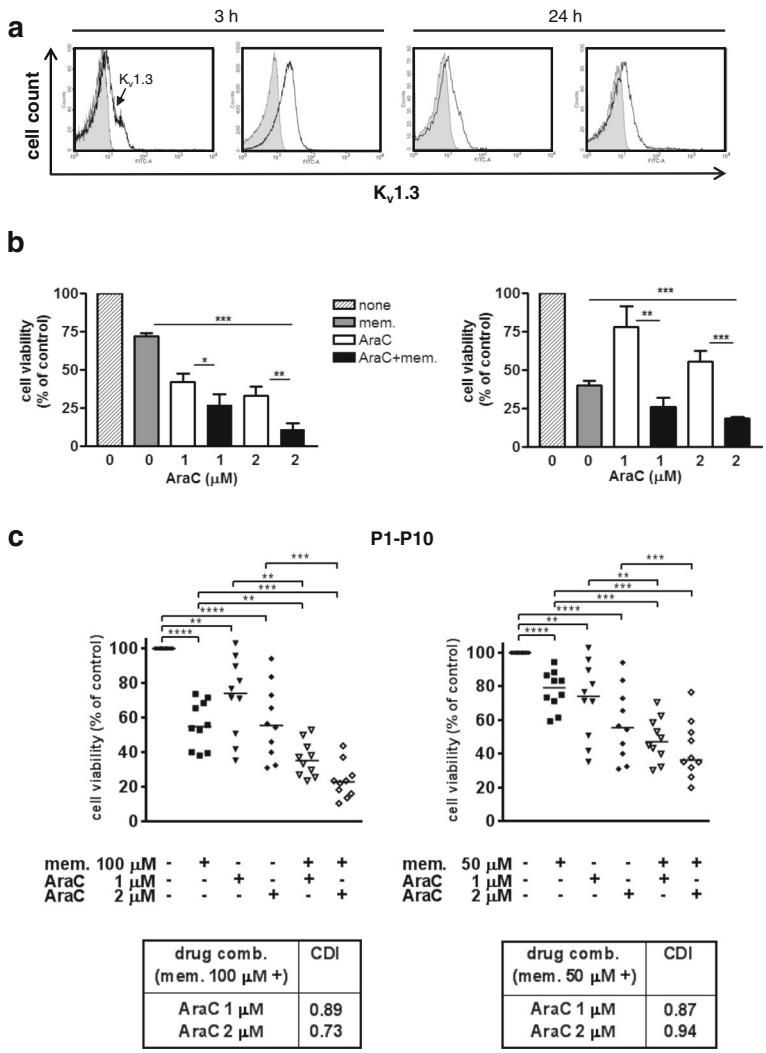

drug comb. (mem. 100 μM +)	CDI
AraC 1 μM	0.89
AraC 2 μM	0.73

drug comb. (mem. 50 μM +)	CDI
AraC 1 μM	0.87
AraC 2 μM	0.94

Fig. 6 Memantine potentiates cell death of patients' myeloid leukemic blasts. **a** Bone marrow (BM) cells of AML patients were analysed for surface expression of K_v1.3 by flow cytometry. Histograms show K_v1.3 profiles of viable $CD117^+$ leukemic blasts cultured for 3 or 24 h and are representative for eight BM samples. Cells without K_v1.3 staining are depicted in grey histograms. **b.** and **c.** BM cells of 10 AML patients (Additional file 1: Table S1) were cultured without any drug, with memantine alone (100 μM lower left graph, 50 μM lower right graph), with 1 μM and 2 μM AraC alone, and with AraC plus memantine for 48 h. Cell death was determined with SYTOX/Annexin-V staining and flow cytometry. $SYTOX^-$Annexin-V^- cells were considered as viable cells. For each patient, cell viability of untreated (control) AML cells was set as 100% and cell viability of treated AML cells was related to the corresponding control sample. **b** The graphs show data of two representative patients (cells were treated with 100 μM memantine). **c** Graphs provide the relative cell viability of BM cells of 10 AML patients. Coefficient of drug interaction (CDI) values for combined memantine and AraC treatments are provided in the boxes; CDI < 1 indicates synergism and CD > 1 antagonism

produced at the mitochondria upon apoptosis induction [23, 25].

Using murine lymphocytes, we previously reported that memantine blocks K_v1.3 and K_{Ca}3.1 channels [37]. Therefore, we do not exclude a possibility of memantine affecting K_{Ca}3.1 channels (and maybe other ion channels) [50, 54, 56, 57] which might contribute to memantine's potentiation of AraC cytotoxicity. Compared to memantine treatment alone, knockdown of K_v1.3 mRNA in Jurkat cells was more effective in inducing cell death. This could in part be due to transient pharmacological blockade of cell surface K_v1.3 channels by memantine and a compensatory up-regulation of K_v1.3 channel expression and activity as a mechanism of drug resistance [39, 54].

The PI3K-AKT-mTOR and ERK1/2 signaling pathways are commonly activated in acute leukemia and confer poor prognosis [52]. PI3K-AKT-mTOR inhibitors have been used in clinical trials [13, 58], however, the induction of feedback and compensatory mechanisms, like aberrant ERK1/2 activation leading to phosphorylation of ribosomal protein S6, may have contributed to drug resistance [6]. Further, treatment of T-ALL cell lines

with PI3K and mTOR inhibitors led to an up-regulation of MYC [59, 60]. Here we found that memantine co-treatment targets several central signaling cascades as it concurrently decreased AKT, ERK1/2 and MYC signaling while increasing mitochondrial CytC release and Caspase-9/Caspase-3 activation. Since memantine/AraC co-treatment led to effective killing of lymphoid and myeloid leukemia cell lines and patients' leukemic blasts with different genetic background, memantine may act through 'common' mechanisms that feed into or extend the AraC-induced cell death machinery. Beside inhibition of AKT-mTOR and ERK1/2 signaling, these may include inhibition of calcium signaling and cell cycle by altering the membrane potential [49] and increase of intracellular potassium concentrations, which inhibited AKT-mTOR activity in T-effector cells by unknown mechanisms [61].

Memantine is an orally given drug with excellent bioavailability and long half-life. Steady-state memantine concentrations in serum of treated (10–20 mg/day) Alzheimer patients were reported to be < 1.0 μM [35, 36]. In our study, effective memantine concentrations (given only once at begin of cell culture) ranged from 25 to 100 μM. However, daily therapeutic doses of memantine block $K_v1.3$ channels on blood T cells and inhibit T cell function in vivo, whereas inhibition of human T cell function in vitro required higher memantine concentrations [39]. Various pharmacologic factors such as drug metabolites, half-life, daily dosing, and niche specific drug-cell interactions might account for the difference of in vitro versus in vivo drug effectiveness. Memantine is being tested in several disease settings without showing severe side effects even in elderly patients and at higher drug doses. As a licensed drug proven to inhibit $K_v1.3$ channels in vivo, memantine seems to be suited for testing a potential cooperative action in AraC therapy of acute leukemia.

Conclusion

Our data support the concept of targeting $K_v1.3$ channels in ALL and AML therapy and, though in vivo studies remain to be performed, suggest memantine as a potential intensifier of AraC-based treatments of different subtypes of acute leukemia, particular in palliative low-dose AraC monotherapy of patients.

Additional files

Additional file 1: Table S1. Characteristics of AML patients. **Figure S1.** a $K_v1.3$ expression on Jurkat cells; grey histogram shows isotype staining. b Knockdown of $K_v1.3$ mRNA in Jurkat cells via lentivirus harboring Sh-$K_v1.3$ (1), Sh-$K_v1.3$ (2) or scrambled (Sh-scr) sequence. Data give the relative mean + SEM expression of $K_v1.3$ mRNA from triplicate cultures of one experiment at day 3, $n = 6$. c $K_v1.3$ expression on CEM cells; grey histogram shows unstained cells. **Figure S2.** a Jurkat cells were cultured without drug, 100 μM memantine, 60 nM AraC, and memantine+AraC for 72 h. Caspase-8 and β-actin expression was analysed by Western blot. Data show mean + SD relative expression of Caspase-8; $n = 4$. b Parental A3 and Caspase-8-deficient C8 cells were treated with AraC±memantine for 72 h; mean ± SD percentage of PI^+ cells was calculated from $n = 5$. Western blot shows Caspase-8 and β-actin expression. Student´s *t*-test: $P^{**} < 0.01$, $P^{***} < 0.001$, ns = not significant. **Figure S3.** a $K_v1.3$ expression on HL-60, Molm-13, OCI-AML-3; grey histograms show unstained cells. b Number of $K_v1.3$ channels/cell of HL-60, Molm-13, and OCI-AML-3. Data show mean ± SEM $K_v1.3$ channel number of $n = 4$-5 experiments for each cell line and mean $K_v1.3$ number of all cells. c HL-60, Molm-13, OCI-AML-3 cells were cultured with AraC and memantine at fixed drug ratios for 72 h; percentage of PI^+ cells was determined. For each cell line, combination index (CI) and dose reduction index (DRI) for AraC were calculated from $n = 4$-5 using Chou-Talalay method. CI < 1 drug synergism, CI = 1 additivity, CI > 1 drug antagonism. d Molm-13 cells were cultured without drug, 100 μM memantine, 250 nM AraC, and memantine+AraC for 46 h. Cytoplasmic expression of indicated proteins was analysed by Western blot; $n = 2$-3. (PDF 226 kb)

Abbreviations

AraC: cytarabine; CI: combination index; CytC: cytochrome c; DRI: dose reduction index; Mem: memantine; PI: propidium iodide

Acknowledgements

The authors like to thank M. Heine, J. Lindquist, V. Reddycherla, and L. Simeoni for discussion, JE6-1 cells and antibodies.

Funding

This work was supported by grants from the Deutsche Forschungsgemeinschaft (DFG) (SFB854–1/2 to F.H.H. and T.F. (A20), I.S. (A23N), U.S. (A24N), B.S. (B19), U.B. (B9)) and the German Jose-Carreras Leukemia Foundation (DJCLF SP12/08 to F.H.H. and T.F.). T.L. was supported by a stipend from the Medical Faculty of the Otto-von-Guericke-University Magdeburg.

Availability of data and materials

The datasets used and/or analysed during the current study are available from the corresponding author on reasonable request.

Authors' contributions

T.L., F.H.H., and U.B. designed the study; T.L., T.B., T.S., S.C.N., C.C., and U.B. performed experiments. T.L., T.B., F.H.H., T.F., S.C.N., C.C., and U.B. analyzed data and prepared figures. T.F., F.H.H., I.S., B.S., and U.S. provided patient cells, cell lines, reagents, discussion and scientific advice. T.L., F.H.H., U.S., T.B., S.C.N., and U.B. wrote and revised the manuscript. All authors approved the final manuscript.

Ethics approval and consent to participate

The study was approved by the Institutional Review Board and Ethics Committee (MD 115/08, MD 40/13) of the Medical Faculty of the Otto-von-Guericke-University Magdeburg, Germany. Patient material for research purposes was obtained after informed and written consent of all donors and according to the Helsinki Declaration.

Consent for publication

Not applicable.

Competing interests

The authors declare that they have no competing interests.

Publisher's Note

Author details

[1]Institute of Molecular and Clinical Immunology, Health Campus Immunology, Infectiology and Inflammation (GC-I3), Otto-von-Guericke-University Magdeburg, Leipziger Str. 44, 39120 Magdeburg, Germany. [2]Department of Hematology and Oncology, GC-I3,

Otto-von-Guericke-University Magdeburg, Magdeburg, Germany. [3]Leibniz Institute on Aging, Fritz-Lipmann Institute, Jena, Germany. [4]Innere Medizin II, Universitätsklinikum Jena, Jena, Germany. [5]Leibniz Institute of Neurobiology, Magdeburg, Germany. [6]Friedrich Loeffler Institute for Medical Microbiology, University Medicine Greifswald, Greifswald, Germany. [7]Systems-Oriented Immunology and Inflammation Research Group, Helmholtz Centre for Infection Research, Braunschweig, Germany. [8]Department of Immune Control, Helmholtz Centre for Infection Research, Braunschweig, Germany. [9]Present address: Department of Hematology, Oncology, and Stem Cell Transplantation, Faculty of Medicine, Freiburg University Medical Center, Freiburg, Germany. [10]Present address: Institute for Clinical Neuroimmunology, Ludwigs-Maximilians-University, Munich, Germany.

Received: 23 October 2018 Accepted: 28 December 2018
Published online: 16 January 2019

References

1. Peyrade F, Gastaud L, Re D, Pacquelet-Cheli S, Thyss A. Treatment decisions for elderly patients with haematological malignancies: a dilemma. Lancet Oncol. 2012;13:e344–52.
2. Ossenkoppele G, Lowenberg B. How I treat the older patient with acute myeloid leukemia. Blood. 2015;125:767–74.
3. Barata JT, Silva A, Brandao JG, Nadler LM, Cardoso AA, Boussiotis VA. Activation of PI3K is indispensable for interleukin 7-mediated viability, proliferation, glucose use, and growth of T cell acute lymphoblastic leukemia cells. J Exp Med. 2004;200:659–69.
4. Kornblau SM, Womble M, Qiu YH, Jackson CE, Chen W, Konopleva M, et al. Simultaneous activation of multiple signal transduction pathways confers poor prognosis in acute myelogenous leukemia. Blood. 2006;108:2358–65.
5. Gutierrez A, Sanda T, Grebliunaite R, Carracedo A, Salmena L, Ahn Y, et al. High frequency of PTEN, PI3K, and AKT abnormalities in T-cell acute lymphoblastic leukemia. Blood. 2009;114:647–50.
6. Steelman LS, Franklin RA, Abrams SL, Chappell W, Kempf CR, Basecke J, et al. Roles of the Ras/Raf/MEK/ERK pathway in leukemia therapy. Leukemia. 2011; 25:1080–94.
7. Gupta M, Hendrickson AE, Yun SS, Han JJ, Schneider PA, Koh BD, et al. Dual mTORC1/mTORC2 inhibition diminishes Akt activation and induces puma-dependent apoptosis in lymphoid malignancies. Blood. 2012;119:476–87.
8. Kerkhoff E, Houben R, Loffler S, Troppmair J, Lee JE, Rapp UR. Regulation of c-myc expression by Ras/Raf signalling. Oncogene. 1998;16:211–6.
9. Tsai WB, Aiba I, Long Y, Lin HK, Feun L, Savaraj N, et al. Activation of Ras/PI3K/ERK pathway induces c-Myc stabilization to upregulate argininosuccinate synthetase, leading to arginine deiminase resistance in melanoma cells. Cancer Res. 2012;72:2622–33.
10. Eilers M, Eisenman RN. Myc's broad reach. Genes Dev. 2008;22:2755–66.
11. Luo H, Li Q, O'Neal J, Kreisel F, Le Beau MM, Tomasson MH. c-Myc rapidly induces acute myeloid leukemia in mice without evidence of lymphoma-associated antiapoptotic mutations. Blood. 2005;106:2452–61.
12. Herranz D, Ambesi-Impiombato A, Palomero T, Schnell SA, Belver L, Wendorff AA, et al. A NOTCH1-driven MYC enhancer promotes T cell development, transformation and acute lymphoblastic leukemia. Nat Med. 2014;20:1130–7.
13. Teachey DT, Obzut DA, Cooperman J, Fang J, Carroll M, Choi JK, et al. The mTOR inhibitor CCI-779 induces apoptosis and inhibits growth in preclinical models of primary adult human ALL. Blood. 2006;107:1149–55.
14. Nishioka C, Ikezoe T, Yang J, Yokoyama A. Inhibition of MEK signaling enhances the ability of cytarabine to induce growth arrest and apoptosis of acute myelogenous leukemia cells. Apoptosis. 2009;14:1108–20.
15. Chiarini F, Fala F, Tazzari PL, Ricci F, Astolfi A, Pession A, et al. Dual inhibition of class IA phosphatidylinositol 3-kinase and mammalian target of rapamycin as a new therapeutic option for T-cell acute lymphoblastic leukemia. Cancer Res. 2009;69:3520–8.
16. Martelli AM, Tabellini G, Ricci F, Evangelisti C, Chiarini F, Bortul R, et al. PI3K/AKT/mTORC1 and MEK/ERK signaling in T-cell acute lymphoblastic leukemia: new options for targeted therapy. Adv Biol Regul. 2012;52:214–27.
17. Schubbert S, Cardenas A, Chen H, Garcia C, Guo W, Bradner J, et al. Targeting the MYC and PI3K pathways eliminates leukemia-initiating cells in T-cell acute lymphoblastic leukemia. Cancer Res. 2014;74:7048–59.
18. Walz S, Lorenzin F, Morton J, Wiese KE, von Eyss B, Herold S, et al. Activation and repression by oncogenic MYC shape tumour-specific gene expression profiles. Nature. 2014;511:483–7.
19. Loosveld M, Castellano R, Gon S, Goubard A, Crouzet T, Pouyet L, et al. Therapeutic targeting of c-Myc in T-cell acute lymphoblastic leukemia, T-ALL. Oncotarget. 2014;5:3168–72.
20. Fransecky L, Mochmann LH, Baldus CD. Outlook on PI3K/AKT/mTOR inhibition in acute leukemia. Mol Cell Ther. 2015;3:2.
21. Cahalan MD, Chandy KG. The functional network of ion channels in T lymphocytes. Immunol Rev. 2009;231:59–87.
22. Szabo I, Bock J, Jekle A, Soddemann M, Adams C, Lang F, et al. A novel potassium channel in lymphocyte mitochondria. J Biol Chem. 2005;280:12790–8.
23. Szabo I, Bock J, Grassme H, Soddemann M, Wilker B, Lang F, et al. Mitochondrial potassium channel Kv1.3 mediates Bax-induced apoptosis in lymphocytes. Proc Natl Acad Sci U S A. 2008;105:14861–6.
24. Leanza L, Henry B, Sassi N, Zoratti M, Chandy KG, Gulbins E, et al. Inhibitors of mitochondrial Kv1.3 channels induce Bax/Bak-independent death of cancer cells. EMBO Mol Med. 2012;4:577–93.
25. Leanza L, Romio M, Becker KA, Azzolini M, Trentin L, Manago A, et al. Direct pharmacological targeting of a mitochondrial Ion Channel selectively kills tumor cells in vivo. Cancer Cell. 2017;31:516–31 e510.
26. Felipe A, Bielanska J, Comes N, Vallejo A, Roig S, Ramon YCS, et al. Targeting the voltage-dependent K(+) channels Kv1.3 and Kv1.5 as tumor biomarkers for cancer detection and prevention. Curr Med Chem. 2012;19:661–74.
27. Chimote AA, Hajdu P, Sfyris AM, Gleich BN, Wise-Draper T, Casper KA, et al. Kv1.3 channels mark functionally competent CD8+ tumor-infiltrating lymphocytes in head and neck Cancer. Cancer Res. 2017;77:53–61.
28. Leanza L, Trentin L, Becker KA, Frezzato F, Zoratti M, Semenzato G, et al. Clofazimine, Psora-4 and PAP-1, inhibitors of the potassium channel Kv1.3, as a new and selective therapeutic strategy in chronic lymphocytic leukemia. Leukemia. 2013;27:1782–5.
29. Alizadeh AA, Eisen MB, Davis RE, Ma C, Lossos IS, Rosenwald A, et al. Distinct types of diffuse large B-cell lymphoma identified by gene expression profiling. Nature. 2000;403:503–11.
30. Wulff H, Castle NA, Pardo LA. Voltage-gated potassium channels as therapeutic targets. Nat Rev Drug Discov. 2009;8:982–1001.
31. Arcangeli A, Pillozzi S, Becchetti A. Targeting ion channels in leukemias: a new challenge for treatment. Curr Med Chem. 2012;19:683–96.
32. Panyi G, Beeton C, Felipe A. Ion channels and anti-cancer immunity. Philos Trans R Soc Lond Ser B Biol Sci. 2014;369:20130106.
33. Teisseyre A, Gasiorowska J, Michalak K. Voltage-gated potassium channels Kv1.3--potentially new molecular target in Cancer diagnostics and therapy. Adv Clin Exp Med. 2015;24:517–24.
34. Leanza L, Manago A, Zoratti M, Gulbins E, Szabo I. Pharmacological targeting of ion channels for cancer therapy: in vivo evidences. Biochim Biophys Acta. 1863;2016:1385–97.
35. Rammes G, Danysz W, Parsons CG. Pharmacodynamics of memantine: an update. Curr Neuropharmacol. 2008;6:55–78.
36. Alam S, Lingenfelter KS, Bender AM, Lindsley CW. Classics in chemical neuroscience: Memantine. ACS Chem Neurosci. 2017;8:1823–9.
37. Kahlfuss S, Simma N, Mankiewicz J, Bose T, Lowinus T, Klein-Hessling S, et al. Immunosuppression by N-methyl-D-aspartate receptor antagonists is mediated through inhibition of Kv1.3 and KCa3.1 channels in T cells. Mol Cell Biol. 2014;34:820–31.
38. Simma N, Bose T, Kahlfuss S, Mankiewicz J, Lowinus T, Luhder F, et al. NMDA-receptor antagonists block B-cell function but foster IL-10 production in BCR/CD40-activated B cells. Cell Commun Signal. 2014;12:75.
39. Lowinus T, Bose T, Busse S, Busse M, Reinhold D, Schraven B, et al. Immunomodulation by memantine in therapy of Alzheimer's disease is mediated through inhibition of Kv1.3 channels and T cell responsiveness. Oncotarget. 2016;7:53797–807.
40. Samraj AK, Sohn D, Schulze-Osthoff K, Schmitz I. Loss of caspase-9 reveals its essential role for caspase-2 activation and mitochondrial membrane depolarization. Mol Biol Cell. 2007;18:84–93.
41. Seol DW, Li J, Seol MH, Park SY, Talanian RV, Billiar TR. Signaling events triggered by tumor necrosis factor-related apoptosis-inducing ligand (TRAIL): caspase-8 is required for TRAIL-induced apoptosis. Cancer Res. 2001; 61:1138–43.
42. Waterhouse NJ, Trapani JA. A new quantitative assay for cytochrome c release in apoptotic cells. Cell Death Differ. 2003;10:853–5.
43. Grissmer S, Dethlefs B, Wasmuth JJ, Goldin AL, Gutman GA, Cahalan MD, et al. Expression and chromosomal localization of a lymphocyte K+ channel gene. Proc Natl Acad Sci U S A. 1990;87:9411–5.

44. Ghanshani S, Wulff H, Miller MJ, Rohm H, Neben A, Gutman GA, et al. Up-regulation of the IKCa1 potassium channel during T-cell activation. Molecular mechanism and functional consequences. J Biol Chem. 2000;275:37137–49.
45. Schnoder TM, Arreba-Tutusaus P, Griehl I, Bullinger L, Buschbeck M, Lane SW, et al. Epo-induced erythroid maturation is dependent on Plcgamma1 signaling. Cell Death Differ. 2015;22:974–85.
46. Chou TC. Drug combination studies and their synergy quantification using the Chou-Talalay method. Cancer Res. 2010;70:440–6.
47. Tallarida RJ. The interaction index: a measure of drug synergism. Pain. 2002; 98:163–8.
48. Conforti L. The ion channel network in T lymphocytes, a target for immunotherapy. Clin Immunol. 2012;142:105–6.
49. Feske S, Wulff H, Skolnik EY. Ion channels in innate and adaptive immunity. Annu Rev Immunol. 2015;33:291–353.
50. Valle-Reyes S, Valencia-Cruz G, Linan-Rico L, Pottosin I, Dobrovinskaya O. Differential activity of voltage- and ca(2+)-dependent potassium channels in leukemic T cell lines: Jurkat cells represent an exceptional case. Front Physiol. 2018;9:499.
51. McCubrey JA, Steelman LS, Abrams SL, Bertrand FE, Ludwig DE, Basecke J, et al. Targeting survival cascades induced by activation of Ras/Raf/MEK/ERK, PI3K/PTEN/Akt/mTOR and Jak/STAT pathways for effective leukemia therapy. Leukemia. 2008;22:708–22.
52. Brown KK, Toker A. The phosphoinositide 3-kinase pathway and therapy resistance in cancer. F1000Prime Rep. 2015;7:13.
53. Terrisse AD, Bezombes C, Lerouge S, Laurent G, Jaffrezou JP. Daunorubicin- and Ara-C-induced interphasic apoptosis of human type II leukemia cells is caspase-8-independent. Biochim Biophys Acta. 2002;1584:99–103.
54. Leanza L, O'Reilly P, Doyle A, Venturini E, Zoratti M, Szegezdi E, et al. Correlation between potassium channel expression and sensitivity to drug-induced cell death in tumor cell lines. Curr Pharm Des. 2014;20:189–200.
55. Szabo I, Trentin L, Trimarco V, Semenzato G, Leanza L. Biophysical characterization and expression analysis of Kv1.3 potassium channel in primary human leukemic B cells. Cell Physiol Biochem. 2015;37:965–78.
56. Pillozzi S, Brizzi MF, Balzi M, Crociani O, Cherubini A, Guasti L, et al. HERG potassium channels are constitutively expressed in primary human acute myeloid leukemias and regulate cell proliferation of normal and leukemic hemopoietic progenitors. Leukemia. 2002;16:1791–8.
57. Grossinger EM, Weiss L, Zierler S, Rebhandl S, Krenn PW, Hinterseer E, et al. Targeting proliferation of chronic lymphocytic leukemia (CLL) cells through KCa3.1 blockade. Leukemia. 2014;28:954–8.
58. Perl AE, Kasner MT, Tsai DE, Vogl DT, Loren AW, Schuster SJ, et al. A phase I study of the mammalian target of rapamycin inhibitor sirolimus and MEC chemotherapy in relapsed and refractory acute myelogenous leukemia. Clin Cancer Res. 2009;15:6732–9.
59. Park S, Chapuis N, Saint Marcoux F, Recher C, Prebet T, Chevallier P, et al. A phase Ib GOELAMS study of the mTOR inhibitor RAD001 in association with chemotherapy for AML patients in first relapse. Leukemia. 2013;27:1479–86.
60. Shepherd C, Banerjee L, Cheung CW, Mansour MR, Jenkinson S, Gale RE, et al. PI3K/mTOR inhibition upregulates NOTCH-MYC signalling leading to an impaired cytotoxic response. Leukemia. 2013;27:650–60.
61. Eil R, Vodnala SK, Clever D, Klebanoff CA, Sukumar M, Pan JH, et al. Ionic immune suppression within the tumour microenvironment limits T cell effector function. Nature. 2016;537:539–43.